Order Number 9009774

Charge transfer complexes of polymers containing pendant heterocyclic rings

Rodriguez, Libaniel, Ph.D.

City University of New York, 1989

U·M·I
300 N. Zeeb Rd.
Ann Arbor, MI 48106

CHARGE TRANSFER COMPLEXES OF POLYMERS CONTAINING PENDANT HETEROCYCLIC RINGS

by

LIBANIEL RODRIGUEZ

A dissertation submitted to the Graduate Faculty in Chemistry in partial fulfillment of the requirements for the degree of Doctor of Philosophy, The City University of New York.

1989

This manuscript has been read and accepted by the Graduate Faculty in Chemistry in satisfaction of the dissertation requirement for the Degree of Doctor of Philosophy.

6/1/89
date

Chairman of Examining Committee

6/1/89
date

Executive Officer

Howard Hanbenbock

David C. Locke
Supervisory Committee

The City University of New York

Acknowledgements

I would like to express my sincere gratitude to my mentor and friend, Professor Nan-Loh Yang, for his support, guidance and encouragement.

Special thanks are extended to Professors David Locke and Howard Haubenstock, members of my thesis committee, for their interest and advice as well as for the generosity of their time.

Acknowledgement is gratefully made to the following sources of financial support: (a) the Chemistry Department of the College of Staten Island for teaching appointments from 1984 to 1988, (b) Catalyst Research Corporation for partial support and (c) PSC-CUNY grants No. 666379, 667271 and 668253.

I would like to thank my parents for their continuous support love and patience.

Finally I would like to thank my wife Rose for her love, support and understanding, and for her generous help throughout the completion of this thesis manuscript.

Abstract

Charge-Transfer Complexes of Polymers Containing Pendant Heterocyclic Rings

by

Libaniel Rodriguez

Adviser: Professor Nan-Loh Yang

Charge-transfer complexes of a series of three polymers containing pendant heterocyclic polar rings, poly(2-vinylpyridine), P2VP, poly(3-vinylpyridazine), P3VPd, and poly(4-vinylpyridazine), P4VPd, with iodine were studied. The P2VP polymer, upon complex formation with iodine at low temperatures, led to crosslinking and degradation of the polymer as well as generation of paramagnetic centers in the complex. These phenomena were not observed for the polymers P3VPd and P4VPd under the same conditions. The difference in behaviour was ascribed to the higher resonance energy of pyridine compared to pyridazine.

For the study of the P3VPd-I_2 and P4VPd-I_2 systems, two new polymers, P3VPd and P4VPd, and their monomers, 3- and 4-vinylpyridazine, as well as their precursor alcohols, 3- and 4-(β-hydroxyethyl)pyridazine were synthesized and characterized for the first time

by us. Our study of the new polymers showed that the differences in direction and magnitude of the dipole moment of the pendant pyridazine rings were responsible for the stereoregularity of the polymers. Dipole interactions were found to cause significant differences in dilute solution viscosity as well as thermal behaviour of the two polymers. For radical P4VPd, an unusual rigid rod structure leading to liquid crystalline behaviour, not found in P3VPd, was observed. The synthesis of the two new intermediate alcohols, 3- and 4-β-(hydroxyethyl)pyridazine required the development of a new anhydrous molecular formaldehyde reagent solution which we employed successfully. We showed these anhydrous solutions with controlled concentrations of molecular formaldehyde to be effective in the addition of one carbon to organometallic species including Grignard reagents and demonstrated their broad potential for organic synthesis.

Charge-transfer complex formation of the new polymers with iodine resulted in adducts with direct current conductivity at least in the same range as the semi-conductive P2VP-iodine system, i.e. 10^{-5} to 10^{-4} $\Omega \cdot cm^{-1}$.

The two new polymers showed better thermal stability compared to P2VP. This property, combined with semiconductive behaviour and special properties such as rigid rod and liquid crystal behaviour, suggests clearly that polymers with heterocyclic pendant rings can be competitive systems to the unstable, highly conjugated backbone, charge-transfer complexes studied extensively in the past two decades.

TABLE OF CONTENTS

List of Tables

List of Figures

I. INTRODUCTION:

It is the objective of this thesis work to investigate a series of polymeric charge-transfer complexes with systematic structural variations. Three polymers were studied: poly(2-vinylpyridine), poly(3-vinylpyridazine), and poly(4-vinylpyridazine). The latter two polymers were synthesized and characterized for the first time by us for the purpose of this study.

Molecular complexes formed between electron donors and electron acceptors, e.g. pyridine with I_2, are known to exhibit very interesting electronic properties[1] which are absent in the individual components of the complex. An understanding of the manner in which charge-transfer imparts specific and useful characteristics to the complexes formed is highly desirable for the purpose of the controlled design of charge-transfer complexes with new and useful properties.

In recent years a great deal of work has been done in the area of charge-transfer complexes of inorganic as well as organic and polymeric materials. A large part of these studies deal with the effect that complex formation has on the electronic conductivity of polymeric organic materials.[2] In this area, it has been observed that some polymers can form charge transfer-complexes with electron donors such as Li and Na, and with electron acceptors like AsF_5, I_2 and Br_2. These dopants, upon complexing with the polymer, can transform the electronic conductivity of the system from a total insulator in the

However, the majority of the conductive polymers studied and reported up to now contain highly conjugated backbone structures.[3] This rigid structural feature alone makes these polymers rather insoluble. As a result, their characterization requires methods applicable in the solid state. The determination of molecular weights for these polymeric systems has been very difficult and in the best of cases highly qualitative.[3] In addition, most highly conjugated backbone conducting polymeric charge-transfer systems, e.g. doped polyacetylene and poly(p-phenylene sulfide), are not stable in air.[4-5] They are very sensitive to atmospheric water vapor. Their electronic conductivity degrades rapidly when exposed to moisture.[6]

The search for stable and useful charge-transfer polymeric systems has brought attention to polymers containing electron donor or electron acceptor moieties pendant to a vinyl polymer backbone. This feature, in principle, enables the characterization of the initial polymer by various methods, including molecular weight determination before the formation of the complexes. The formation and characterization of the charge-transfer complexes in the solid state can then be studied systematically by methods such as solid state ^{13}C NMR, IR, conductivity measurements etc. Poly(2-vinylpyridine), P2VP, and the two newly synthesized related analog polymers poly(3-vinylpyridazine), P3VPd, and poly(4-vinylpyridazine), P4VPd, carry electron donating heterocyclic pendant rings with variations in direction and magnitude of their dipole moments.

POLYMER	POLARITY OF PENDANT VINYL GROUP (based on methyl derivative)
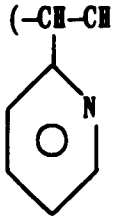 Poly(2-vinylpyridine) P2VP	2.16 D[7]
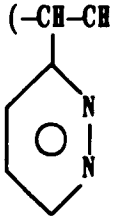 Poly(3-vinylpyridazine), P3VPd	3.86 D[8]
 Poly(4-vinylpyridazine), P4VPd	4.34 D[8]

In addition, the charge-transfer complexes of their monomeric molecular analogs[9-10] as well as those of P2VP[11], show good semiconduc- ting behaviour and much better stability in air and moisture compared with those of the conjugated backbone polymers mentioned above.

In order to compare pendant pyridine/I_2 charge-transfer complexes

and pendant pyridazine/I_2 complexes, polymers with the pyridazine moiety pendant to the macromolecule backbone were prepared. This was achieved by the polymerization of the two new monomers synthesized and characterized by us for the first time: 3-vinylpyridazine and 4-vinylpyridazine. Polymerization gave two new polymers: P3VPd and P4VPd. Thus, we have a series of three structurally related polymers: P2VP, P3VPd and P4VPd. Each polymer contains a pendant heterocyclic ring known to form charge-transfer complexes with iodine.

Investigation of the poly(2-vinylpyridine)-iodine system is a main focus in this thesis work. P2VP/I_2 charge-transfer complexes are used as the cathode material for lithium-iodine cells[12] because of its stability and good semiconductive behavior. Previous studies by Yang et al. showed that the performance of lithium-iodine cells depend significantly on the properties of the cathode material P2VP-I_2. In order to complete the formation of the charge-transfer complex of polymer-I_2, initial heat treatment is required.[13] The physical and chemical changes due to this treatment are not thoroughly understood. In this part of the work we set out to investigate the processes involved when P2VP is heated in the presence of I_2 at the relatively low temperatures of 65°C to 60°C. For this purpose, P2VP samples of two different molecular weights were doped with iodine in a ratio of one pyridine ring per 20 I_2 molecules.

Solubility studies, ^{13}C NMR, ESR and GPC investigations established the generation of paramagnetic centers in the cathode material and the crosslinking of the polymer as well as its concurrent degra-

dation as a function of polymer molecular weight, temperature and duration of heat treatment.

Parallel to the P2VP-I_2 studies considerable effort was invested in the synthesis and characterization of the two new polymers P3VPd and P4VPd. This involved the synthesis of 3- and 4-(β-hydroxyethyl)pyridazines followed by their dehydration to give the respective monomers and subsequent polymerization to obtain their polymers.

Several attempts to synthesize the intermediate alcohol 3-(β-hydroxyethyl)pyridazine and the 3-vinylpyridazine monomer were made previous to this thesis work. One successful method resulting from that effort yielded the 3-vinylpyridazine monomer in an acceptable yield (25%) and high purity[14] (see Scheme 2 in section IV.A.1.a). In this method, no attempt was made to characterize or isolate the intermediate 3-(β-hydroxyethyl)pyridazine. The same method and its variations for the synthesis of 4-(β-hydroxyethyl)-pyridazine and the 4-vinylpyridazine monomer always resulted in the polymer P4VPd.

Since control over the polymerization reaction was desired, a new method for the synthesis of the 4-vinyl monomer needed to be developed. The result was the method shown in Scheme 1.[15]

This method involved the metalation of methylpyridazine by lithium diisopropylamide (LDA) at low temperature and anhydrous conditions followed by the condensation of the lithiated methylpyridazine with anhydrous THF formaldehyde solution. The resulting alkyllithiumpyridazinyl anion was then reacted with water to obtain the

SCHEME 1

Synthesis of n-vinyl pyridazines

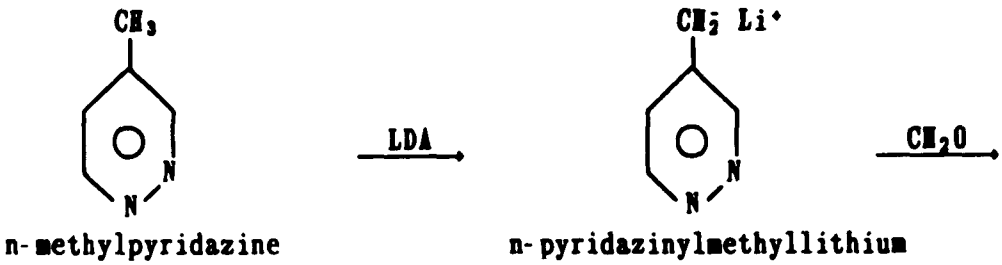

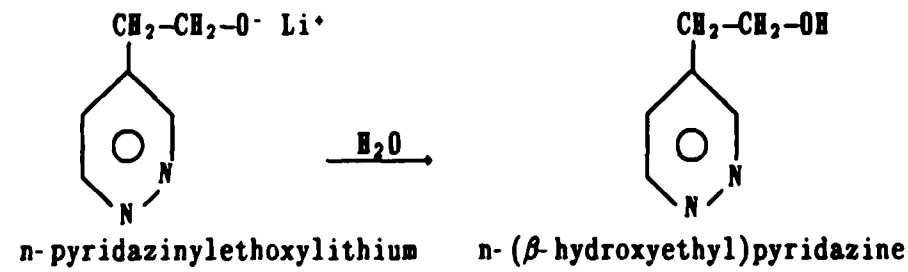

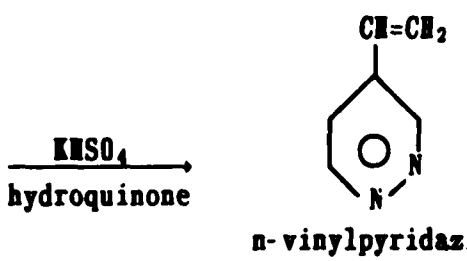

desired alcohol. These alcohols were in general obtained in good yield. Dehydration of the alcohol was effected by fused potassium hydrogen sulfate in the presence of hydroquinone as a radical inhibitor. The 4-vinylpyridazine monomer was obtained by this method in a satisfactory yield, i.e. 47%.

This process was also successful in the synthesis of 3-(β-hydroxyethyl)pyridazine and 3-vinylpyridazine.

The new method proved to be more efficient than the previous high temperature and pressure method for the following reasons:

1. It requires only low temperature and pressure (i.e. -78°C and 1 atm).
2. It allows the isolation in good yields and characterization of the 3- and 4-pyridazine alcohols.
3. It gives acceptable yields for both monomers.
4. Finally, no special equipment is needed as opposed to the previous method in which a pressure reactor was required.

By this new procedure, three new molecules were isolated and characterized by ^{1}H and ^{13}C NMR as well as elemental analysis.

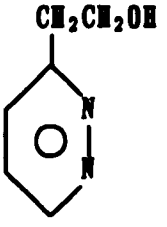

3-(β-Hydroxyethyl)pyridazine

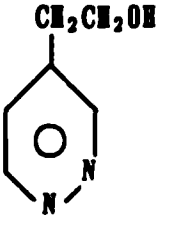

4-(β-Hydroxyethyl)pyridazine

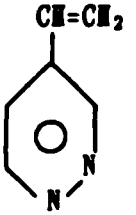

4-vinylpyridazine

3-Vinylpyridazine, which had been previously synthesized by a different method,[14] was also synthesized by the new method in a satisfactory yield.

In the search for the procedure shown in Scheme 1, we developed an anhydrous THF molecular formaldehyde solution with controlled concentration. This solution proved to be stable at temperatures as high as 0°C. ^{1}H NMR studies of this solutions at 0°C showed formaldehyde to exist in its pure molecular form, and not in equilibrium with paraform or methylols as in the case of aqueous solutions of formaldehyde.[16]

The monomers obtained by the new method were successfully polymerized in bulk and in solution by radical, thermal and anionic initiation. The respective polymers obtained were characterized by solution and solid ^{13}C NMR as well as by elemental analysis. Viscosity measurements on dilute solutions of the two new polymers revealed rigid rod solution behavior for P4VPd not readily observable for P3VPd. This phenomenon, we believe was caused by the direction and large magnitude of the dipole moment of the pendant pyridazine ring in P4VPd. Thermal analysis of both polymers revealed their thermal stability. Studies of the charge-transfer formation of the polymers

with I_2 were made by use of ESR and iodine uptake. Conductivity measurements showed that the new polymers upon forming charge-transfer complexes with iodine become semi-conductors and conduct direct current at least at the same level as the charge-transfer complexes of P2VP with iodine, i.e. 10^{-5} - 10^{-3} $\Omega \cdot cm^{-1}$.

II. LITERATURE REVIEW

In this section some basic background in the areas of charge-transfer and polymeric charge-transfer complexes is provided. The poly(2-vinylpyridine) polymeric system is then reviewed, concentrating mainly on its charge-transfer complexes with I_2 and the use of these complexes as the cathode material in lithium iodine cells. Finally some general background on pyridazine will be discussed.

II.A. CHARGE-TRANSFER COMPLEXES

Charge-transfer complexes are formed as a result of partial electron transfer from the donor to the acceptor. The fraction of electron transfer varies greatly, from close to zero to almost one, depending on the electron donor-acceptor pair and on the electronic state of the complex. Charge-transfer complexes are also viewed as a quantum mechanical resonance between a no-bond structure and a structure with a bond $D^{+}-A^{-}$.[17]

The forces leading to the formation of charge-transfer complexes are thought to be highly directional and favored only when the ground and electronically excited states of the acceptor and donor belong to the same group theoretical species and are of the same symmetry. This requirement allows the maximum overlap between the odd electrons in the excited molecular orbital of the donor and the lowest excited states of the acceptor. Once the charge transfer complex is formed,

it shows a special class of intense electronic absorption spectra characteristic of the complex D•A and non-existing in either partner D or A alone.[17]

The discussion above applies in general to charge-transfer complexes in solution. However, Mulliken observed in 1952 that charge-transfer forces operate in more or less localized fashion in the solid as in the liquid. He made this suggestion in view of the fact that some molecular complexes existing in solution can often appear as crystalline solids.[17]

Pyridine-iodine is an example of a charge-transfer complex known to exist in solution as well as in the solid state. In solution, these complexes exist as the quaternized pyridinium ion[18] as well as the π I_2-pyridine complex.[19] In the solid state, as the polymeric P2VP-I_2 charge-transfer complex, however, the details in donor acceptor interaction are still not well understood.

Formation of the pyridine-iodine complex has been studied by UV, IR[18] and ^{13}C NMR.[19] In ^{13}C NMR the formation of the charge-transfer complex has been ascertained by a comparison of the spectrum of the uncomplexed pyridine to that of the molecule in the complex. It was observed experimentally that some carbon absorptions in the complex shift downfield by as much as 13 ppm.[19] This shift is caused by the new electronic distribution upon complexation and has been found to be consistent with predictions of theory.[19] The same type of shifts in magnitude and direction has been observed by us for the poly(2-vinyl-pyridine)-iodine charge-transfer complexes in solid state ^{13}C NMR

spectra. This is not surprising since in general, the electronic state of the pendant molecule is very similar to that of the isolated molecule.[3] Thus, the electronic interactions of the pendant charge-transfer complexes are essentially the same as those of a randomly oriented ensemble of the small molecule charge-transfer complexes.[3]

II.B. POLY(2-VINYLPYRIDINE)-IODINE SYSTEM

The presence of the heterocyclic nitrogen in poly(vinylpyridine) imparts basic properties to the polymers. Poly(2-vinylpyridine) undergoes most of the chemical reactions reported for alkylpyridines. Among the most important ones are: reaction with acids, quaternization with alkyl halides and N-oxidation. The polymer resembles pyridine in its ability to form complexes with several metal ions including Cu^{2+}, Co^{2+} and Mn^{2+}. It also forms molecular complexes with I_2,[18-19] phenol, SO_2 and many Lewis bases.

Poly(2-vinylpyridine) exhibits good thermal stability when dry. Its glass transition temperature has been shown to be in the range of 100° to 120°C depending on the molecular weight of the polymer.[20-21] The thermal stability of the polymer decreases upon protonation or conversion to 1-alkylpyridinium salt.[22] In general the thermal stability of the polymer decreases with the extent of quaternization.[22]

Poly(2-vinylpyridine) is moderately hygroscopic, soluble in methanol, THF, acetic acid and pyridine. It is insoluble in benzene, toluene and cyclohexane. The polymer shows weaker basicity than its

monomeric counterpart. For example, 2-ethylpyridine has a pK_a of 5.89 while P2VP shows a pK_a of 3.5.[23]

Dry poly(2-vinylpyridine) in relatively pure form exhibits electronic insulating properties typical of most vinyl polymers. However, quaternization of the free base with alkyl halides or the addition of water or acids, including Lewis acids can impart semiconducting properties to the polymer. P2VP has been complexed with TCNQ (7,7,8,8-tetracyanoquinodimethane). The conductivity of the complex has been controlled over several orders of magnitude by varying the amount of TCNQ. Conductivities as high as $10^{-3}\Omega \cdot cm^{-1}$ have been obtained in these systems.[24] The uses of P2VP range from agricultural and medical uses to photographic and battery applications. [11-12]

Charge-transfer complexes of P2VP with molecular iodine have been utilized as the cathode material in small solid state batteries in which long life under low current drain is required.[12] Applications of these batteries include implantable cardiac pacemakers. The use of P2VP/I_2 as a cathode material offers many advantages: it provides high energy density,[11] long shelf life and in addition, no gas is generated during the operation of the battery.[13]

II.C. PYRIDAZINE

Pyridazine and its derivatives have been known since the 19th Century.[8] Although the basic syntheses and reactivity were investigated in the early years, interest in these compounds was not

very intense. Unlike the other two diazines, pyrimidine and pyrazine, and their bicyclic compounds, pyridazines do not occur commonly as natural products.

Several extensive reviews on pyridazine and its derivatives are available.[8 25-27] Studies on pyridazines range from the theoretical[28-29a] to their anti-viral[30] and anti-cancer[31] activities. However, studies on the charge-transfer complexes of pyridazine are rather limited.

In general pyridazines are completely miscible with water and alcohols due to the lone electron pair in the nitrogen being capable of forming hydrogen-bond with hydroxylic solvents. The basicity of the pyridazine ring is lower than that of pyridine (pK_a 2.33 for pyridazine and 5.23 for pyridine). Pyridazine has a high dipole moment of 3.45 D, perhaps among the highest for organic moieties.[29b] It has a relatively high boiling point of 208°C which has been attributed to electrostatic forces arising from the high permanent dipole moment.[8]

A few pyridazine-iodine charge-transfer complexes have been reported recently. The formation of these complexes has been studied by ^1H NMR,[10] x-ray crystallography, IR and elemental analysis.[9] The complexation of pyridazine to iodine in a ratio of one pyridazine to 1.0-1.4 I_2 molecules was found[9]. The resulting adducts are reported to possess low electronic resistivity, high stability to ambient conditions and excellent thermal stability.

More recently, pyridazine-iodine charge-transfer complexes have

been used in combination poly(2-vinylpyridine)-iodine complexes as the cathode material for lithium-iodine cells. This cathode material mixture results in longer shelf life for the batteries and higher current densities. The reasons for the improvement of properties upon use of this material as opposed to P2VP/I_2 alone as the cathode material are not yet understood.[32]

Studies of pyridazine from the point of view of polymer chemistry are scarce. The most recent report, is that for poly(3-vinylpyridazine), by our group in Chemical Communications.[14]

III. POLY(2-VINYLPYRIDINE)-IODINE SYSTEM

Poly(2-vinylpyridine) is used as the cathode material in lithium-iodine cells. The performance of these cells depends significantly on the properties of the polymeric charge-transfer material. In order to complete the formation of the conductive charge-transfer complex, initial heat treatment is required. This treatment causes physical and chemical changes previously not understood. We report here our findings reflecting these changes.

III.A. EXPERIMENTAL

III.A.1. Heat treatment of the cathode material

Samples of poly(2-vinylpyridine), P2VP, (Catalyst Research Corp.) of molecular weights 2 X 10^4 and 4 X 10^5 were ground and passed through a standard 270 mesh sieve. Before use, each sample was dried under vacuum for at least 24 hours and then dry mixed with iodine in a ratio 1/20, polymer/I_2, in a rolled glass jar for twenty minutes. The material was then pressed into a pellet 21.3 mm in diameter and 0.66 mm thick using 3.6 kilograms of force with a hydraulic press. The pellet was hermetically sealed into a cell case which it completely filled. The amount of material in each cell was about 0.75 grams. The cells were subjected to heating at 60° and 65°C for various durations. The cathode material was then removed from the cell for determination of crosslinking and centration of paramagnetic centers.

III.A.2. Determination of percent crosslinked polymer

For each determination, cathode material from two cells was added to 80 mL of 20% NaOH aqueous solution. The slurry was subjected to continuous stirring for at least two hours until the polymer lost its violet-black color. The mixture was then filtered through Millipore HVLPO 2500 filter disks. The polymer was removed from the filter disk and dried at 75°C for at least two hours in a vacuum oven connected to a mechanical pump. The weight of the dried polymer was taken as the total weight of the polymer, crosslinked and noncrosslinked. The dried polymer was then treated with methanol at 45°C for initial removal of the noncrosslinked polymer. The mixture was filtered. The polymer remaining on the filter disk was washed with distilled water and collected. It was further treated with 0.1 N $S_2O_3^{2-}$ to remove I_2 possibly remaining.

The $S_2O_3^{2-}$/polymer mixture was filtered, the polymer was washed with distilled water and removed for treatment with concentrated HCl. The precipitate after HCl treatment was again filtered, washed and dried. The weight of this dried polymer was taken to be the weight of the crosslinked polymer.

III.A.3. Spin density measurements

Electron spin resonance absorption of the heat-treated cathode material was monitored with a JEOL model JES-ME-3X ESR spectrometer operated at X-Band. Spectra were obtained at a microwave power level where the peak-to-peak signal intensity response to the square root of

the microwave power was linear and at modulation amplitudes of less than one-fourth of the line width. A manganese marker, consisting of manganese ion dispersed in magnesium oxide, was fitted to the microwave dual cavity as a standard to correct for any change in the cavity Q between runs. Samples of pure DPPH of accurately known weight were used as spin density standards.

All first derivative curves were doubly integrated by the Wyard method.[33] Spin density calculations are based on the assumption of one spin per DPPH (1,1-diphenyl-2-picrylhydrazyl) molecule. The quantity of DPPH was also determined experimentally by measurement of its optical density in benzene, λ_{max} = 519 nm, log ϵ = 4.89. The agreement in spin density between this determination and that from the double integration was satisfactory.

g Values for the ESR absorptions were calculated using the equation: g = 6651 / (3357 - ΔH), assuming a g value for the fourth line of the Mn^{++} marker equal to 1.980 and a microwave frequency of 9300 MHz. ΔH is measured from the fourth Mn^{++} line to the center of the ESR absorption peak linewidth. The relative error involved in this determination is ± 0.0005.

III.A.4. Gel permeation chromatography, GPC

The gel permeation chromatography instrument used was a Waters Associates Model 15C high temperature GPC System with a Model 730 Data Module. Dimethylformamide at 50°C was used as the mobile phase. Soluble portions of the P2VP-I_2 system after heat treatment were

examined for molecular weight changes. For this purpose, standard P2VP samples of known molecular weight were mixed with I_2 in a ratio of twenty I_2 molecules per pyridine ring. These samples were packed into glass ampules which were then evacuated for 15 minutes at room temperature with a mechanical pump and then sealed under vacuum. Heat treatments were carried out for 24 hours at 60°C ±1°C. At the end of the heating period, the ampules were opened and the contents were mixed with concentrated NaOH solution to extract I_2 from the polymer. The solid remaining was subjected to NaOH treatment again, then filtered, washed with distilled water and dried under vacuum. The brown polymeric material was then treated with methanol. Part of it dissolved to give a yellowish solution, containing an undissolved brown solid crosslinked material. The soluble polymer, presumably degraded, was recovered from the methanol solution. This step was achieved by evaporating the methanol under vacuum, dissolving any impurities remaining in the recovered polymer with ether and filtering again. The P2VP thus recovered, approximately 6% of the total polymer treated, was dried under vacuum, dissolved in DMF and its average molecular weight determined by GPC using the same standards and conditions under which the M_w of the original untreated P2VP was determined.

III.A.5. Solid state ^{13}C MAS/CP NMR

Solid state ^{13}C MAS/CP NMR spectra were obtained at 50.3 MHz through the use of an IBM WP 200 FT NMR spectrometer with a solid

state attachment for magic angle spinning and cross polarization, MAS/CP. Contact times were between 1.3 to 2.5 milliseconds. Line broadening was optimized to obtain the best signal to noise ratio without affecting the linewith.

III.A.5.a. T_1 experiment

The measurement of T_1 for untreated P2VP and crosslinked P2VP was done on the same instrument described above. ^{13}C CP/MAS spectra were obtained at 50.3 MHz and contact times of 2.0 milliseconds for crosspolarization. In this experiment the inversion recovery pulse sequence, 180-τ-90 was utilized. The time allowed for longitudinal relaxation of the spin system to occur, τ, was varied from 0.4 seconds to 120 seconds and a waiting time of 6 seconds was allowed in between pulse sequences. The samples used were: untreated standard poly(2-vinylpyridine) M_w 2.4 X 10^5 and crosslinked poly(2-vinyl-pyridine). The crosslinked P2VP was obtained by treating a sample of the standard P2VP, (M_w 2.4 X 10^5), in the same manner described in the GPC experiment above. The null method[34] was used in order to estimate T_1 for the carbons of interest. In this method, at null amplitude of the signal, T_1 is equal to τ/ln 2.

III.B. RESULTS AND DISCUSSION

Figure 1 shows the formation of crosslinks in P2VP during the course of heat treatment. The high molecular weight, 4 X 10^5, polymer formed crosslinks at a much faster rate than that with the lower

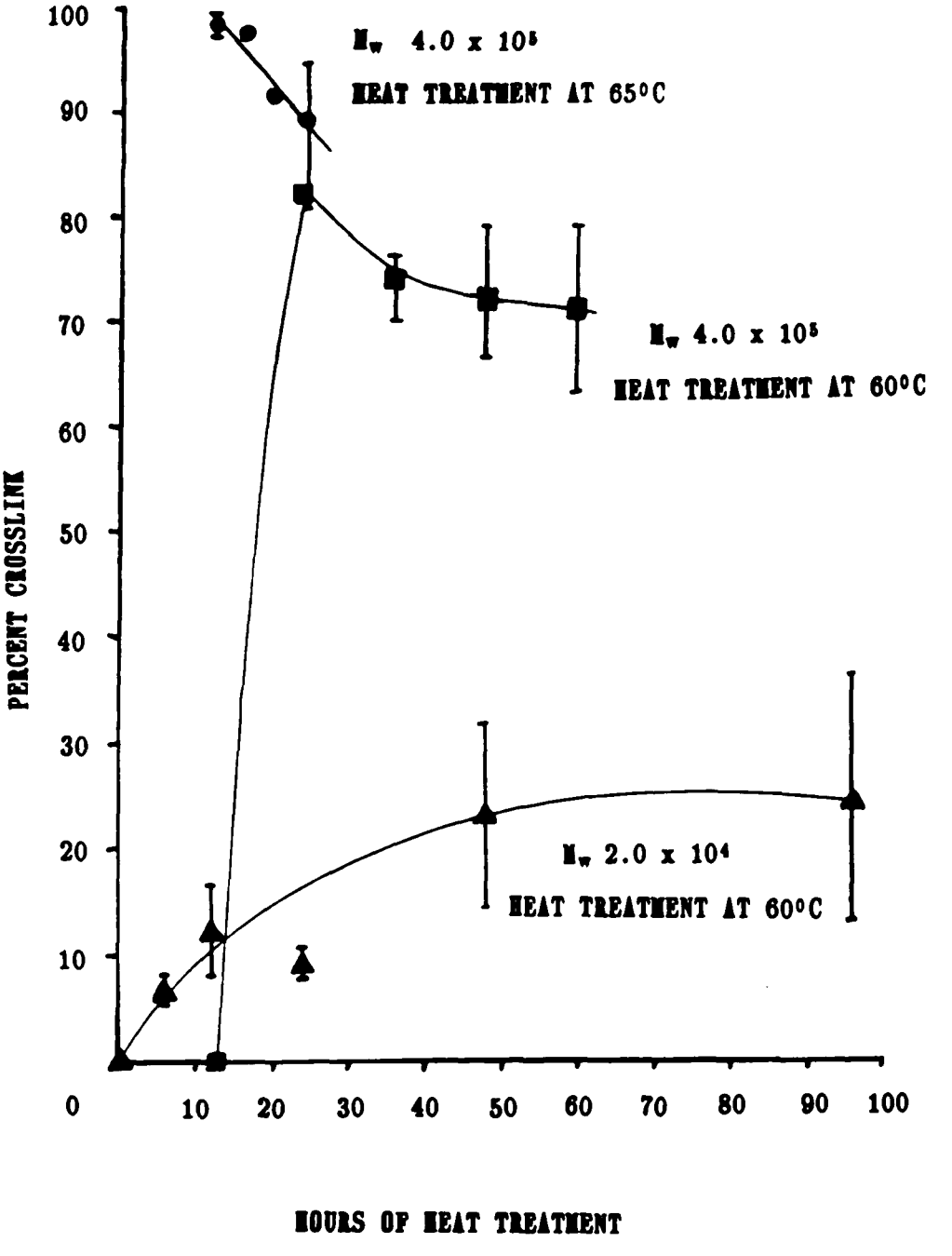

Figure 1. Percent P2VP crosslinked as a function of molecular weight, temperature and duration of heat treatment.

molecular weight of 2 X 10^4. A comparison of the curves at 65°C and 60°C for the sample with the molecular weight of 4 X 10^5 indicates the marked difference in the time required for the onset of crosslinking due to a five degree difference in temperature. Higher temperature leads to a much faster initial rate in the crosslink formation. The decrease in the net percent of polymer crosslinked during later stage heating indicates that degradation of the polymer takes place concurrently with the process of crosslinking. The degradation of P2VP was further substantiated through GPC studies of the samples with crosslinking. For the same heat treatment temperature of 60°C, the low molecular weight polymer attained a much lower level of crosslinking than the higher molecular weight polymer. This is to be expected, because lower molecular weight polymer would require a higher number of interchain linkages per unit mass to become crosslinked. Controlled experiments demonstrated that poly(2-vinylpyridine), when heated by itself, does not become crosslinked.

Additional evidence for the crosslinking of P2VP was obtained through solid state ^{13}C MAS/CP NMR studies. Figure 2 shows the solid state ^{13}C NMR spectra of P2VP-I_2 systems heat-treated (spectrum A) and without heating (spectrum B). The two spectra indicate that heat-treatment leads to considerable broadening of the absorption lines for C_2 and $C\alpha+\beta$. The half height line width for C_2 is broadened considerably from 238 Hz to 374 Hz; the combined $C\alpha+\beta$ carbon peak, from 335 Hz to 622 Hz. These carbon atoms are the ones on and

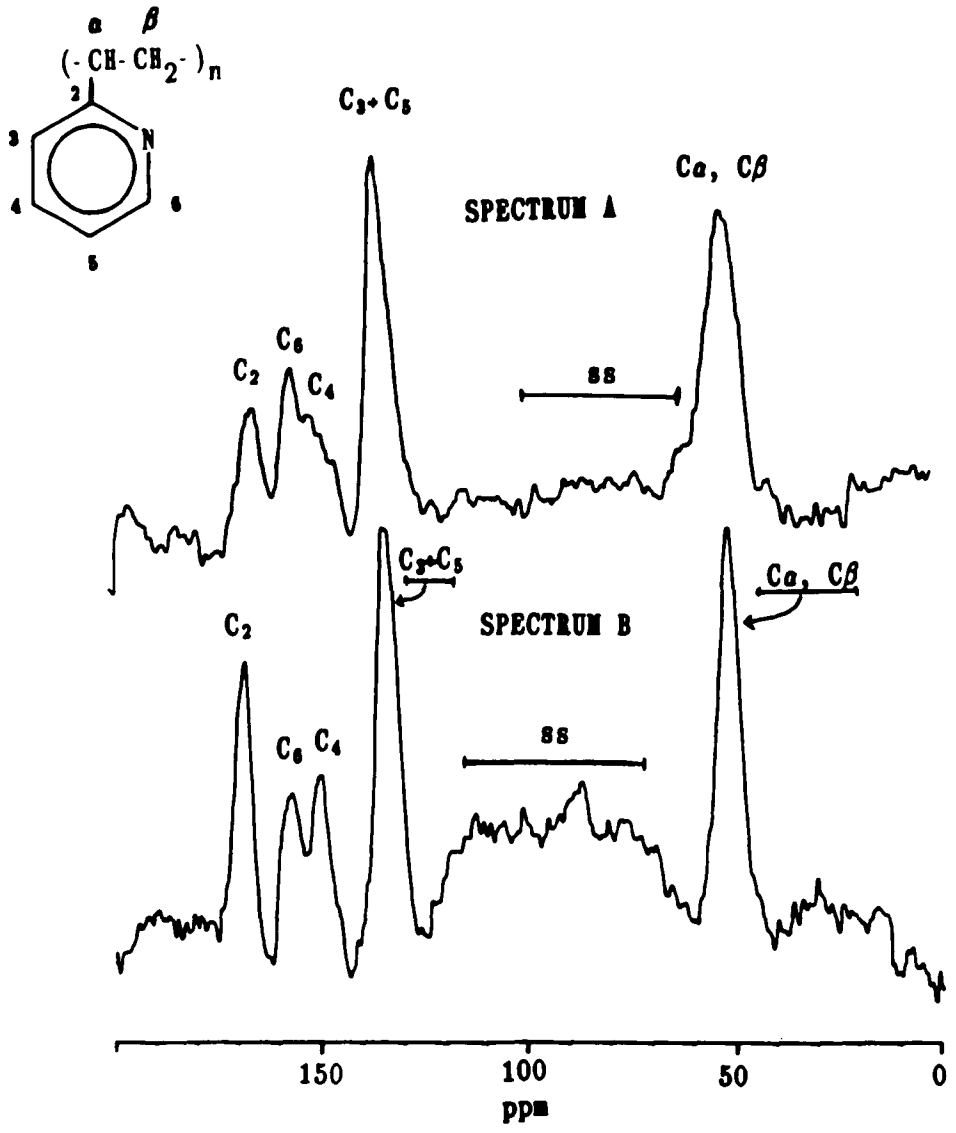

FIGURE 2. Solid state ^{13}C NMR spectra of P2VP-I_2 system.

A. HEAT TREATED

B. CONTROL

ss = Spinning Sidebands

adjacent to the P2VP backbone and hence their mobility would be considerably hindered because of the reduction in polymer backbone segmental motion due to crosslinking. Thus, a lower level of motional averaging of local magnetic field and hence broader NMR absorptions are to be expected[35]. The P2VP-I_2 systems, untreated and heat treated, show no significant difference in ^{13}C NMR absorption chemical shifts. This indicates that the heat-treatment at 60°C and 65°C did not significantly alter the structure of the polymer. Evidence here strongly supports that poly(2-vinylpyridine) as a cathode component can become crosslinked due to heat treatment at these low temperatures. Furthermore, the dissolution processes in our experimental scheme were extremely harsh, i.e. concentrated HCl was used to remove non-crosslinked polymer and $S_2O_3^{2-}$ to remove I_2. In addition, we have performed quantitative determination of I_2 removed and results indicated I_2 was almost completely removed. The crosslinked material was observed to remain insoluble even after a two days of treatment with concentrated HCl.

Linewidths and relaxation times derived from nuclear magnetic resonance are sensitive indications of molecular motion in polymers.[35] Spin lattice relaxation times of ^{13}C in polymers are of particular interest since they are dilute nuclei, therefore each carbon shows a characteristic T_1 reflective of their specific domain.[35] The spin lattice relaxation mechanism is dominated by dipolar interaction of carbon with attached protons[36] and it is therefore greatly affected by molecular motions (i.e. segmental motion, tumbling etc.).

Relaxation studies on atactic polystyrene revealed that above a certain molecular weight (10^4), the relaxation mechanism is dominated by segmental motion and not by overall reorientation of the whole molecule.[37-38] For such a system, any factor hindering segmental motion would slow the relaxation mechanism. Thus long T_1's would result.

By analogy to the system above, our P2VP systems, treated and untreated, should be affected in the same manner.

Figures 3 and 4 show spectra for the T_1 measurement of untreated P2VP and crosslinked P2VP respectively. Our interest centers on determining the T_1 of C_2 and that of the combined absorption for carbons α and β, $C\alpha+\beta$. These carbons would be the most affected by a decrease of segmental motion of the polymer,

T_1's were calculated by estimating from the graphs, the time τ, at which the absorptions for C_2 and $C\alpha + \beta$ were null. The null absorption, τ_0, was estimated by direct correlation between the intensity of the absorptions and the time τ needed for the absorption peaks to recover from a low negative to a low positive value.

Table 1 T_1 Values for Carbons 2 and $\alpha + \beta$ of Untreated and Crosslinked Poly(2-vinylpyridine)

Carbon	P2VP Untreated $T_1 = \tau/0.69$	P2VP Crosslinked $T_1 = \tau/0.69$
2	52 sec ± 5	72 sec ± 5
$\alpha + \beta$	50 sec ± 5	65 sec ± 5

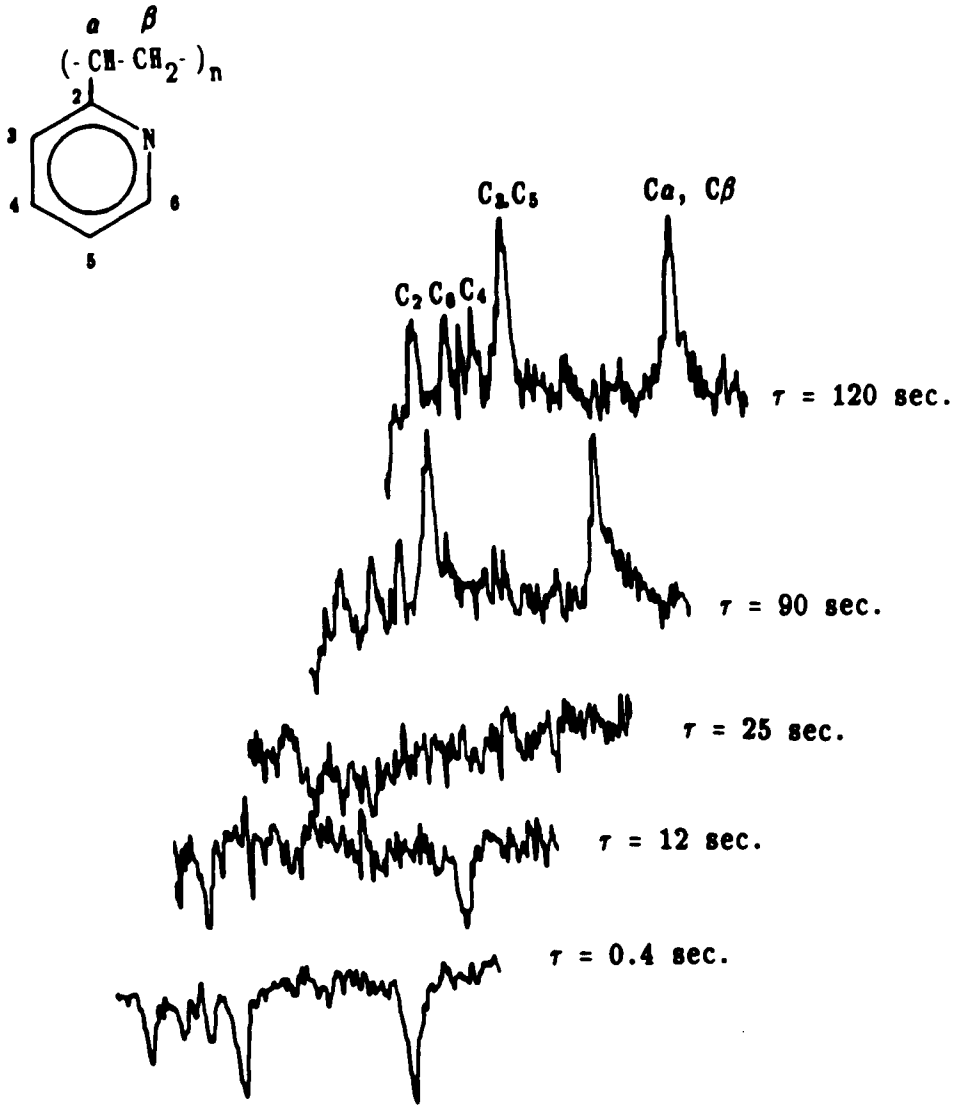

Figure 3. Solid state ^{13}C MAS/CP T_1 experiment for P2VP.

C_2, A_0 at t $\cong$ 37 sec. T_1 = 52 sec.

$C\alpha + \beta$, A_0 at t $\cong$ 35 sec. T_1 = 50 sec.

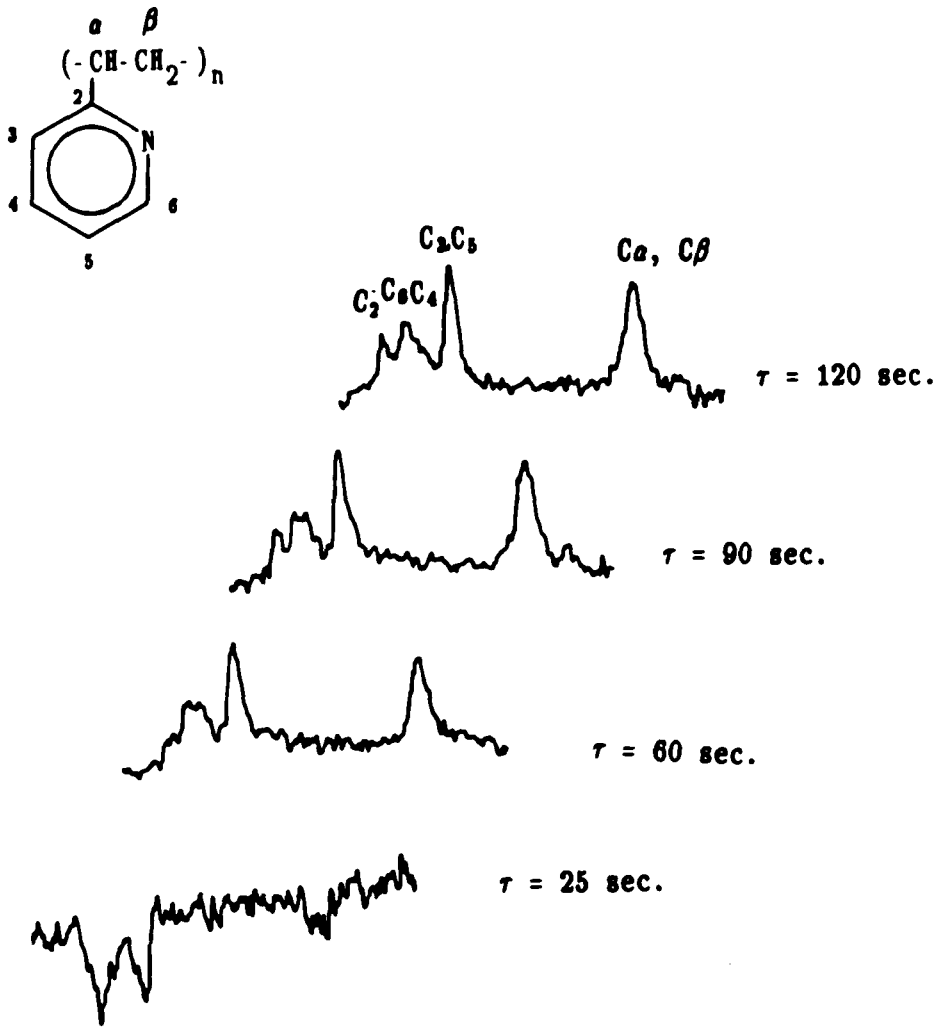

Figure 4. Solid state ^{13}C MAS/CP T_1 experiment for crosslinked P2VP.

C_2, A_0 at t ≅ 50 sec. T_1 = 72 sec.

$C\alpha + \beta$, A_0 at t ≅ 45 sec. T_1 = 65 sec.

Data from Table 1 indicate in a qualitative manner an increase in the average T_1 value for the carbons on or close to the backbone after crosslinking of the polymer. Quantitative results[47] from data in Figures 3 and 4 indicate for C_2 of the crosslinked polymer, an increase in T_1 by 4 seconds and no change in T_1 for the $C_{\alpha+\beta}$ absorption. The value obtained for C_2 follows the trend in Table 1. However, difficulty in baseline determination for Figures 3 and 4 together with the lack of a τ_∞ data point for the crosslinked polymer lead to erroneously low T_1 values and render the quantitative results inconclusive. The increase in T_1 however, suggests that the average segmental mobility of the polymer molecules decrease due to crosslinking and therefore the relaxation process becomes less effective (longer T_1's). This result along with the broadening of the absorptions for C_2 and $C\alpha + \beta$ in Figure 2, give support to our finding that P2VP crosslinks after being heated in the presence of I_2.

The degradation of P2VP concurrently with the crosslinking process during heat treatment is clearly indicated by GPC studies on the soluble polymer portions. Poly(2-vinylpyridine)-I_2 systems with two different molecular weight polymer samples were examined. Figure 5 shows the GPC chromatograms from a system with a narrow molecular weight distribution, M_w = 1.1 X 10^5: "curve A" for untreated polymer: "curve B" for soluble fraction after treatment.

The chromatogram shows substantial degradation of the polymer molecules accompanying the crosslinking process. The soluble portions of the systems contain a fraction of polymer with an average molecular

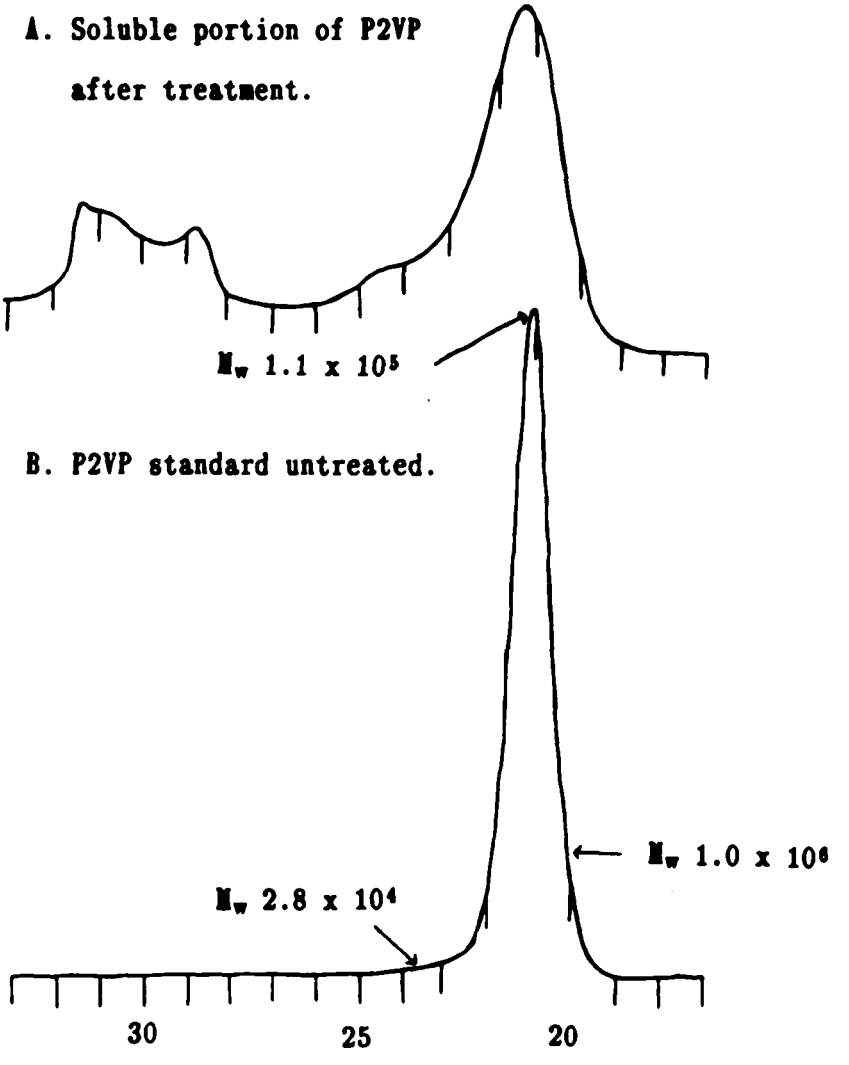

Figure 5. GPC of P2VP: A. Soluble portion of P2VP after treatment, B. Untreated P2VP standard.

weight close to that of the original sample plus a fraction of polymer with very low molecular weights. Systems with different P2VP molecular weights show similar behaviors.

Thus, the formation of a charge transfer complex of P2VP with I_2 at a temperature of 60°C leads to crosslinking of most of the polymer molecules with an accompanying degradation of the chain. This is consistent with the observation of maxima or plateaus in the percent crosslinking vs. time curves (Figure 1). Figure 6 shows a typical ESR absorption of heat treated cathode material. The maximum slope line width, ΔH_{msl} ranges from 15 to 20 gauss. Longer treatment time leads to a signal at a narrower line widths. Heating produced paramagnetic centers in the system with higher rate at higher temperature (Figure 7). Lower molecular weight polymers lead to higher spin density. A spin density of 9 X 10^{15} spin/g of cathode material corresponds to ca. one spin per 3 X 10^5 pyridine rings. Controlled heat treatment experiments on freshly prepared P2VP-I_2 samples revealed ESR hyperfine structures at early stages of heating. These structures resemble a triplet absorption with a hyperfine splitting constant of 10 Gauss, superimposed on a singlet. As heat treatment continues, the fine structures disappear and only the singlet absorption is observed. This observation is consistent with observations by David et al.[39-40] on irradiated P2VP and P4VP. They suggested that the two types of absorptions, the triplet and the singlet, correspond to a benzilic-type radical and a ring carbon radical respectively. In our case, it is then possible that as the benzilic-type of radical is formed,

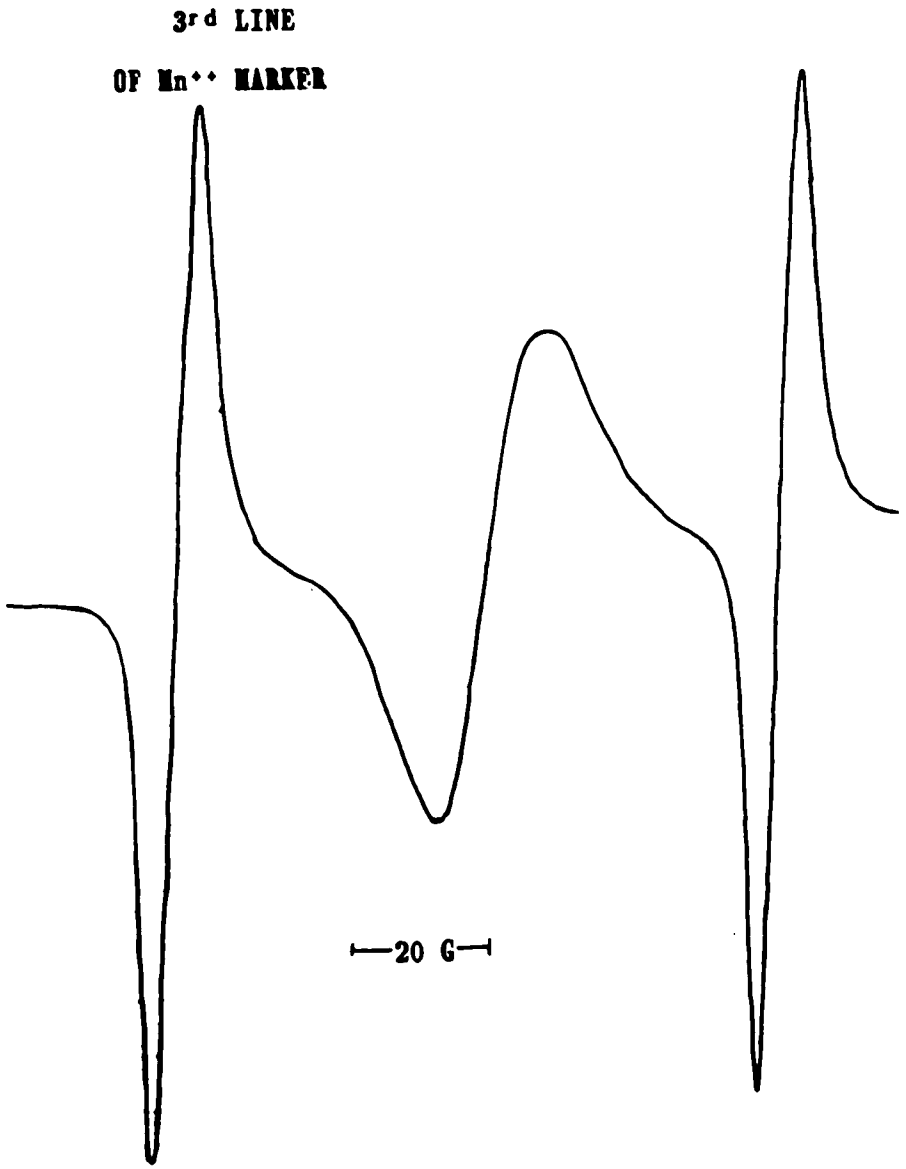

Figure 6. Typical ESR absorption of heat treated cathode material.

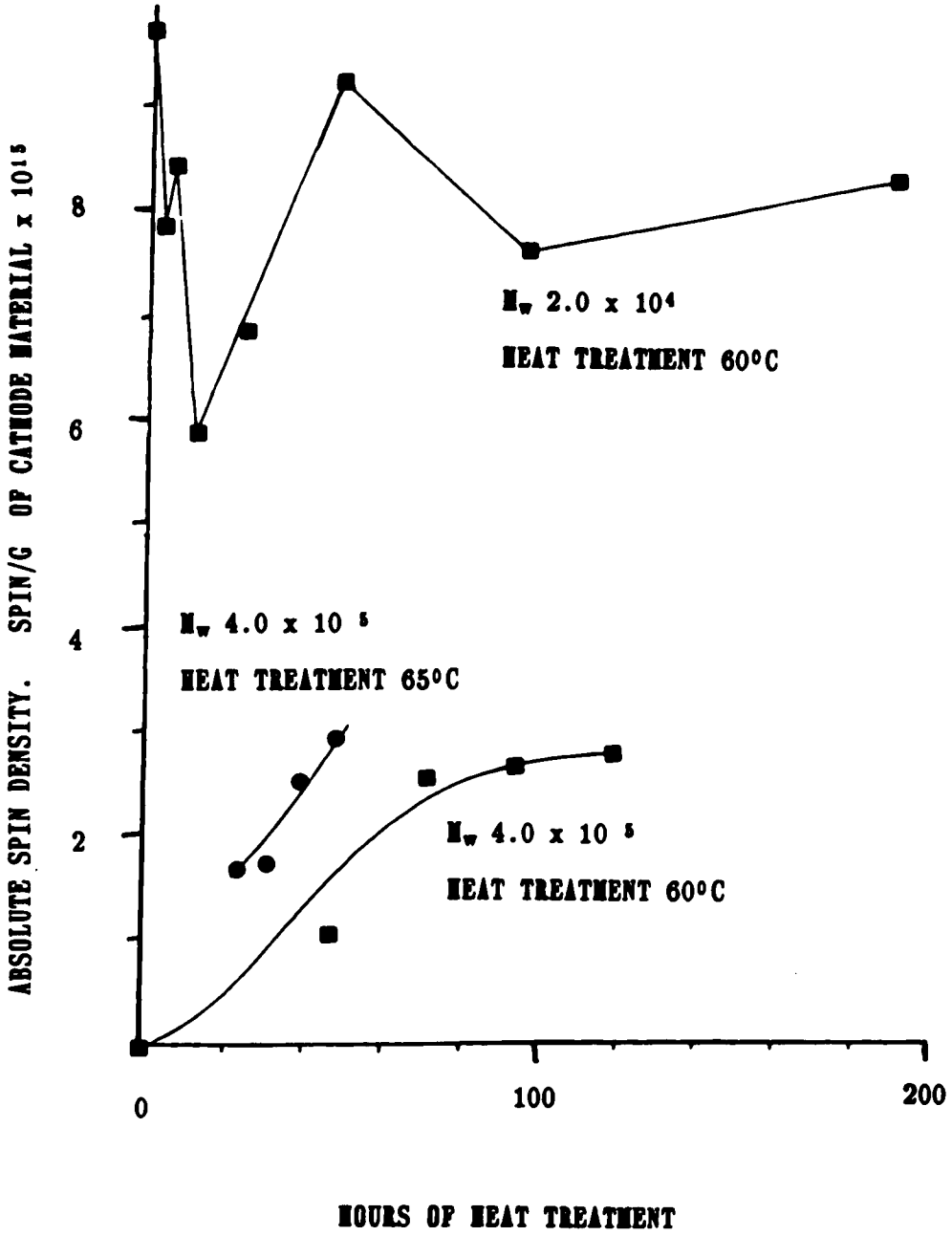

Figure 7. Absolute spin density of heat treated cathode material as a function of molecular weight, temperature and duration of heat treatment.

crosslinking of the polymer occurs and in the latter stages of treatment, the only radicals remaining in the sample are those on the ring carbons. Furthermore, ESR observations of a freshly mixed P2VP/I_2 sample at room temperature showed a singlet absorption whose intensity increases with time. However no hyperfine structures were observed for this sample at low temperatures.

Solubility studies of this room temperature sample showed no crosslinking of the polymers. This experiment suggests that the singlet absorption is due to a ring carbon radical and that moderate heating of the P2VP/I_2 material is needed in order to generate the radicals responsible for crosslinking of the polymer.

III.C. CONCLUSION

Heat treatment at 60°and 65°C of P2VP-I_2 cathode material for lithium-iodine cells leads to the following physicochemical changes.

1. Delocalized electrons are generated. The rate of generation increases with temperature and is higher for low molecular weight polymers.
2. The polymer component, P2VP, of the cathode becomes chemically crosslinked without substantial alteration of its chemical structure. The crosslinking process is accompanied by degradation resulting in generation of monomer and oligomer. The crosslinking process is favored by higher treatment temperature and higher molecular weight.

IV. POLY(VINYLPYRIDAZINES)

Pyridazine-iodine charge-transfer complexes exhibit improved semiconductive behavior[9-10] and are more stable to ambient conditions in comparison to pyridine-iodine adducts. Analogous to the P2VP-I_2 system, this suggests that vinyl polymers containing pendant pyridazine rings may lead to interesting polymeric charge-transfer systems.

Poly(3-vinylpyridazine) and poly(4-vinylpyridazine) were the polymers of choice. The starting monomers could in principle be obtained by the modification of the methyl group in 3-methylpyridazine and 4-methylpyridazine. Having the pyridazine moiety pendant to the polymer at these positions would enable us to make relative comparisons between the new polymers and the well-established poly(2-vinylpyridine) system.

In this work the synthesis of two new monomers, 3- and 4-vinylpyridazine, and their polymers, P3VPd and P4VPd, was conducted. Characterization was accomplished by elemental analysis and NMR spectroscopy.

IV.A. EXPERIMENTAL

IV.A.1. Synthesis of 3- and 4-vinylpyridazine

IV.A.1.a. Synthesis of 3-vinylpyridazine (Pressure reactor method)

The monomer 3-vinylpyridazine was synthesized using 3-methylpyridazine as the starting heterocyclic material. 3-Methylpyridazine

starting material is a dark brown liquid (FW 94.12, b.p. 214°C, d 1.031). 3-Methylpyridazine (20.5 g, 0.22 mol in 40 mL of H_2O) was hydroxymethylated by mixing it with 37% aqueous formalin (30 g, 0.33 mol) in the presence of a catalytic amount of piperidine (0.7 g). The reaction was carried out in a series 4560 Parr bench top pressure mini-reactor equipped with a series 4840 temperature controller and a mechanical stirrer under a nitrogen pressure of 175 psi. The reaction was allowed to proceed for 6 hours at 150°C with continuous stirring. At the end of the reaction period, the reactor was cooled to room temperature and the nitrogen pressure released. The resulting reaction mixture, a brown liquid, was removed from the reactor. Excess water, formalin and starting material were removed from this mixture, by controlled evaporation in a Kugelrohr distillation apparatus. The material left after this treatment, 3-(β-hydroxyethyl)pyridazine, was a dark brown viscous liquid.

The alcohol obtained by the procedure above was subsequently dehydrated by a base. 3-(β-hydroxyethyl)pyridazine (19.7 g) in a 50 mL round bottom flask with (0.1 g) of 4,4'-methylenebis(2,6-di-t-butyl)phenol as a radical inhibitor, was dehydrated with powdered sodium hydroxide (1.5 g) under reduced pressure (1.0 mm Hg) at 120°C in a Kugelrohr apparatus. This procedure yielded a clear yellow liquid, 3-vinylpyridazine, (4.9 g), 25% yield. This procedure is depicted in Scheme 2.

SCHEME 2

Synthesis of 3-vinylpyridazine

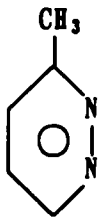

3-METHYLPYRIDAZINE

37 percent formalin
CH_2O
$C_5H_{10}NH$
piperidine
150 psi

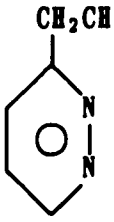

3-(β-HYDROXYETHYL)PYRIDAZINE

NaOH
radical inhibitor
1 mmHg, 120°C

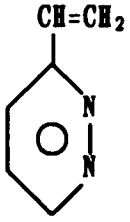

3-VINYLPYRIDAZINE

IV.A.1.b. Synthesis of 4-vinylpyridazine (pressure reactor method)

The method used here was exactly as the one described in the section above. Variations in temperature and pressure were made after the initial unsuccessful attempts. For example 100°C, instead of 150°C and 70 psi instead of 150 psi. Every variation in pressure and/or temperature gave always polymer P4VPd; no alcohol could be isolated.

The synthesis of the 4-vinyl monomer became rather involved. The starting material 4-methylpyridazine is extremely expensive as compared to its counterpart 3-methylpyridazine. In order to have reasonable amounts of 4-methylpyridazine available, it was synthesized in our laboratory. This synthesis and the variations we observed are briefly described below.

IV.A.1.c. Synthesis of 4-methylpyridazine

The synthetic route is depicted in Scheme 3. The method mainly followed a publication by Mizzoni et al.[41] in 1954. The only differences in procedure were the hydrogenation and the yield. In their paper they hydrogenate until the theoretical amount of hydrogen is consumed. They report a final 4-methylpyridazine yield of 91.4%. We hydrogenated until no more hydrogen was consumed and our yield was consistently 40%. The colorless clear liquid obtained in our synthesis was shown by coupled and decoupled ^{13}C NMR to be pure 4-methylpyridazine.

SCHEME 3

Synthesis of 4-methylpyridazine

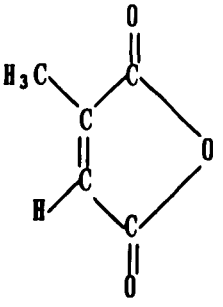

CITRACONIC ANHYDRIDE

+ $H_2N-NH_2 \cdot 2HCl$ (HYDRAZINE DIHYDROCHLORIDE)

reflux in H_2O

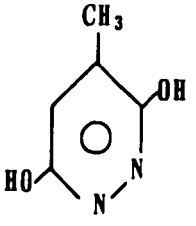

4-METHYL-3,6-PIRIDAZINEDIOL

$POCl_3$

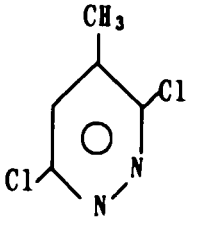

4-METHYL-3,6-DICHLOROPYRIDAZINE

H_2, Pd-CHARCOAL (5%), 60 psi

4-METHYLPYRIDAZINE
yield 40%

IV.A.1.d. Synthesis of 4-(β-hydroxyethyl)pyridazine (method based on molecular formaldehyde solution reagent)

The reaction scheme is shown in Scheme 1 on page 6 of this thesis. A 1000 mL three neck round bottom flask containing a magnetic stirring bar was stoppered with rubber septa. The septa were secured to the necks of the flask by copper wire. Dry nitrogen gas was passed through the flask by needles connected to a nitrogen tank at one end and to an oil bubbler at the other. The flask was flame dried and dry nitrogen gas allowed to flow continuously through the flask in order to ensure the dryness of the vessel. Once cooled, the dry flask with all of its attachments was placed in a dry ice acetone bath (-78°C).

Lithium diisopropylamide (LDA) was prepared by first injecting into the dry cooled flask 200 mL of dry THF and 12.04 g (0.119 mol) of diisopropylamine. Diisopropylamine was previously dried by refluxing over calcium hydride for several days, then distilled under nitrogen, discarding the first fraction and collecting only the middle fraction of the distillate. All transferences to reaction vessels or to measurement vessels throughout this method were done through long stainless steel needles. Fluids were transferred by displacement with dry nitrogen.

To the THF diisopropylamide stirred mixture, 45.6 mL (31.6 g, 0.114 mol) of 2.5 M butyllithium in hexanes were slowly added. Butyllithium was used as received from Aldrich. After addition, the mixture was removed from the dry ice-acetone bath and allowed to reach room temperature. Stirring was maintained at all times. The mixture was kept at room temperature for 30 minutes, then cooled again to

-78°C in a dry ice-acetone bath.

To the cooled mixture 10 g of 4-methylpyridazine (0.104 mol) in 100 mL of dry THF were added. The reaction mixture immediately turned a purple color and started to solidify. After this addition was completed the reaction vessel was removed from the dry ice-acetone bath and allowed to warm up to room temperature. Dry THF (500 mL) was added in order to facilitate stirring. After 30 minutes at room temperature, the solution turned from purple to a dark brown color.

While at room temperature, 200 mL of THF containing 0.130 mol (3.9 g) of anhydrous molecular formaldehyde (prepared as described below (IV.A.1.e)) were added to the stirred reaction mixture. The color of the reaction mixture changed from dark brown to a light yellow as the condensation reaction proceeded.

After addition of the formaldehyde solution, the reaction mixture was stirred for 1 hour, at the end of which water was added to the reaction mixture until LiOH precipitated. The solid LiOH was removed from the resulting mixture by filtration and washed several times with THF. The washings were combined with the initial solution. The alcohol 4-(β-hydroxyethyl)pyridazine was recovered by removal of THF in a rotary evaporator (60°C, 10mm Hg). The yield was 91.9% (12.12 g).

3-(β-hydroxyethyl)pyridazine was obtained by the same method in 45.5% yield. The starting material, 3-methylpyridazine, was distilled under vacuum before use (45°C, 1mm Hg). The distillate was a clear, light-green liquid.

The setup used to generate formaldehyde and solubilize it is shown in Scheme 4 along with the vessel described in the procedure above.

IV.A.1.e. Preparation of anhydrous molecular formaldehyde solutions

The solutions with controlled concentrations of molecular formaldehyde were prepared as follows. The apparatus as shown in Scheme 4, consisted of two round bottom flasks (500 mL three neck and 50 mL one neck) connected through a Drierite-filled glass drying tube. The smaller flask was fitted with a high vacuum stopcock as a nitrogen gas inlet. The larger flask was equipped with a glass tube reaching close to its bottom, a nitrogen gas outlet, a magnetic stirring bar and a high vacuum connection. The entire system could be evacuated. The apparatus was flame dried under vacuum and then flushed with dry nitrogen gas before use. Formaldehyde gas was generated under vacuum by heating a desired quantity of *a*-poly(oxymethylene), *a*-POM, inside the small flask slowly with a flame. The *a*-POM was made as described below and dried overnight under vacuum at room temperature before use. The required amount of dry THF was transferred into the larger flask through a connecting needle under nitrogen. THF was dried by refluxing over calcium hydride for several days then distilling and collecting the middle fraction under nitrogen. The use of *a*-POM and not paraform is critical. Formaldehyde molecules generated from paraform exhibit a great tendency to repolymerize. Paraform is known to contain larger amounts

SCHEME 4

SETUP FOR SOLUBILIZATION OF FORMALDEHYDE

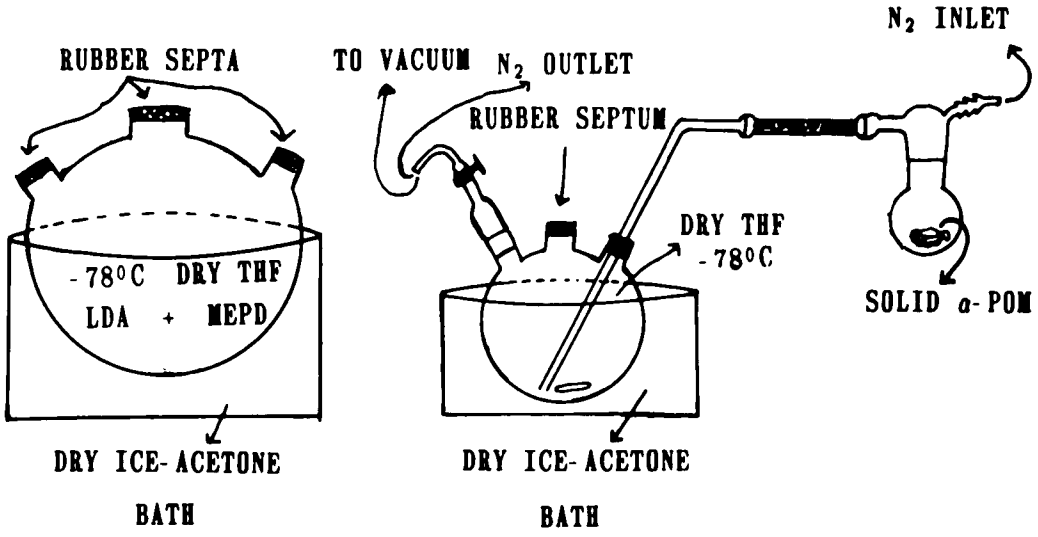

of water than α-POM.[16]

Formaldehyde gas generated by pyrolysis was carried through the Drierite tube under vacuum and condensed into stirred dry THF at -78°C. The solutions thus generated were observed to remain clear at 0°C for several days. ^{1}H NMR spectra of this solutions at 0°C allowed us to quantify the amount of molecular formaldehyde in solution.

IV.A.1.f. Preparation of α-poly(oxymethylene)[16]

α-POM was obtained by KOH polymerization of a methanol free 40% aqueous formaldehyde solution.

An aqueous formaldehyde solution was prepared by refluxing 400 g of paraform in 600 mL of distilled water in a 2000 mL round bottom flask, fitted with a long wide stem condensor. Reflux was maintained until the solution was clear. This required about four days at moderate refluxing rates. Slow reflux is needed since vigorous reflux tends to deposit too much paraform in the stem of the condensor, leading to blockage and build-up of pressure inside the refluxing vessel. This pressure build-up may lead to rupture of the vessel or condensor. At the end of the reflux period, the solution was allowed to cool and was then filtered into a large Erlenmeyer flask. Potassium hydroxide (7.6 g) was then dissolved in the solution, which was allowed to sit for 3 days. After that period of time a large amount of crystals deposited in the bottom of the flask. The crystals were scratched off the flask, recovered by filtration and washed several times with hot distilled water. The yield was 280 g, (70%).

IV.a.1.g. Dehydration of 4-(β-hydroxyethyl)pyridazine

The alcohol obtained by the new method was acid-dehydrated in the presence of a radical inhibitor.[42] A 50 mL round bottom flask containing a small magnetic stirring bar and 12.0 g (0.096 mol) of 4-(β-hydroxyethyl)pyridazine was fitted with a reflux condenser. The alcohol in this setup was mixed with 0.12 g. of fused potassium hydrogen sulfate and 0.12 g of hydroquinone as a radical inhibitor. This mixture was refluxed under stirring for 8 hours at 100°C. At the end of this period the flask was fitted with a microdistillation condenser equipped with a thermometer and a vacuum connection. Distillation of the monomer was carried out at 1.0 mm Hg and a temperature range of 58°C to 75°C for the 4-vinyl monomer, and 34°C to 55°C for the 3-vinyl monomer. The distillate resulting from this procedure proved to be a mixture of starting material plus vinyl monomer by ^{13}C NMR. Redistillation of these mixtures yielded the relatively pure monomers 4-vinylpyridazine (bp 1mm Hg, 62°C to 64°C, 47% yield); and 3-vinylpyridazine (bp 1mm, 47°C-51°C, 40% yield).

Base dehydration was attempted for the new alcohols as described in III.A.1.a. Yields of the monomer were very poor and a large amount of polymer was left in the dehydration vessel.

From the acid dehydration, a brown solid material also remained in the round bottom flask containing the initial alcohol. This material was shown by ^{13}C NMR to be the vinyl polymer.

IV.A.2. Polymerization

Solution and bulk polymerization of the two new monomers was conducted by means of radical and anionic initiation. Adventitious thermal polymerization of the nascent macromolecule occurred in situ during dehydration of the alcohols. Large amounts of the two polymers, were obtained through this route.

IV.A.2.a. Anionic polymerization in toluene.

Phenyl magnesium bromide was used as the initiator for anionic polymerization of 3-vinylpyridazine. Toluene (40 mL, previously dried by CaH_2, then redistilled) was stirred in a 100 mL three neck round bottom flask stoppered with rubber septa. One mL of 3.0 M PhMgBr (in ether) was added to the toluene through a septum. All manipulations were performed under nitrogen. The monomer 3-vinylpyridazine (4.9 g in 10 mL of toluene) was added dropwise. The molar ratio of monomer to the catalyst was ca. 15:1. Polymerization was carried out for two hours in a water bath at room temperature. The solution became dark brown and the viscosity increased progressively. At the end of the polymerization reaction, 50 mL of water were added and stirring continued to allow the dissolution of the polymer and some monomer into the water layer. After separation of the water layer from the toluene layer, the water was removed in a rotary evaporator. A brown crude polymer was obtained. The crude polymer was first washed with toluene and then dried under vacuum at 120°C for 0.5 hours. The polymer was obtained as a brown colored material. The yield was 15%.

IV.A.2.b. Anionic polymerization in THF.

Polymerization of 4-vinylpyridazine and 3-vinylpyridazine were also carried out in dry THF solution by PhMgBr initiation.[43a] Two 20 x 150 mm pyrex glass tubes were stoppered with rubber septa wrapped in Teflon tape. The tubes were flame dried and flushed with dry nitrogen to minimize moisture. Dry THF, 30 mL, were transferred into each tube through a needle under a nitrogen atmosphere. The rest of the manipulations were conducted in a dry box.

To each of the tubes, 0.5 g of 4-vinylpyridazine and 3-vinylpyridazine were added respectively. The vinyl monomers were kept over molecular sieves and under nitrogen before use. To each of the tubes containing the monomer solutions, 5 μL of 3 M PhMgBr were added. A white cloudy precipitate formed immediately and no further reaction occurred in both reaction mixtures. This precipitate was removed from solution by filtration and washed several times with THF to remove unreacted monomer. In each case, a very small amount of highly hygroscopic polymer was obtained. Both polymers turned to a dark brown color and gummy appearance upon exposure to air moisture. They were dried in a vacuum oven under continuous evacuation at 60°C overnight to remove solvent and water. Small amounts of polymer were recovered after this step, brown brittle hygroscopic material in the case of P3VPd and pink powdery material in the case of P4VPd. Elemental analysis of these polymers indicated that both contained a large amount of oxygen contaminants, perhaps originating from water and $Mg(OH)_2$.

IV.A.2.c. Anionic polymerization in bulk

The two monomers were polymerized in bulk by PhMgBr. All manipulations were carried out in a dry box. To two small (10 mL) round bottom flasks stoppered with rubber septa, 1.5 g of 4-vinylpyridazine and 3-vinylpyridazine were added respectively followed by 20 μL of 3.0 M PhMgBr (in ether) to each monomer solution. Polymerization occurred immediately in both cases. For the case of 4-vinylpyridazine solid formed immediately. After a few minutes, both flasks were opened and their contents poured in separate beakers containing THF. The polymers precipitated in the THF and were recovered by filtration followed by several washings with THF and dried under vacuum. Both polymers were obtained in low yield (ca. 6%) with P4VPd in better yield than P3VPd. Solid state ^{13}C NMR indicated that these materials obtained from this type of polymerization were indeed the polymers sought.

IV.A.2.d. Thermal polymerization

As indicated before, base or acid dehydration yielded the monomer plus a brown solid. This brown solid proved to be in every case the polymer of the respective vinyl monomer. These polymers were isolated by dissolving in methanol and reprecipitating in ether, and then by heating the collected solid at 180°C under high vacuum in a Kugelrohr apparatus.

Base dehydration and the pressure reactor method produced also a fraction of polymers of apparent high molecular weight insoluble in

methanol. They were soluble only in acidified water. These polymers were purified in some cases in a Soxhlet apparatus by refluxing methanol for several days. ^{13}C solid state NMR of the polymers thus obtained, proved them to be the desired polymers.

IV.A.2.e. Radical polymerization in bulk

Bulk polymerization of the two new monomers was successfully initiated by hydrogen peroxide as the thermal initiator. The polymerization was conducted as follows:

1.0 mL of freshly distilled monomer was placed in a 1 x 10 pyrex tube. A small magnetic stirrer was placed inside the tube and predetermined amounts, in the range of μL, of hydrogen peroxide were added by means of a microsyringe. Monomer/initiator ratios of 120-270 were typically used. The polymerization tube was placed in a thermostatted oil bath and polymerization was allowed to proceed overnight at a temperature of 105°C with stirring. When the clear yellowish monomer-initiator mixture was placed in the hot oil bath, the color of the mixture turned to a deep purple color within the first 5 to 10 minutes. The viscosity of the stirred mixture increased slowly with time. At the end of the polymerization period the reaction mixture solidified. The polymer was recovered by dissolution in methanol and reprecipitation in ether. This procedure was repeated until the methanol-ether solution above the precipitated polymer was clear. The polymer was then recovered by filtration, washed with THF and dried under vacuum at 75°C for several days. The resulting

materials were a dark brown brittle solid in the case of poly(3-vinylpyridazine), and a dark purple powder in the case of poly(4-vinylpyridazine). The yields of polymers were in the range of 12 to 25%, consistently lower for P3VPd. ^{13}C NMR along with elemental analysis were used to establish the identity of the polymer products.

IV.A.2.f. Radical polymerization in solution

4-Vinylpyridazine was polymerized by radical initiation in water and in 1.0 N H_2SO_4 solutions. A typical experiment was conducted as follows: predetermined amounts of monomer and hydrogen peroxide initiator were mixed with a small volume of the desired solvent (monomer/solvent ratio ca. 1/10) in a 25 mL round bottom flask containing a magnetic stirrer. The flask was then placed in a thermostatted oil bath (95°C) and allowed to reflux with stirring overnight. In the case for non-acidic water the polymerization mixture changed color from clear yellow to purple. As the polymerization proceeded, a purplish precipitate was observed. At the end of the polymerization, the polymer was recovered by filtration, washed with THF, dried and studied by ^{13}C NMR. The polymer was obtained in very low yields, i.e. 7-9%, and was rather hygroscopic. For the H_2SO_4 aqueous medium, the polymerization proceeded without polymer precipitation. The color of the solution turned from its initial light purple to intensely purple. The polymer was recovered by evaporation of water, washing thoroughly with THF and drying in a vacuum oven at 70°C for several days. The yield was again very low.

IV.A.3. Polymer Characterization

IV.A.3.a. Nuclear magnetic resonance (NMR)

^{1}H and ^{13}C NMR solution spectra were obtained in a IBM WP 200 FT-NMR spectrometer. A 5 mm probe was used to obtain the spectra of the small molecules and a 10 mm probe was used to obtain the solution spectra of the polymers. ^{1}H NMR was obtained at 200 MHz, sample concentrations ranged from 2 to 5%, and relaxation delay between 3 and 5 seconds. The solvents used were methanol-d_4 with tetramethylsilane (TMS) as an internal reference, D_2O with 3-(trimethylsilyl) propionic acid, sodium salt (TSP) as an internal reference.

^{13}C NMR spectra were obtained at 50.3 MHz at concentrations between 5 and 10% with the same solvents as indicated above. In these experiments a large relaxation delay was allowed (9 to 15 seconds) in order to obtain good signal intensity for the quaternary carbons.

For the polymers, high concentration 15-20% and long relaxation delay times,15-20 seconds were required even when a 10 mm probe was used. The solvent used was D_2O with TSP as an internal reference and a trace amount of D_2SO_4 to improve the solubility of the polymers.

Experimental details for ^{13}C solid state CP/MAS NMR have been described in section II.A.5.

IV.A.3.b. Viscosity measurements

Viscosity measurements of the P3VPd and the P4VPd dilute methanol solutions were conducted in a thermostatted water bath 21± 0.1°C with an Ubelohde viscometer. The concentration range for each case was

from 0.2 to 1 gm/dl. The samples were allowed to equilibrate thermally in the water bath for 30 minutes before measurements. The viscosity measurements conducted in the Ubelohde dilution viscometer showed relatively short efflux times (i.e. 90-100 seconds). The differences in the efflux times between the most concentrated and the least concentrated solutions was about 2 seconds.

In view of this disadvantage further measurements were conducted in a Cannon-Manning semi-micro calibrated viscometer designed for extra low charge. The calibration constant for this viscometer was 0.003765 centistokes/second at 24°C. The measurements were conducted in a thermostated water bath at 24°C with DMF as the solvent. The viscometer was thoroughly cleaned between measurements. The size of each sample was 0.2 mL and efflux times were of the order of 250-280 seconds with significant difference in efflux times between samples of different concentrations.

IV.A.3.c. Electron Spin Resonance (ESR)

ESR spectra for poly(vinylpyridazines) were obtained following the procedure given for P2VP (see section II.A.3). The area under the curve for the signal A_s was estimated based on the relationship.

$$A_s = h(\Delta H_{s\,pl})^2$$

i.e. the area is proportional to the product of height of the first derivative curve(h), with the square of the linewidth $\Delta H_{s\,pl}$.

IV.A.3.d. Direct current conductivity

The measurements were carried out using two methods.

Method 1, Direct measurement: The polymer sample was compressed in an IR press between the two dies of an IR pellet maker using a polypropylene ring guide. The direct current electrical resistance was measured at room temperature using a Keithley model 160 digital multimeter. The direct current conductivity of the sample was calculated from the measured resistance, the thickness of the pellet and the contact area.

Method 2, Kirchhoff's Law method: The schematic for measurement of resistance by Kirchhoff's law is shown below.

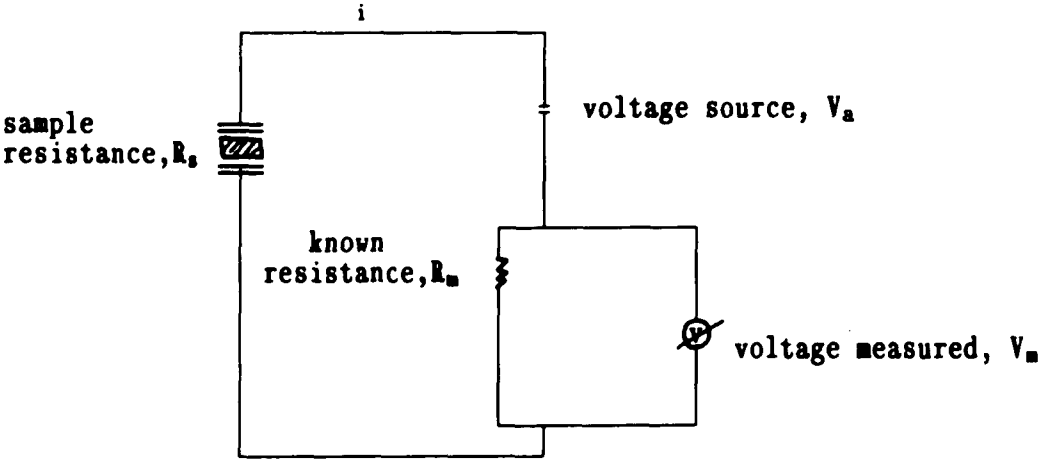

The sample was compressed between two metal dies. Pressure was supplied to the polymer-iodine sample until a pellet was formed. The pressure was released before measurements. R_m is set by a variable resistor adjusted to a resistance at the same level of that of the

sample measured directly. V_a is provided by a standard voltage supply. V_m, the potential drop across the variable resistor, is measured by a multimeter.

An equation correlating V_a with V_m can be derived from Kirchhoff's law:[43b]

$$V_a = \frac{R_s + R_m}{R_m} V_m$$

By changing the applied voltage V_a, a series of V_m values can be obtained. From the slope of the plot of V_a vs. V_m and the known value for R_m, the resistance R_s and conductivity σ_s of the sample can be calculated.

$$\sigma_s = \frac{L}{R_s \cdot A} = \frac{L}{[(\text{slope})R_m - R_m] \cdot A}$$

L and A are the thickness and the area of the pellet respectively. The voltage supplied, V_a was always in the range leading to a constant slope in the plot, indicating no electrochemical reaction taking place during measurement.

IV.A.3.e. Doping with iodine

Doping of the polymers (P3VPd and P4VPd) with iodine for conductivity measurements was carried out at 60°C under vacuum. Polymer iodine samples were mixed in the desired ratios (1:1.5, 1:3,

1:7, 1:10 polymer:iodine) in glass ampules. The ampules were evacuated with a mechanical vacuum pump for 20 minutes, sealed under vacuum, and then placed in an oven at 60°C for 24 hours. At the end of this period the ampules were opened and the contents stored in screw cap vials until the time of the measurements. The material after heat treatment was a lustrous granular material with metallic appearance.

ESR measurements and conductivity measurements on these doped samples as well as on the native samples were conducted.

IV.A.3.f. Iodine uptake

Iodine uptake by the polymers was measured in order to determine the ratio by which the polymer combines with iodine in the charge transfer complex. This measurement was made by exposing a weighed amount of polymer powder to molecular iodine vapors and determining the equilibrium weight gain by the polymer sample. Weighed samples of polymer were placed in glass vials of known weight. The weight of the vials plus the polymer samples was recorded. The samples were placed in a glass vacuum dessicator, with its bottom lined with iodine crystals. The dessicator was covered and evacuated for 20 minutes with the aid of a high vacuum pump at room temperature. At the end of this period, the vacuum valve of the dessicator was turned off and the evacuated dessicator placed in a thermostated oven at 60°C for 24 hours. After this treatment the dessicator was removed from the oven. The vials containing sample and iodine were removed and weighed

accurately. After weighing, the samples containing iodine were placed in another empty glass vacuum dessicator. Vacuum was continuously applied to the sample in order to remove uncomplexed iodine. The weight of the sample plus iodine was recorded periodically until a constant value was arrived at. At this point the weight gain of the sample was determined and the ratio by which molecular iodine combines with the polymer pyridazine rings, was calculated.

IV.A.3.g. Thermal analysis

Differential Scanning Calorimetry, DSC and Thermal Gravimetric Analysis, TGA thermograms of P3VPd and P4VPd were obtained with a Du Pont 990 thermal analyzer with a 910 DSC module and a 950 TGA module. DSC and TGA were conducted at a nitrogen flow rate of 10 ml/min and a 10 ^{o}C/min heating rate. The DSC thermogram for each sample was recorded as the sample was heated to a predetermined temperature (i.e. 200^{o}C). Then the sample was cooled slowly to room temperature and its DSC thermogram recorded again up to 200^{o}C.

IV.B. RESULTS AND DISCUSSION

IV.B.1. Synthesis of monomers and alcohol intermediates

IV.B.1.a. High pressure method for monomer synthesis

The high pressure method was used successfully for the first synthesis of 3-vinyl pyridazine. For the synthesis of 4-vinyl-pyridazine only polymer was produced by this method.

The monomer 3-vinylpyridazine, a clear yellowish oily liquid, was obtained in 25% yield. The monomer, like its parent compound, is a high boiling liquid. It boils at 120°C at 1.0 mm Hg. The 3-vinylpyridazine monomer was found to be soluble in chloroform, methylene chloride, toluene and water. It is insoluble in cyclohexane and hexanes, forming two phases. In ethyl ether it precipitates as a white powder which liquefies upon removal of the ether. The clear yellow oily liquid 3-vinylpyridazine was observed to turn brown upon storage, even when stored over molecular sieves and at low temperatures, (i.e. -17°C to 0°C). The general procedure used to dry the monomer before polymerization was to dilute it in methylene chloride and store the solution over anhydrous magnesium sulfate. The monomer solution was filtered to remove magnesium sulfate before use. Methylene chloride was then removed by evaporation.

In Figure 8, a ^{13}C NMR spectrum of 3-vinylpyridazine, spectrum B, is presented together with that of its parent compound 3-methyl-pyridazine, spectrum A. The 3-vinylpyridazine spectrum is consistent

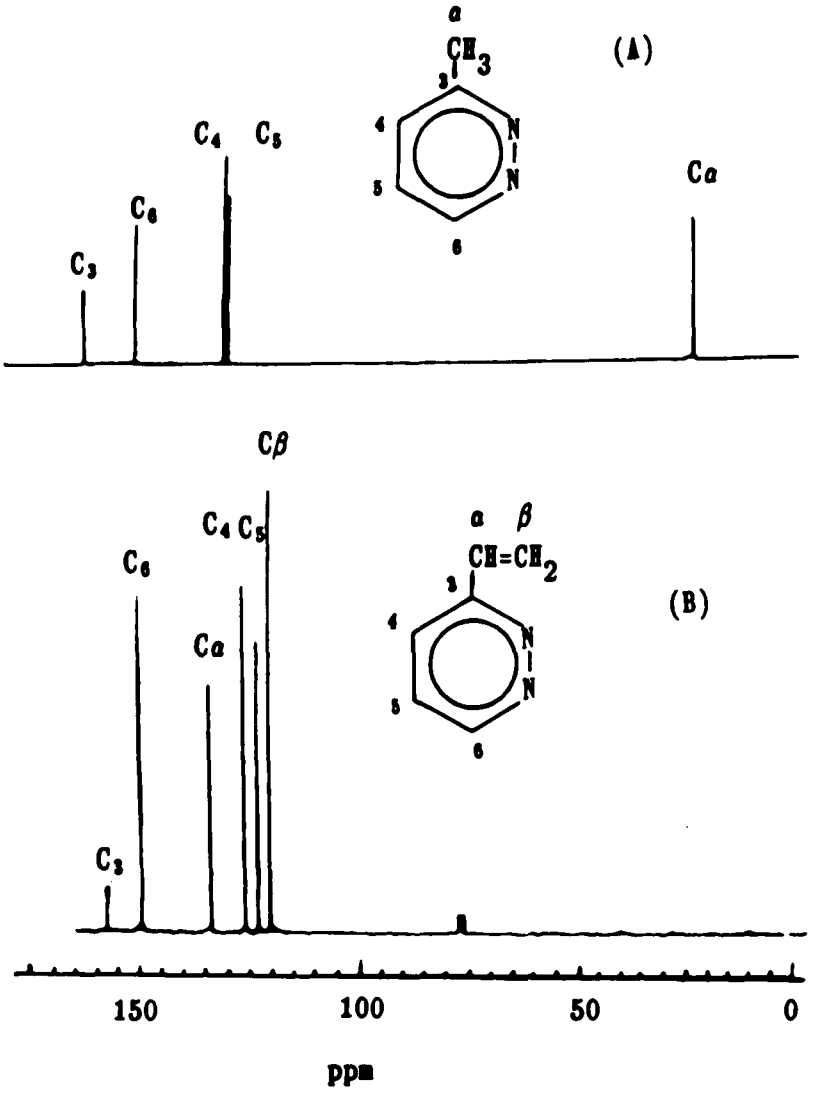

Figure 8. Solution ^{13}C NMR spectra of 3-methylpyridazine A, and 3-vinylpyridazine B.

with the absorptions of analogous vinyl monomers. The absorptions of the new monomer were assigned by comparison a with those of methylpyridazine as well as by proton coupled ^{13}C NMR.

Figure 8 clearly substantiates the identity of the 3-vinylpyridazine monomer and its purity. The intensity of the peak absorption for carbon 3, a quaternary carbon of the pyridazine, is much weaker compared to other absorptions, perhaps due to its lack of NOE enhancement and longer relaxation times.

Attempts to synthesize 4-vinylpyridazine by the high pressure method were unsuccessful. The starting material 4-methylpyridazine was synthesized and characterized by ^{13}C NMR. Figure 9 shows ^{13}C NMR spectra of 4-methylpyridazine; spectrum A, proton coupled, spectrum B, decoupled. The decoupled spectrum indicates the high purity of the compound and the coupled spectrum verifies the chemical shift assignments. Values for the J_{c-h} coupling constants are indicated.

This pure material was used in the pressure reactor method. The resulting reaction mixture after hydroxymethylation in the pressure reactor was a brown liquid plus a solid. This was in contrast to the hydroxymethylation of 3-methylpyridazine system in which after the same reaction no solid was present. The liquid and solid resulting from the reaction mixture were separated. The solid was washed with methanol, then with water and oven dried at 60°C under vacuum for 24 hours. This solid was apparently a high molecular weight polymer insoluble in methanol, THF, water and ethanol. It was soluble in water containing trace amounts of acid. This material was shown by

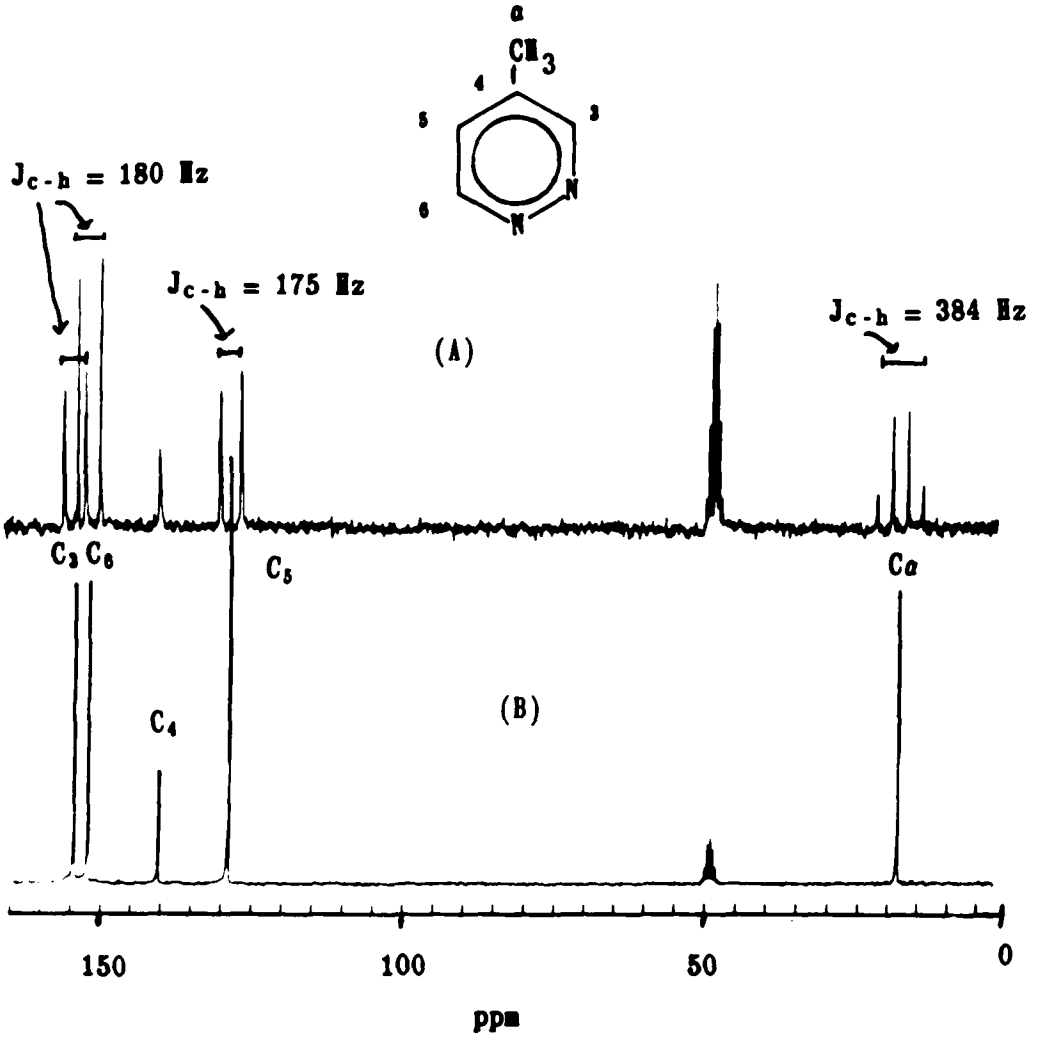

Figure 9. ^{13}C NMR spectrum of 4-methylpyridazine in methanol-d_4.

A, proton coupled

B, proton decoupled

^{13}C solid NMR to be the polymer P4VPd. The liquid resulting from the hydroxymethylation reaction was treated in a rotary evaporator to remove water. The resulting dark brown sticky material was soluble in methanol. It was shown by ^{13}C NMR in solution to be the polymer P4VPd. However, its high solubility in several solvents (i.e. water, methanol, etc.) and sticky nature indicate a low molecular weight fraction.

Figure 10 shows a solid state ^{13}C NMR spectrum of the apparently high molecular weight fraction obtained from this procedure. Broad absorptions are observed for all the aromatic carbons as well as for the α and β aliphatic carbons. The absorption peak due to C_4 cannot be observed unless a very long relaxation delay is allowed and a large number of FID's are collected. (i.e. RD > 25 seconds and NS > 1000 scans). The pyridazine ring is attached through C_4 to the vinyl backbone of the macromolecular chain. Due to the low mobility of the chain, the relaxation time of this carbon becomes much longer compared to that of the small molecule. The same effect is observed in solution. Figure 11 shows the solution ^{13}C NMR spectrum of the apparently low molecular weight P4VPd obtained from this method. The relaxation delay was 26 seconds and more than 2000 transients were collected. Again, the peak assigned as C_4, was not observed when relaxation delay times shorter than 20 sec were used between pulses.

IV.B.1.b. 3- and 4-(β-hydroxyethyl) pyridazines, method based on molecular formaldehyde solution reagent

The two new alcohols were obtained in good yield following the

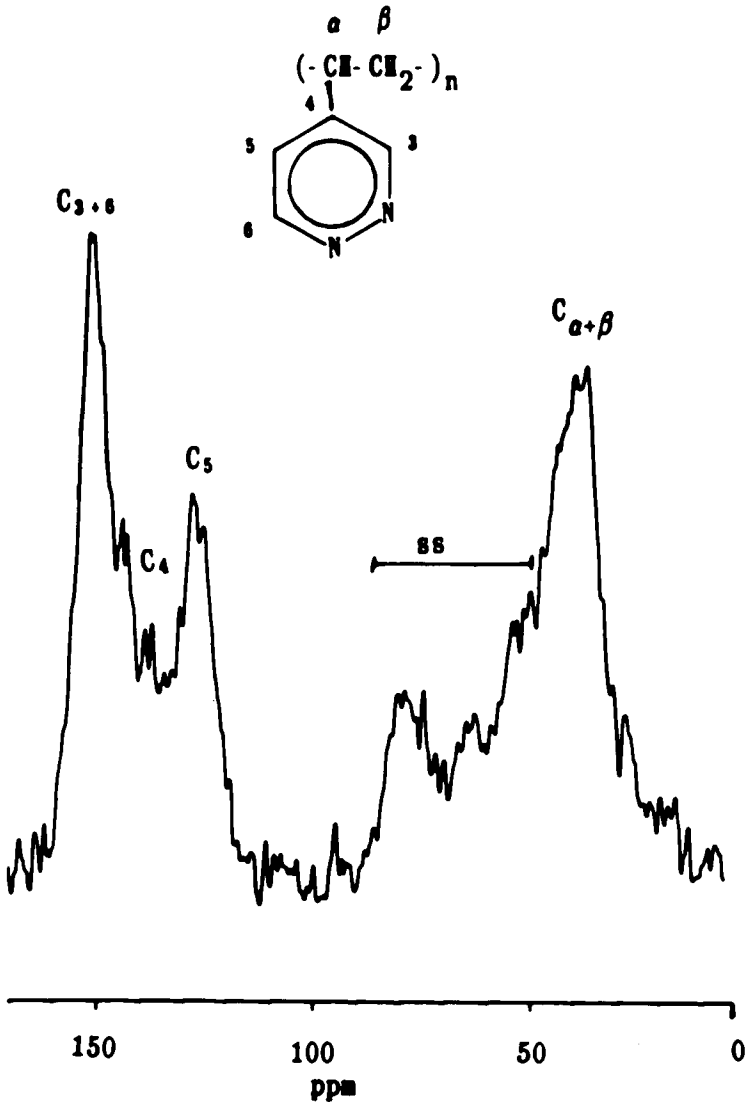

Figure 10. Solid state ^{13}C CP/MAS NMR spectrum of poly(4-vinylpyridazine).
Spinning rate 4.0 KHz.

ss = Spinning Sidebands

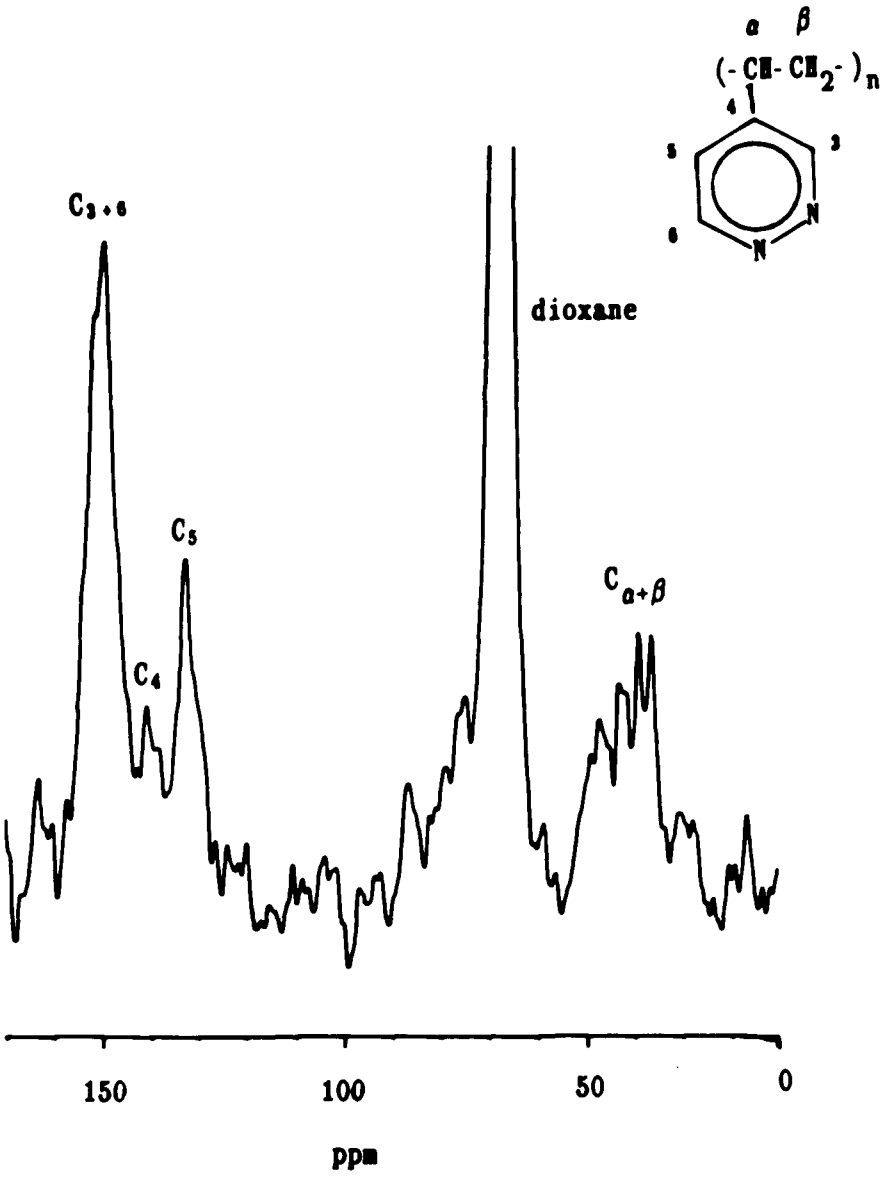

Figure 11. Solution ^{13}C NMR spectrum of poly(4-vinylpyridazine) from pressure reactor method.
Solvent is D_2O, reference dioxane.

reaction scheme shown in Scheme 1, (section II.A.). The resulting alcohol in both cases was a dark brown non-viscous liquid with a reddish to purple hue. These alcohols solidified at -17°C. Attempt to distill them to improve their purity resulted in thermal polymerization of the vinyl monomers produced by the thermal dehydration of the alcohol. The temperatures required to distill these alcohols were rather high (160°C at 1.0 mm Hg in the Kugelrohr apparatus). At this high temperature other side reactions could also take place. Dehydration is one of the reactions known to occur for this type of alcohols at high temperatures.[44] [45] In our case, this resulted in the generation of large amounts of polymer, P3VPd or P4VPd, inside the distilling flask. Another possible type of side reaction is dehydroxymethylation [46] either at high temperature or in basic media. This process is favored when the hydroxy proton is close enough to the nitrogen atoms in the ring to form a new six member ring through hydrogen bonding. The loss of the hydroxymethyl group then occurs as shown below.[60].

SCHEME 5

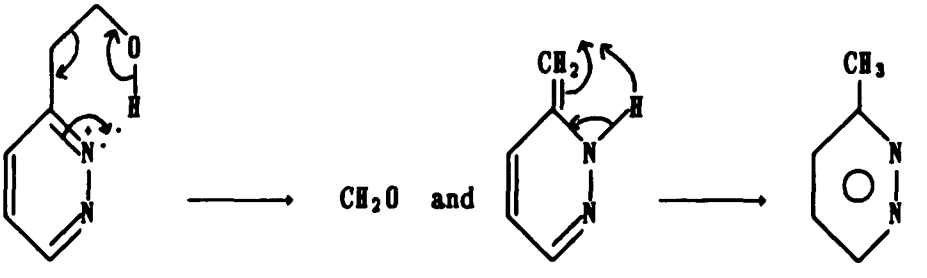

This results in the loss of the alcohol and its conversion back to the starting material. This process was observed by Ohsawa [15] in

secondary and tertiary substituted 2-pyridazinylethanols. ^{13}C NMR of the newly synthesized alcohols show evidence of this phenomenon. Figure 12 shows a ^{13}C NMR spectrum of 3-(β-hydroxyethyl)pyridazine. The peak assignments were based on coupled and decoupled ^{13}C NMR spectra as well as on the comparison of NMR data from 2-hydroxyethyl alcohols attached to other oxygen, nitrogen and sulfur heterocyclic rings [47]. The spectrum clearly shows the presence of pure alcohol together with the starting molecule, 3-methylpyridazine. In this spectrum one can observe a small absorption at 63.4 ppm downfield from the C_β absorption of the alcohol. We assigned this peak to the absorption of the C_β with its hydroxy groups involved in hydrogen bond with the N-2 in the pyridazine ring. Spectra from 3-(β-hydroxyethyl)-pyridazine samples with lower content of starting material have also been obtained. Figure 14 shows a ^{13}C NMR spectrum of 3-(β-hydroxy-ethyl)pyridazine in methanol-d_1. Compared to the spectrum in Figure 12, this sample contains a very low concentration of the starting material. The alcohol in such a pure state could only be obtained through redistillation at the risk of losing a major portion to thermal polymerization. The spectrum in Figure 12 serves as an indication for the cyclization of the 3-alcohol and its effect in dehydroxymethylation as evidenced by the presence of starting compound, 3-methylpyridazine.

Figure 13 shows a proton coupled ^{13}C NMR spectrum of 3-(β-hydroxyethyl)pyridazine in the presence of 3-methylpyridazine. The peaks corresponding to the alcohol are marked. In the aromatic

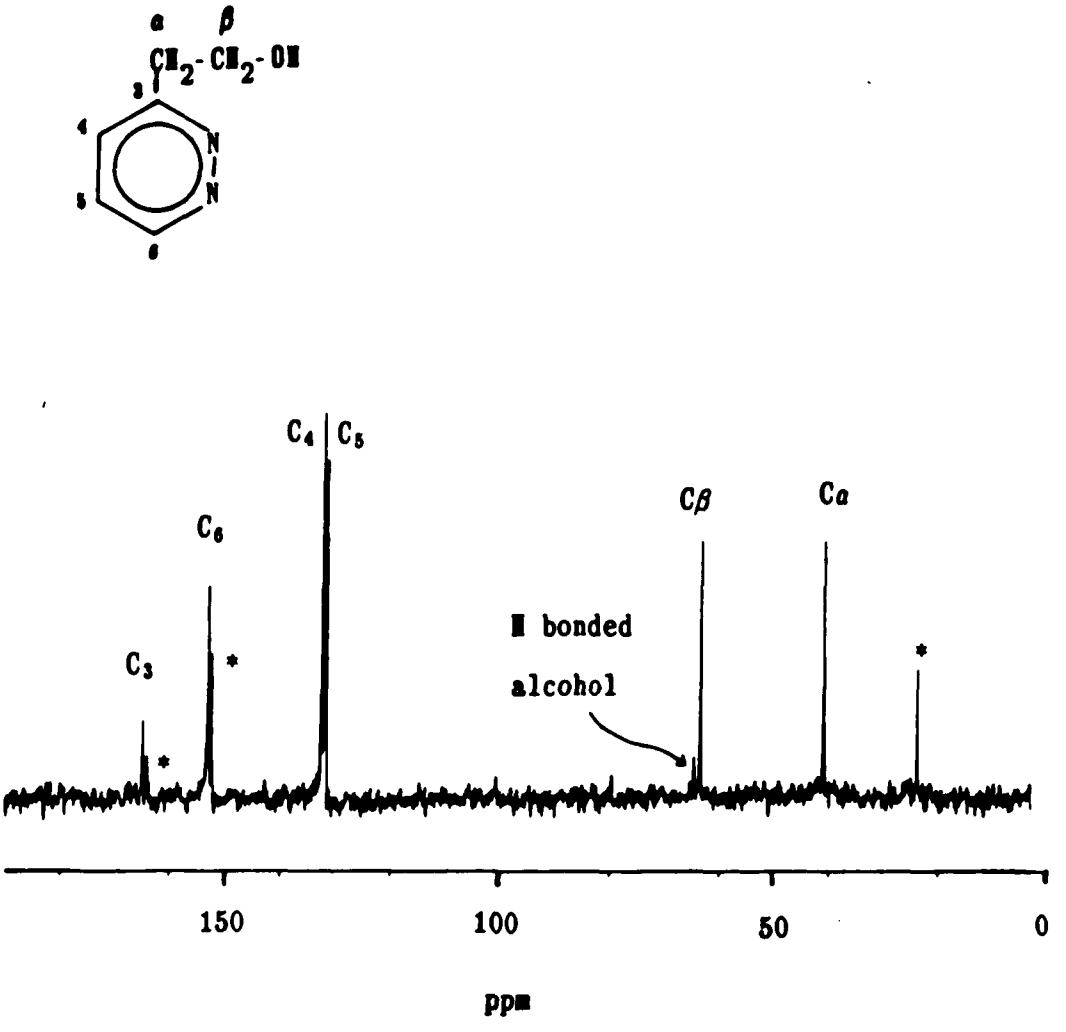

Figure 12. ^{13}C NMR of 3-(β-hydroxyethyl)pyridazine.
Solvent is D_2O, reference TSP.
• Absorptions due to starting material, 3-methylpyridazine.

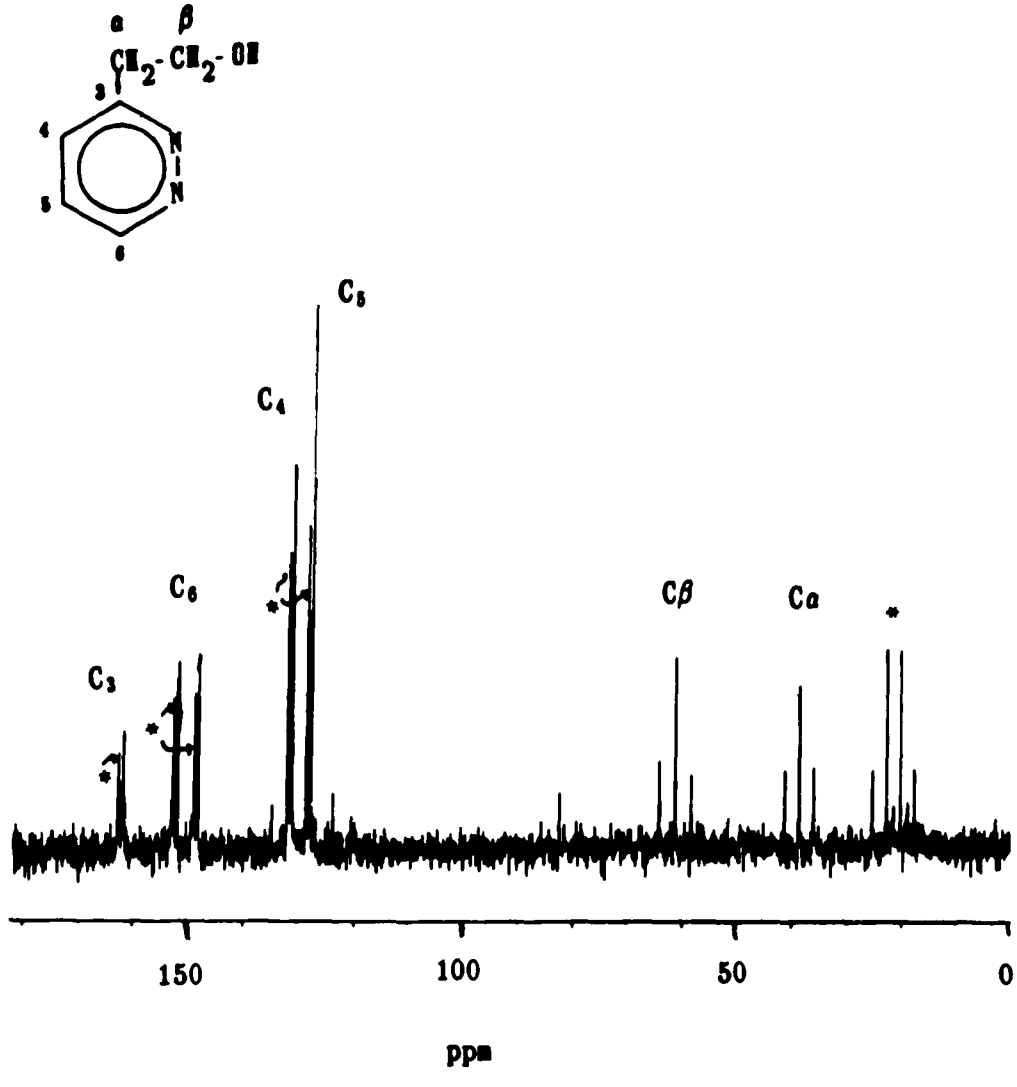

Figure 13. Proton coupled ^{13}C NMR spectrum of 3-(β-hydroxyethyl) pyridazine.
Solvent is D_2O, reference TSP not shown.
* Absorptions due to starting material, 3-methyl-pyridazine.

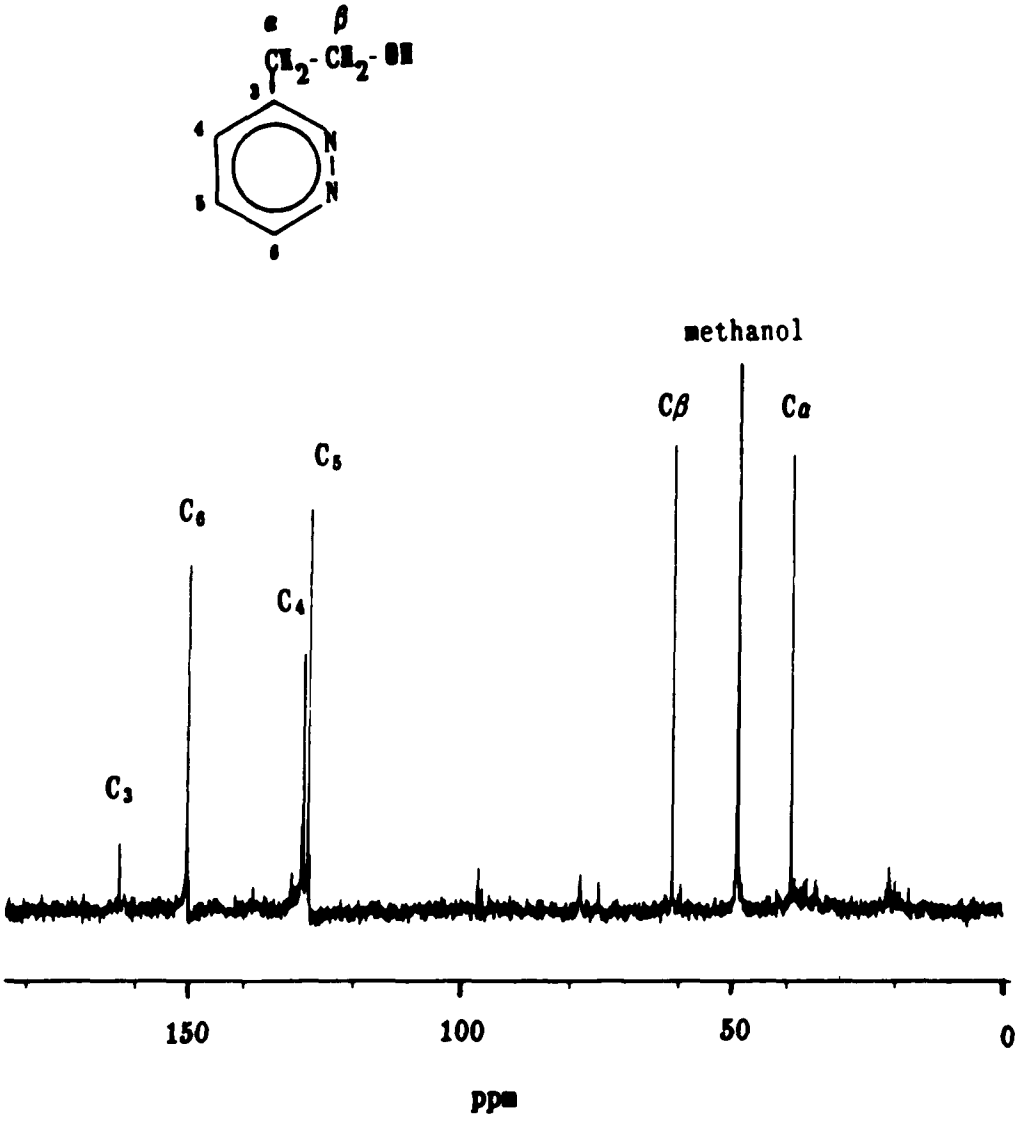

Figure 14. Proton decoupled ^{13}C NMR spectrum of 3-(β-hydroxyethyl)pyridazine. Solvent is methanol-d_1, reference TMS.

region, C_3 absorption for the alcohol appears at 164.6 ppm and C_3 of the starting material at 161.2 ppm. The rest of the peaks show the expected splitting by the attached protons. Table 2 lists the absorption peaks as well as the J_{c-h} coupling constants for the alcohol.

Since this is the first synthesis and isolation of this molecule, characterization by ^1H NMR is also important. Figure 15 shows the ^1H NMR spectrum of 3-(β-hydroxyethyl)pyridazine. The assignments were made by a comparison with related alcohols, mainly 2-(β-hydroxyethyl)-pyridine [47]. Beside the absorption at 2.7 ppm corresponding to the methyl group of 3-methylpyridazine, very few other impurities are observed. Table 3 lists chemical shifts plus J_{h-h} couplings from this spectrum.

Figure 16 shows a proton decoupled ^{13}C NMR spectrum of 4-(β-hydroxyethyl)pyridazine; Figure 17 a proton coupled ^{13}C NMR spectrum. The carbon spectra indicate that this alcohol was obtained in high purity. A very small amount of starting material mixed with this alcohol was evidenced by the low intensity absorption at 19 ppm. Cyclization by hydrogen bond formation occurs less readily for this alcohol as evidenced by the very low intensity of the absortion downfield from the alcohol C_β at 61.7 ppm (Figure 16). Figure 17 shows the expected splitting for each of the alcohol carbons. Table 2 lists the chemical shifts plus the J_{c-h} coupling constants obtained from these spectra for the newly synthesized alcohol. Figure 18 shows a ^1H NMR spectrum of 4-(β-hydroxyethyl)pyridazine. The only

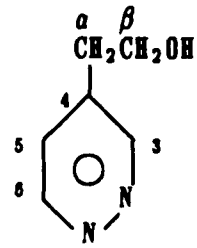

4-(β-hydroxyethyl)pyridazine
1

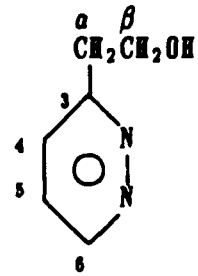

3-(β-hydroxyethyl)pyridazine
2

TABLE 2

^{13}C NMR chemical shifts and J_{C-h} coupling constants for 4-(β-hydroxyethyl)pyridazine, 1, and 3-(β-hydroxyethyl)pyridazine, 2.

Compound	C_3	C_4	C_5	C_6	C_α	C_β	conditions
1 (ppm)	153.3	141.5	128.1	151.2	35.6	60.9	d_4,MeOH
J_{C-h}(Hz)	111.3	0	167.8	112.9	260.9	285.3	r.t.,TMS
2 (ppm)	164.6	132.0	131.4	152.6	40.6	63.2	D_2O
H_{C-h}(Hz)	0	169.3	172.4	184.6	256.3	289.9	r.t.,TSP

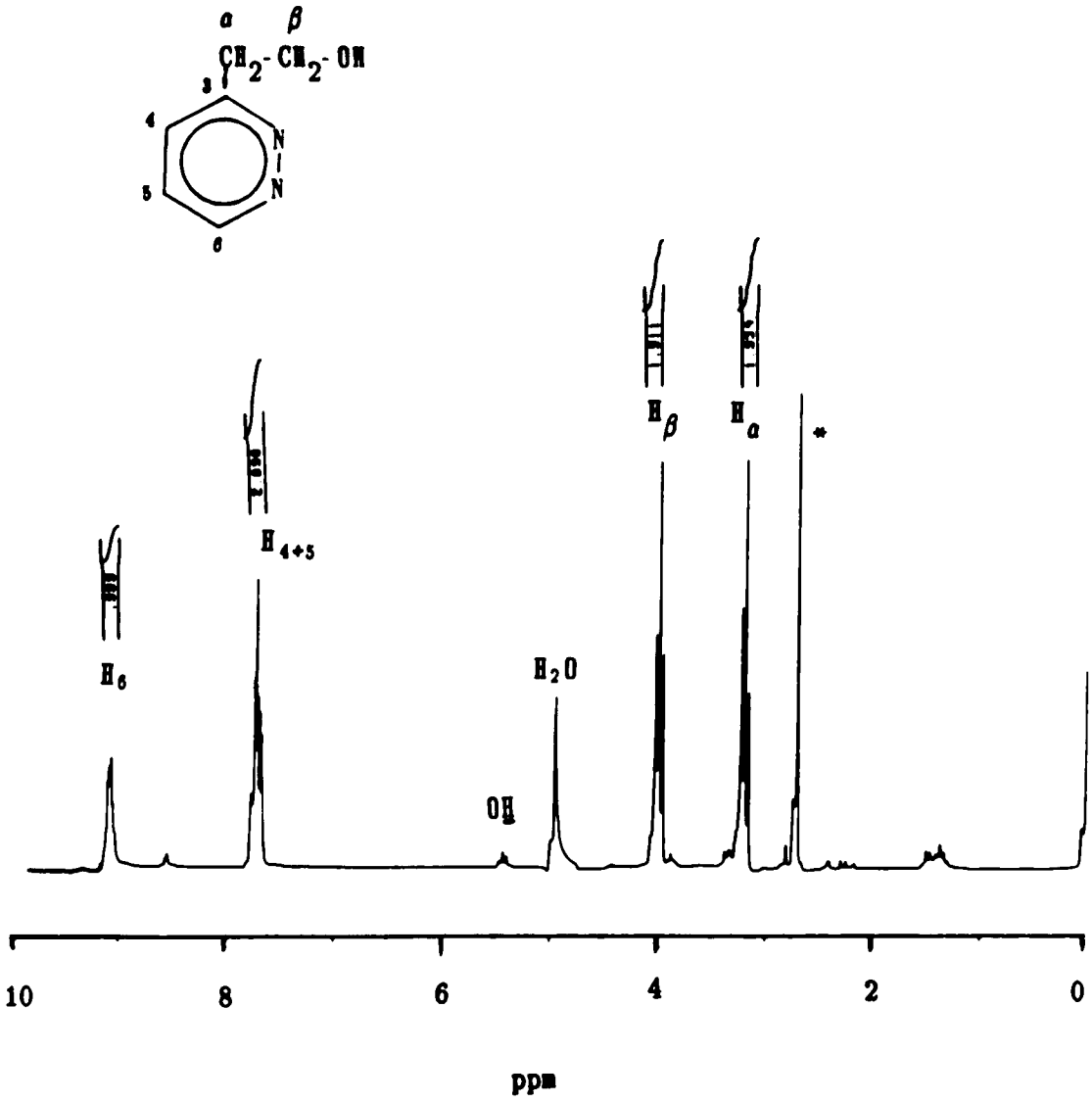

Figure 15. ^{1}H NMR spectrum of 3-(β-hydroxyethyl)pyridazine. Solvent is D_2O, reference TSP.

* Absorptions due to starting material, 3-methylpyridazine.

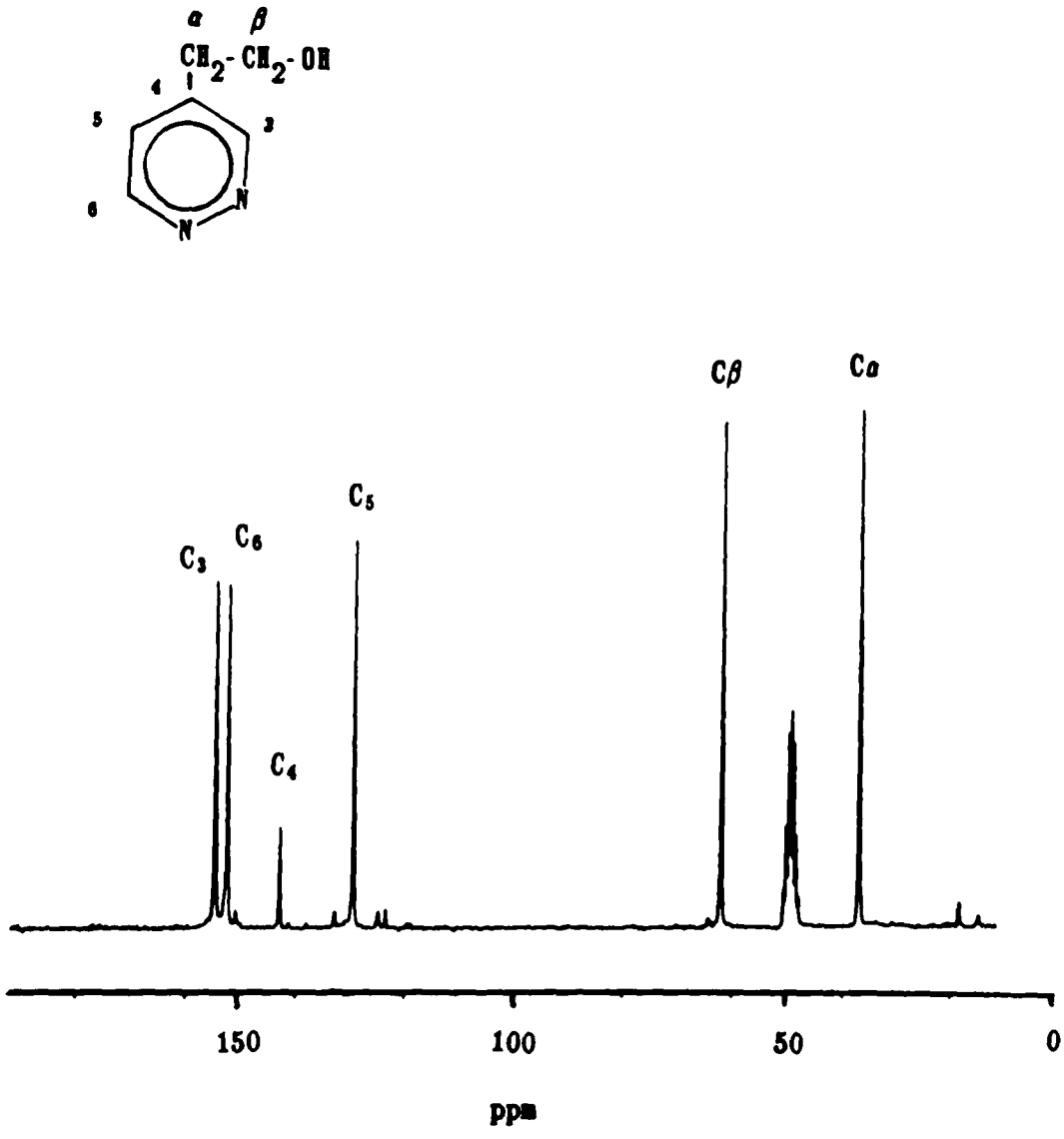

Figure 16. ^{13}C NMR spectrum of 4-(β-hydroxyethyl)pyridazine
Solvent is d_4-methanol, reference TMS

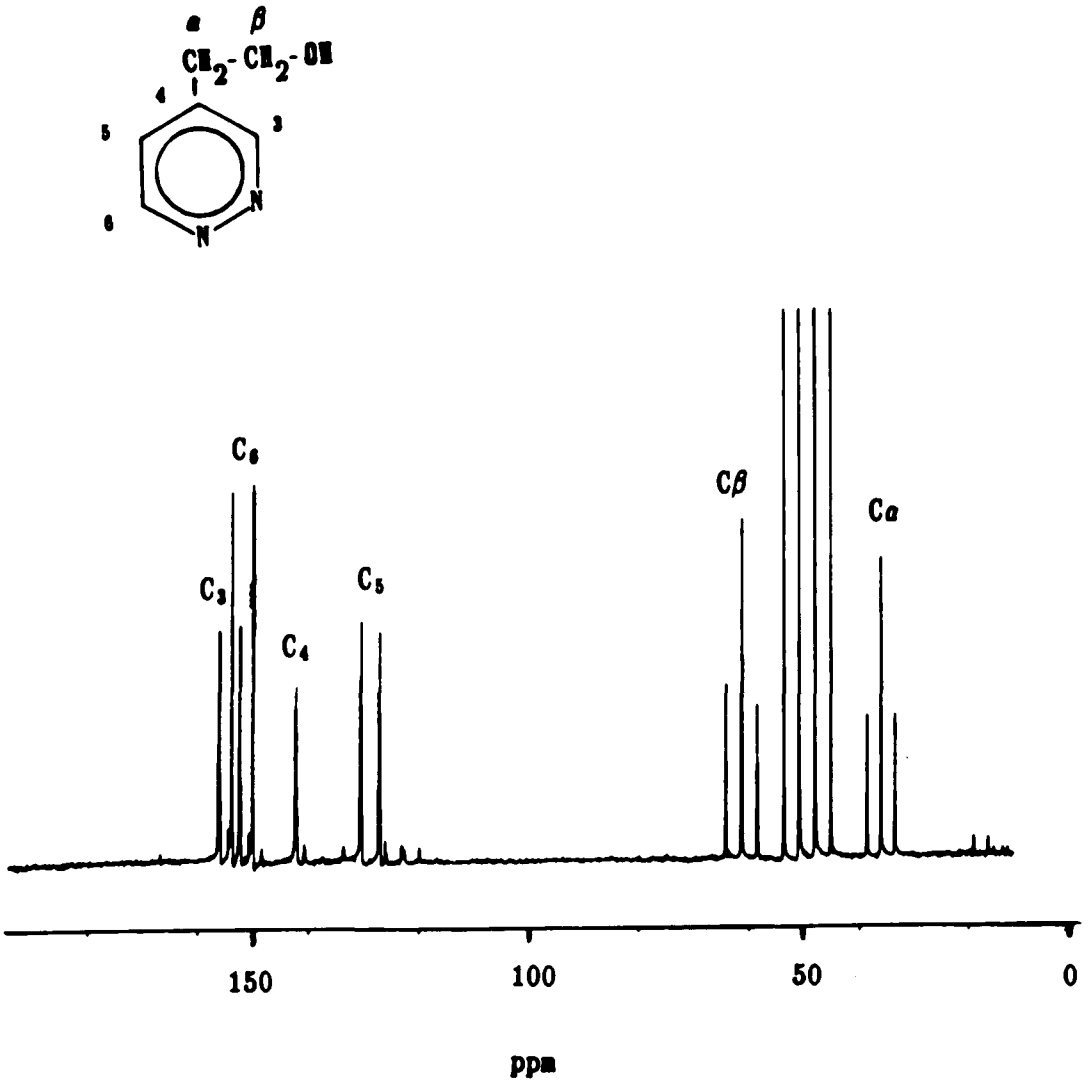

Figure 17. Proton coupled ^{13}C NMR spectrum of 4-(β-hydroxyethyl)pyridazine. Solvent is d_4-methanol, reference TMS.

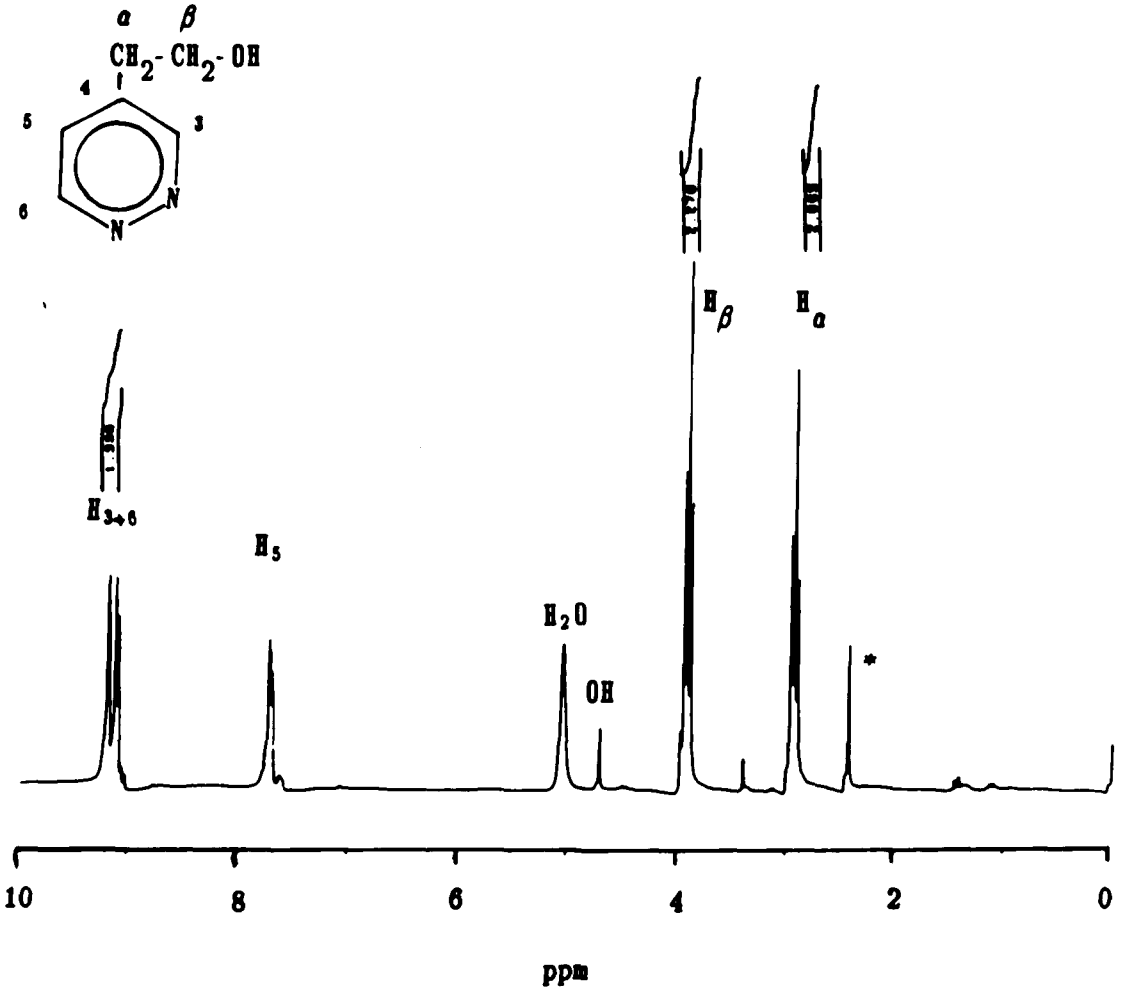

Figure 18. ^{1}H NMR spectrum of 4-(β-hydroxyethyl)pyridazine. Solvent is d_4-methanol, reference TMS.
* Absorptions due to starting material, methylpyridazine

impurity in this case is the starting material and water in relatively small amounts (2.4 ppm). Table 3 lists chemical shifts plus J_{h-h} coupling constants from this spectrum.

NMR spectral data clearly establish the identity of the newly synthesized 4-(β-hydroxyethyl)pyridazine and 3-(β-hydroxyethyl)-pyridazine. A strong tendency for the 3-alcohol to cyclize by forming a hydrogen bond with the ring nitrogen is seen in Figure 12. The 4-alcohol shows very low tendency to cyclize since the hydrogen bonded structure with the closest nitrogen would be subject to unfavorable strain. This is supported by the consistently high yield for 4-(β-hydroxyethyl)pyridazine 91% and low yield for the 3-(β-hydroxy-ethyl)pyridazine 45%. The much lower yield for the 3-alcohol is a direct result of the cyclization and ensuing dehydroxymethylation as shown in Scheme 5.

IV.B.1.c. Anhydrous molecular formaldehyde solutions

The search for a suitable method to synthesize the two new alcohols in acceptable yield led us to the method shown in Scheme 1. This procedure requires the use of anhydrous molecular formaldehyde solution. At first, the common procedure of reacting the activated species, pyridazinylmethyllithiums, with anhydrous formaldehyde gas was attempted. In general, this is achieved by passing anhydrous formaldehyde gas generated from the pyrolysis of paraform, through the solution containing the activated species at either room temperature or -78°C. This method always gave low yields of unrecoverable

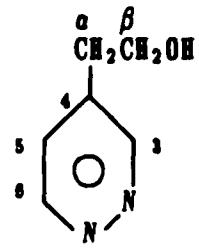

4-(β-hydroxyethyl)pyridazine
1

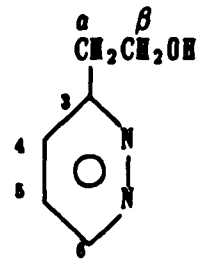

3-(β-hydroxyethyl)pyridazine
2

TABLE 3

^{1}H NMR chemical shifts and J_{h-h} coupling constants for 4-(β-hydroxyethyl)pyridazine, 1, and 3-(β-hydroxyethyl)pyridazine, 2. conditions same as above.

Compound	H_α	H_β	OH	H_6	H_5	H_3	H_{4+5}
1 (ppm)	2.9 t	3.8 t	4.7 b	9.0 d	7.6 m	9.1 s	-
J_{h-h}(Hz)	12.3	12.3	-	5.1	7.8	0	-
2 (ppm)	3.1 t	3.9 t	5.4 b	9.0 m	-	-	7.7 m
J_{h-h}(Hz)	12.6	12.6	-	14.0	-	-	19.5

alcohols plus large amounts of paraform. This is most likely due to the anionic polymerization of formaldehyde at high local concentrations. Formaldehyde gas is a very difficult reagent to control. NMR studies of the crude alcohols obtained in THF consistently showed the presence of small amounts of dissolved molecular formaldehyde suggesting the possibility of preparing THF molecular formaldehyde solutions. Molecular formaldehyde solutions with controlled concentrations in dry THF were then prepared and brought into contact with the activated pyridazinylmethyllithium species to prevent the formation of paraform. With these reagent solutions good yields of recoverable alcohols were obtained without the formation of paraform in the reaction vessel. The anhydrous molecular formaldehyde solution as a synthetic reagent clearly represents an important breakthrough.

Quantitative ^{1}H NMR at 0°C allowed us to ascertain that at least 94% of the *a*-POM pyrolysed becomes molecular formaldehyde and remains as such in solution. Figure 19 shows a ^{1}H NMR spectrum of a formaldehyde solution prepared by pyrolyzing 2.5 g of *a*-POM and then condensing the formaldehyde generated into 165 mL of dry THF. The concentration intended for the solution was 0.5 M; quantitative ^{1}H NMR data showed a concentration of 0.47 M. This method can give formaldehyde concentrations up to 3.3 M. Figure 20 shows a ^{1}H NMR spectrum of a 3.0 M formaldehyde solution in THF.

These solutions were shown to be effective in reacting with Grignard reagents. Reaction of a 0.45 M solution of anhydrous

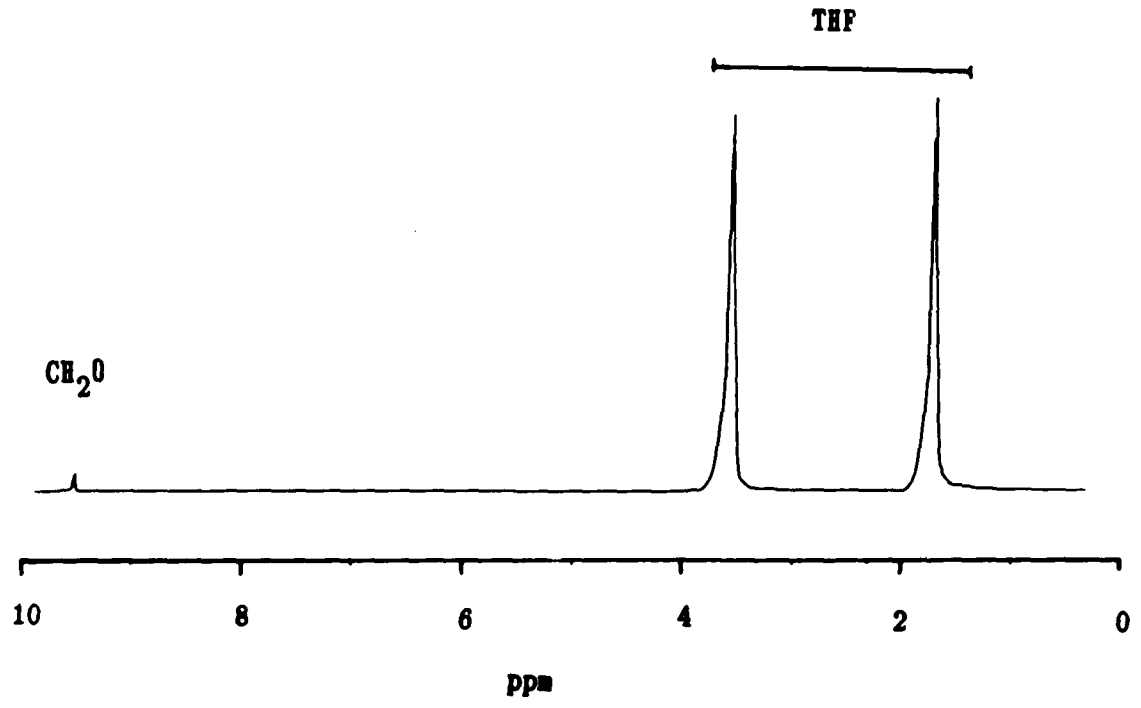

Figure 19. ^1H NMR spectrum of a 0.47 M formaldehyde solution in tetrahydrofuran.
No deuterated solvent.
Reference is THF absorption at 1.73 ppm.

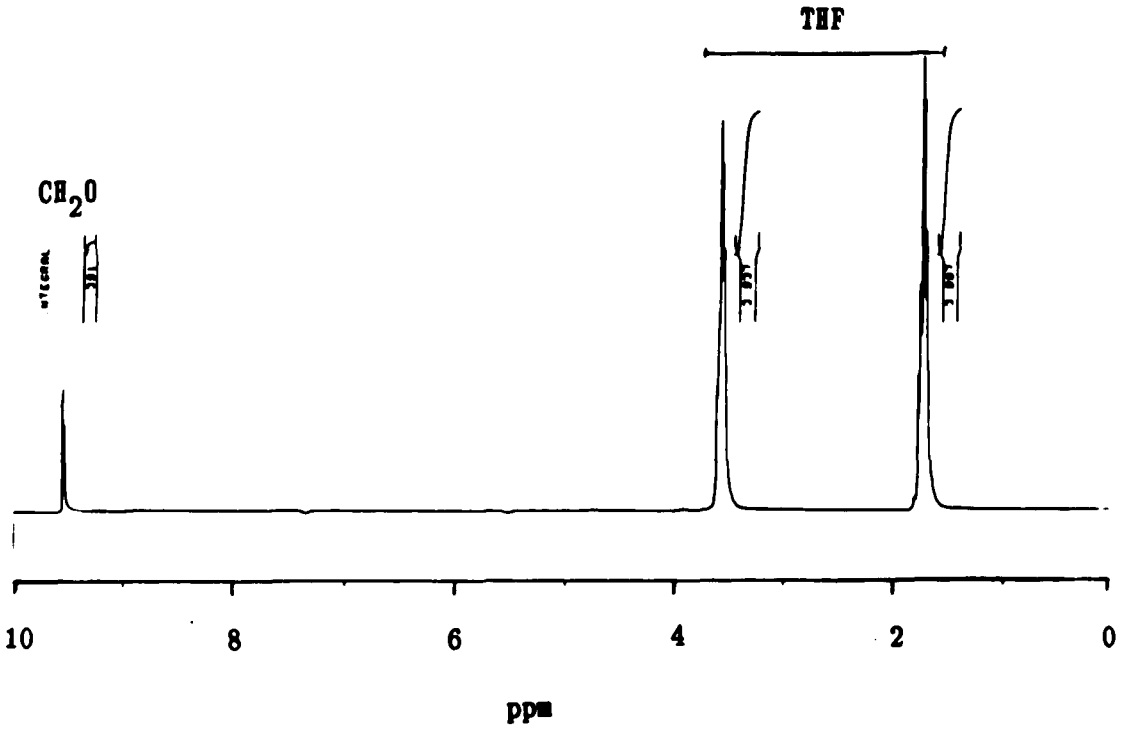

Figure 20. ^1H NMR spectrum of a 3.0 M formaldehyde solution in THF. Conditions as in Fig. 19.

formaldehyde in THF with 0.4 moles of cyclohexyl magnesium chloride in 250 mL THF produced cycohexylcarbinol in 67% yield.

This new reagent of anhydrous formaldehyde solution with controlled concentration represents a major improvement over the conventional method of using formaldehyde gas or formalin solution at high pressure for the synthesis of 3- and 4-(β-hydroxyethyl)-pyridazine. We believe that this reagent solution has far reaching potential as an organic reagent for the addition of one carbon to activated species under anhydrous conditions.

IV.B.1.d. 3- and 4-Vinylpyridazines, acid dehydration

Acid dehydration of the 3- and 4-(β-hydroxyethyl)pyridazines resulted in acceptable yields of the desired monomers. Figure 21 shows a ^{13}C NMR spectrum of 4-vinylpyridazine. The assignments were made based on the proton coupled ^{13}C NMR spectrum (Figure 22). These spectra show that the 4-vinylpyridazine monomer was obtained in high purity. The absorptions at 123 and 132 clearly show the vinyl functional group. Figure 23 shows a proton spectrum of 4-vinyl-pyridazine. This spectrum shows evidence of the presence of 4-methylpyridazine starting material as an impurity in relatively low concentrations. Table 4 lists the ^{13}C NMR chemical shifts of 4-vinylpyridazine along with J_{c-h} coupling constants obtained from the NMR spectra. Table 5 shows ^{1}H NMR chemical shifts along with J_{h-h} coupling constants obtained from the NMR spectrum. Figures 24 and 25 show ^{13}C NMR spectra of 3-vinylpyridazine, proton decoupled and

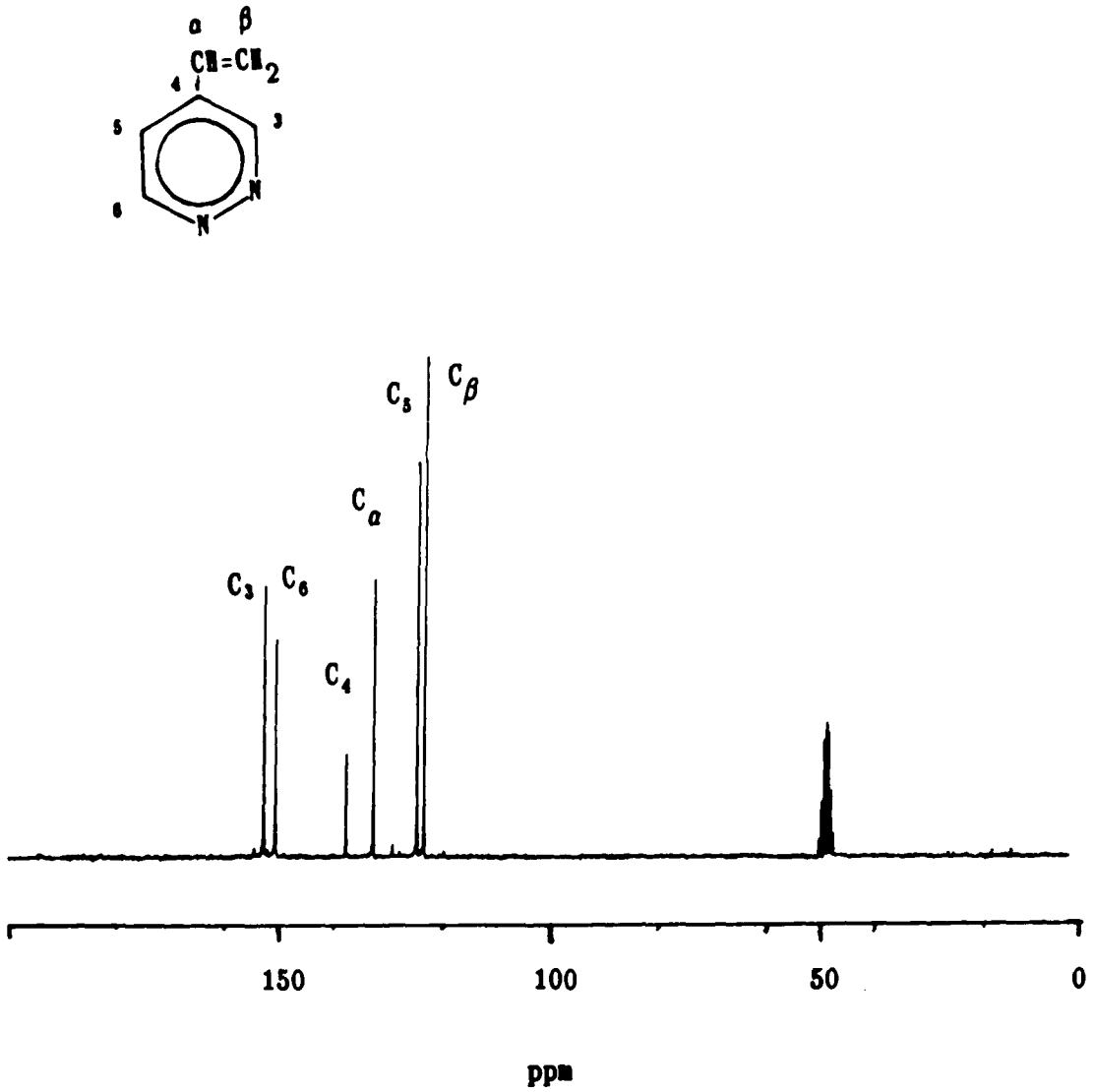

Figure 21. Proton decoupled ^{13}C NMR spectrum of 4-vinylpyridazine. Solvent is d_4-methanol, reference TMS.

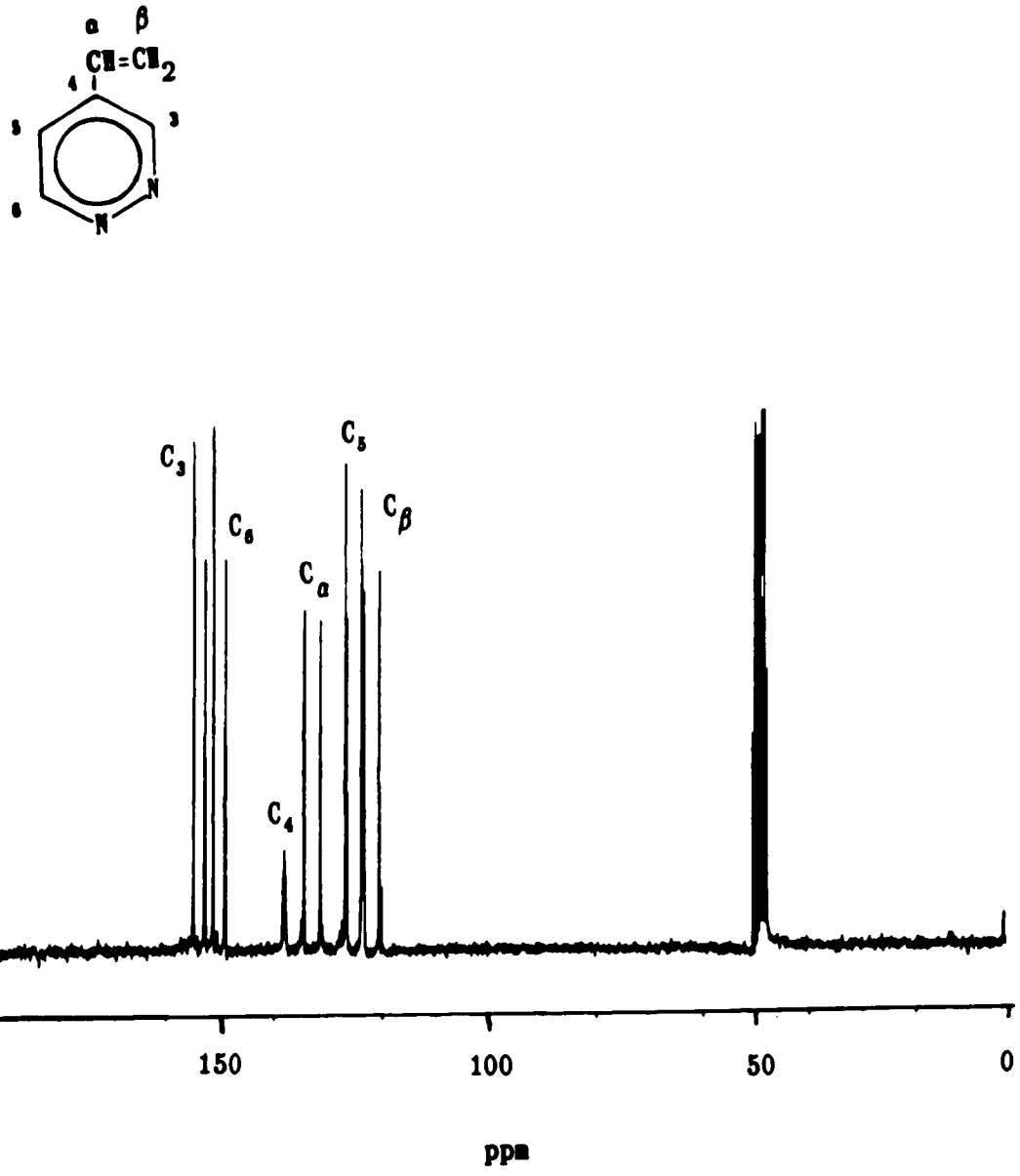

Figure 22. Proton coupled ^{13}C NMR spectrum of 4-vinylpyridazine. Solvent is d_4-methanol, reference TMS.

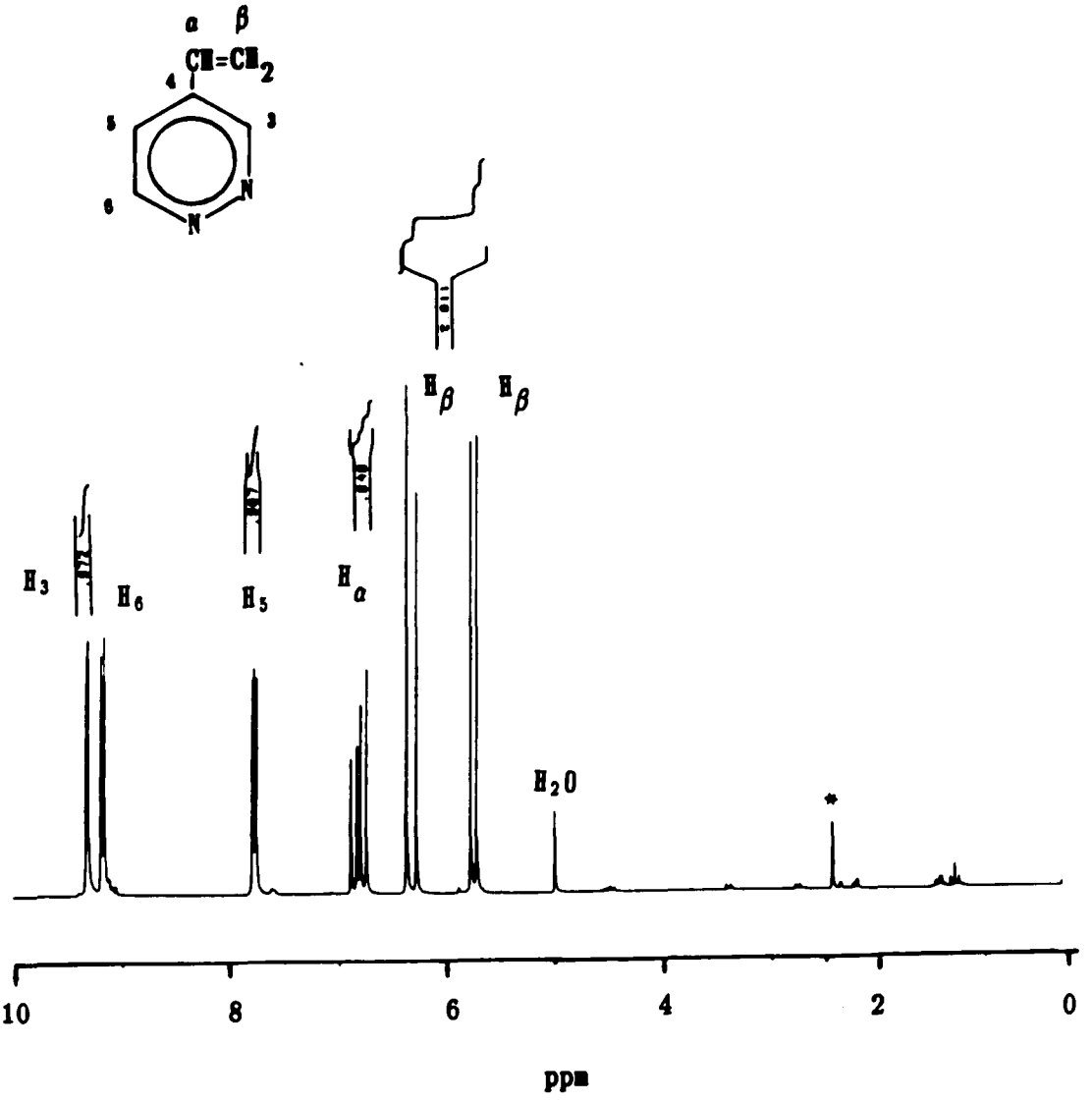

Figure 23. ^{1}H NMR spectrum of 4-vinylpyridazine.
Solvent is methanol-d_4, reference TMS.
* Absorptions due to starting material, methylpyridazine.

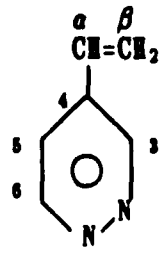

4-vinylpyridazine
3

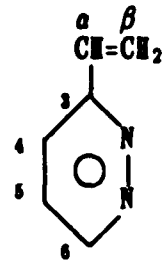

3-vinylpyridazine
4

TABLE 4

^{13}C NMR chemical shifts and J_{C-h} coupling constants for 4-vinylpyridazine, 3, and 3-vinylpyridazine, 4.

Compound	C_3	C_4	C_5	C_6	C_α	C_β	conditions
3 (ppm)	152.6	137.5	124.4	150.5	132.4	123.1	d_4,MeOH
J_{C-h}(Hz)	183.1	0	154.1	183.1	155.6	303.6	r.t.,TMS
4 (ppm)	159.6	128.9	125.6	152.4	135.0	122.1	d_4,MeOH
J_{C-h}(Hz)	0	171.0	174.0	183.1	158.6	318.3	r.t.,TMS

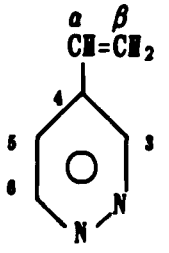

4-vinylpyridazine
3

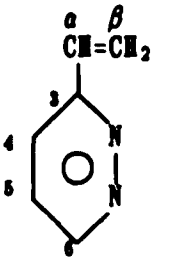

3-vinylpyridazine
4

TABLE 5

^{1}H NMR chemical shifts and J_{h-h} coupling constants for 4-vinylpyridazine, 3, and 3-vinylpyridazine, 4. conditions same as above.

Compound	H_3	H_4	H_5	H_6	H_α	H_β
3 (ppm)	9,31 s	-	7.7 d	9.17 d	6,8 m	6.31+5,75 d
J_{h-h}(Hz)	3.9	0	7.8	5.3	28.8	128.9
4 (ppm)	-	7.69 m	7.95 d	9.08 d	7.04 m	6.36+5.75 d
J_{h-h}(Hz)	0	23.4	6.8	13.1	28.8	135.7

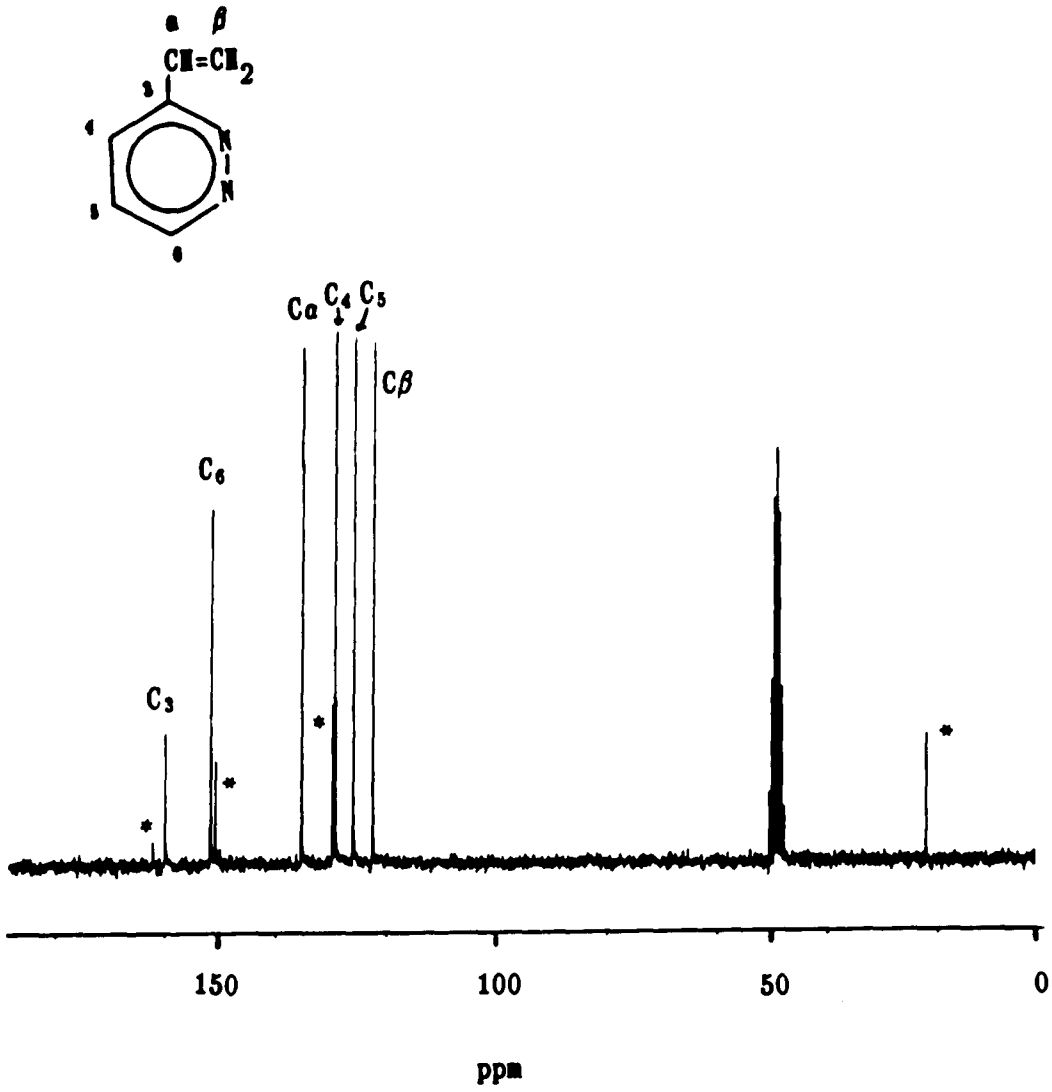

Figure 24. Proton decoupled ^{13}C NMR spectrum of 3-vinylpyridazine. Solvent is d_4-methanol, reference TMS.

* Absorptions due to starting material, 3-methylpyridazine.

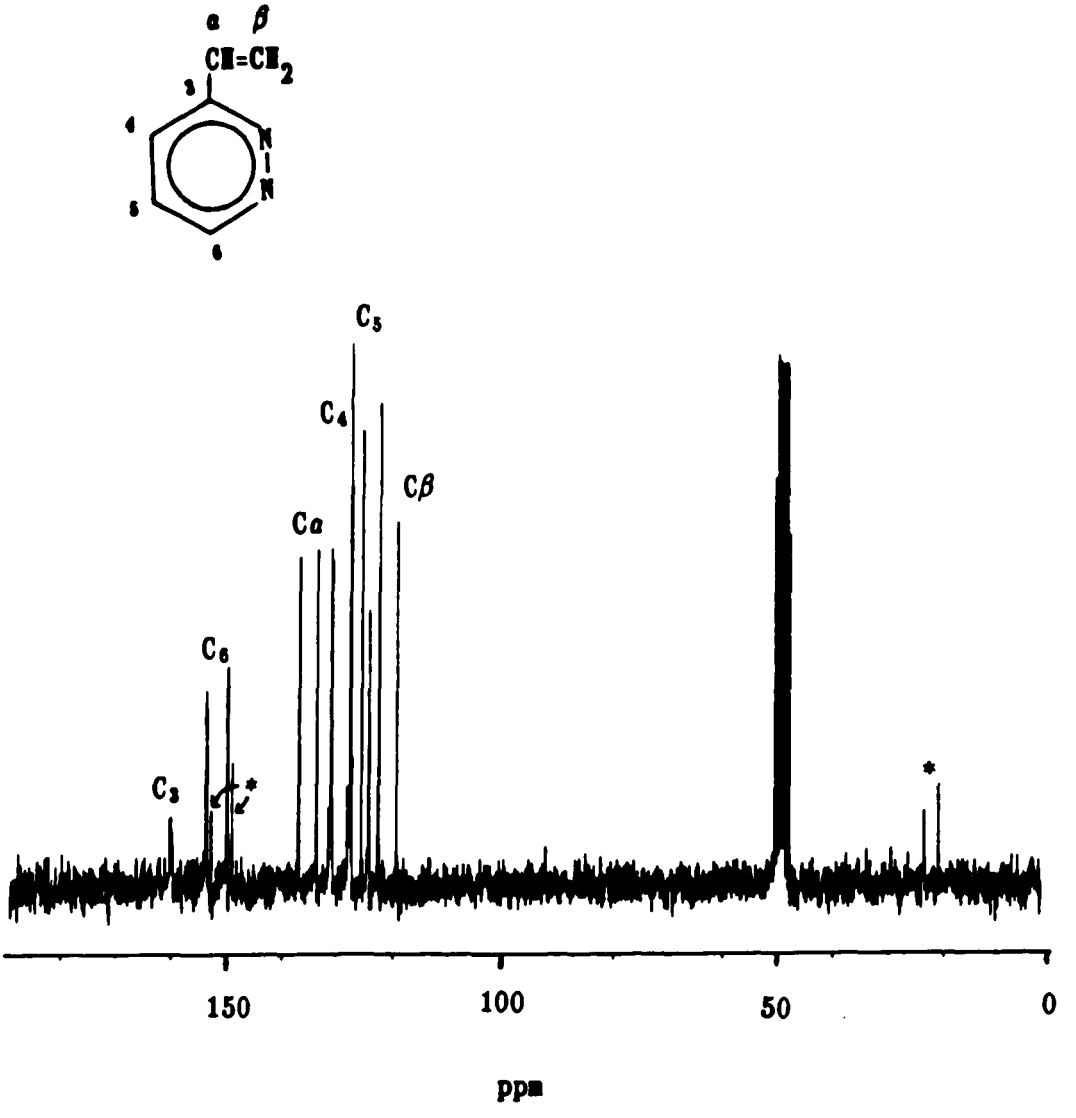

Figure 25. Proton coupled ^{13}C NMR spectrum of 3-vinylpyridazine. Solvent is methanol-d_4, reference TMS.

* Absorptions due to starting material, 3-methylpyridazine.

coupled respectively. These spectra show that although the monomer has been obtained in good yield and high purity, some 3-methylpyridazine starting material is present (methyl, at 21.9 ppm; low intensity absorptions in the aromatic region). Because of cyclization followed by dehydroxymethylation of the 3-alcohol, 3-methylpyridazine is present in both the alcohol and the vinyl monomer.

Figure 26 shows a ^{1}H NMR spectrum of 3-vinylpyridazine. The presence of 3-methylpyridazine, 2.7 ppm, is again in evidence. The absorption peaks of the monomer were all assigned by comparison with spectra of known vinyl heterocyclic monomers as well as by the J_{h-h} coupling expected for each peak.

Tables 4 and 5 show ^{13}C NMR chemical shifts, J_{c-h} coupling constants and ^{1}H NMR chemical shifts along with J_{h-h} coupling constants for 3-vinylpyridazine.

Table 6 shows the results of the elemental analysis (Oneida Research Services) of the newly synthesized 3- and 4-alcohols and 3- and 4-vinyl monomers. The experimental results are in reasonable agreement with the theoretical values. For samples 1 and 2, the experimental value for oxygen is higher than the theoretical value. This is most likely caused by to the presence of water molecules associated with the vicinal nitrogen atoms through double hydrogen bonding [8]. The corrected values were calculated based on assumptions that the value for nitrogen is most reliable and that all excess oxygen content is caused by water. Samples 3 and 4 show a much closer agreement between theory and experiment, with only a small excess of

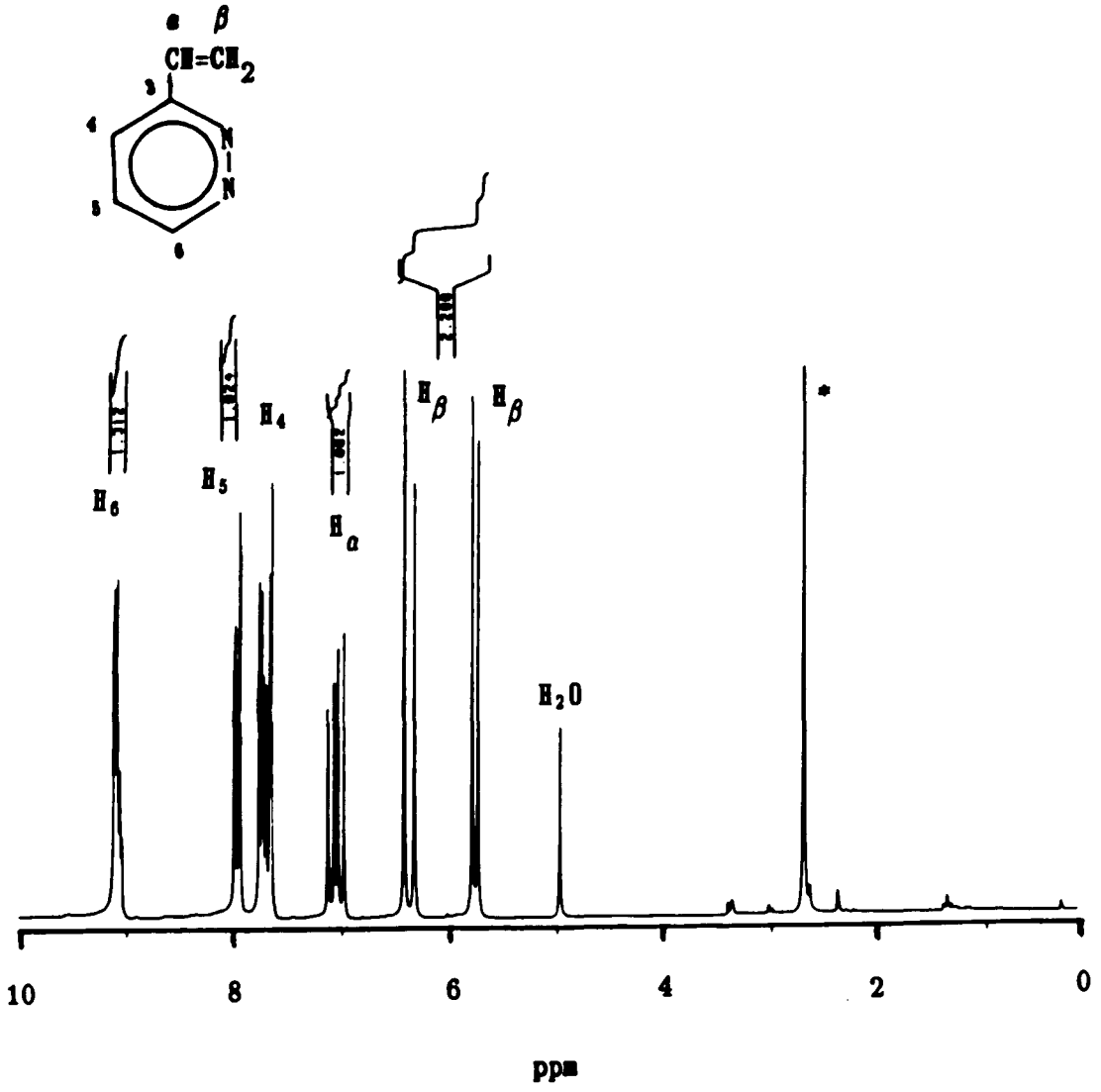

Figure 26. ^{1}H NMR spectrum of 3-vinylpyridazine.
Solvent is d_4-methanol, reference TMS.
• Absorptions due to starting material, 3-methylpyridazine.

TABLE 6: Elemental analysis of alcohols and vinyl monomers

	Sample	C	N	H	O
1	theor.	58.05	22.56	6.49	12.93
	exp.	57.45	21.32	7.20	13.83
	corrected* value	58.66	21.77	7.14	12.41
2	theor.	58.05	22.56	6.49	12.93
	exp.	54.13	19.43	7.20	18.68
	corrected* value	59.53	21.37	6.88	12.21
3	theor.	67.90	26.39	5.97	
	exp.	66.24	26.03	6.03	
4	theor.	67.90	26.39	5.70	
	exp.	66.10	26.61	5.97	

1. 3-(β-hydroxyethyl)pyridazine
2. 4-(β-hydroxyethyl)pyridazine
3. 3-vinylpyridine
4. 4-vinylpyridine

* See text

hydrogen, again due to hydrogen bonded water molecules. The slightly lower values for carbon must be caused by the presence of the unavoidable methylpyridazines.

The two monomers, 3-vinylpyridazine and 4-vinylpyridazine, obtained from acid dehydration of the intermediate alcohols are clear yellowish liquids, soluble in methanol, THF, toluene and water, insoluble in cyclohexane and ethyl ether. Both monomers change color upon storage of a few days. The 3-vinylpyridazine monomer changes to a dark brown color while the 4-vinylpyridazine changes to a deep purple color. Both monomers polymerize upon standing for several days, as evidenced by their polymer precipitation in THF. These self-polymerized polymers are in general of very low molecular weight and highly hygroscopic appearing gummy in nature.

IV.B.2 Polymerization and Characterization

In this work the two pyridazine polymers P3VPd and P4VPd were obtained by three different routes: i, thermal polymerization; ii, ionic polymerization; iii, radical polymerization.

For the thermal polymers there were five sources: the pressure reactor method in the case of P4VPd; acid and base dehydration of the β-hydroxyethylpyridazine alcohols for both P3VPd and P4VPd; heating the two corresponding alcohols at 80°C to 120°C during redistillation; purification of the monomers by redistilling at 60°C to 75°C under vacuum and finally from polymerization of the monomers upon storage at room temperature. The first three processes involving heating produced a dark brown brittle material that could be dried and made into a powder. In the first two cases two fractions of polymer could be distinguished: a methanol-soluble, apparently low molecular weight fraction and an apparently high molecular weight fraction insoluble in methanol but soluble in water containing a trace of acid. For the last three cases, the resulting polymers were completely soluble in methanol.

For ionic polymerization, the resulting polymer appeared to be of very low molecular weight, highly hygroscopic and always turning gummy upon exposure to air. Anionic polymerization of the new monomers, either in toluene or in THF, resulted always in immediate precipitation of the polymerizing molecule. It is apparent that the growing macromolecule precipitated as low molecular weight oligomers. Once precipitation occurred the polymerization came to a stop. The

limited amount of initiator added was apparently depleted, with unreacted monomer remaining in solution. If more initiator was added, more polymer was observed to precipitate. The yields of polymer were always very low for low concentrations of initiator added.

The third and most successful type of polymerization in this work was initiated by hydrogen peroxide in bulk and in solution at temperatures of 92°C to 105°C. This radical polymerization method was the simplest and most reproducible. Unlike anionic polymerization, radical polymerization had the advantage of not having to exclude moisture. In fact, water was used as the solvent in some of the polymerization experiments.

The polymers obtained by radical polymerization in solution were hygroscopic, of low molecular weight and in general their yields were low (i.e. 7%). Radical polymerization in bulk gave better yields (i.e. 25%) and monomer to initiator ratio could be readily controlled. Thus, initiation due to the added initiator could be distinguished from thermal and self-polymerization. Polymerizations at different monomer to radical initiator ratios were conducted. Viscosity measurements of the polymers thus produced showed that the higher monomer-to-initiator ratio led consistently to larger size molecules. This is in agreement with the general relationship between molecular weight and initiator concentrations. Compared to the thermal and anionic polymers, the radical polymers could be purified and characterized more readily.

In general all of the polymers of low molecular weight were

soluble in water, methanol, and DMF, and insoluble in ether, THF and cyclohexane. Figure 27 shows a solution ^{13}C NMR spectrum of P3VPd obtained from NaOH. The initial polymer was purified by dissolving in methanol and reprecipitating in ether several times. The pyridazine impurities remaining after the precipitation treatment were removed by drying in a Kugelrohr distillation apparatus at 150°C for 1 hour at 1.0 mm Hg. The polymer spectrum (A) is displayed together with a spectrum (B) of 3-methylpyridazine. A comparison of the two spectra clearly establishes the identity of poly(3-vinylpyridazine). The aromatic carbons for both compounds correspond closely. Some of the polymer aromatic absorptions shift slightly, possibly due to polymer conformations. The $C\alpha$ and $C\beta$ carbons of the polymer backbone show a broad absorption between 21-44 ppm and appear to be a combination of overlapping peaks. The broadness of the $C\alpha+\beta$ and C_3 absorptions suggests rigidity in the polymeric backbone as well as the lack of stereoregularity for the polymer at high polymerization temperatures.

Figure 28 shows a solution ^{13}C NMR spectrum of P4VPd from spontaneous polymerization. The absorptions are again broad, in general. The sharp lines in the aromatic region are most likely due to oligomers of very small size. The absorption for C_4 (140-144 ppm) is of very low intensity. The aliphatic absorptions are very broad. This again suggests some rigidity of the polymer and lack of stereoregularity even for low molecular weight thermal polymers.

Figures 29 and 30 show solid state ^{13}C NMR of P3VPd and P4VPd thermal polymers from acid dehydration, respectively. The absorption

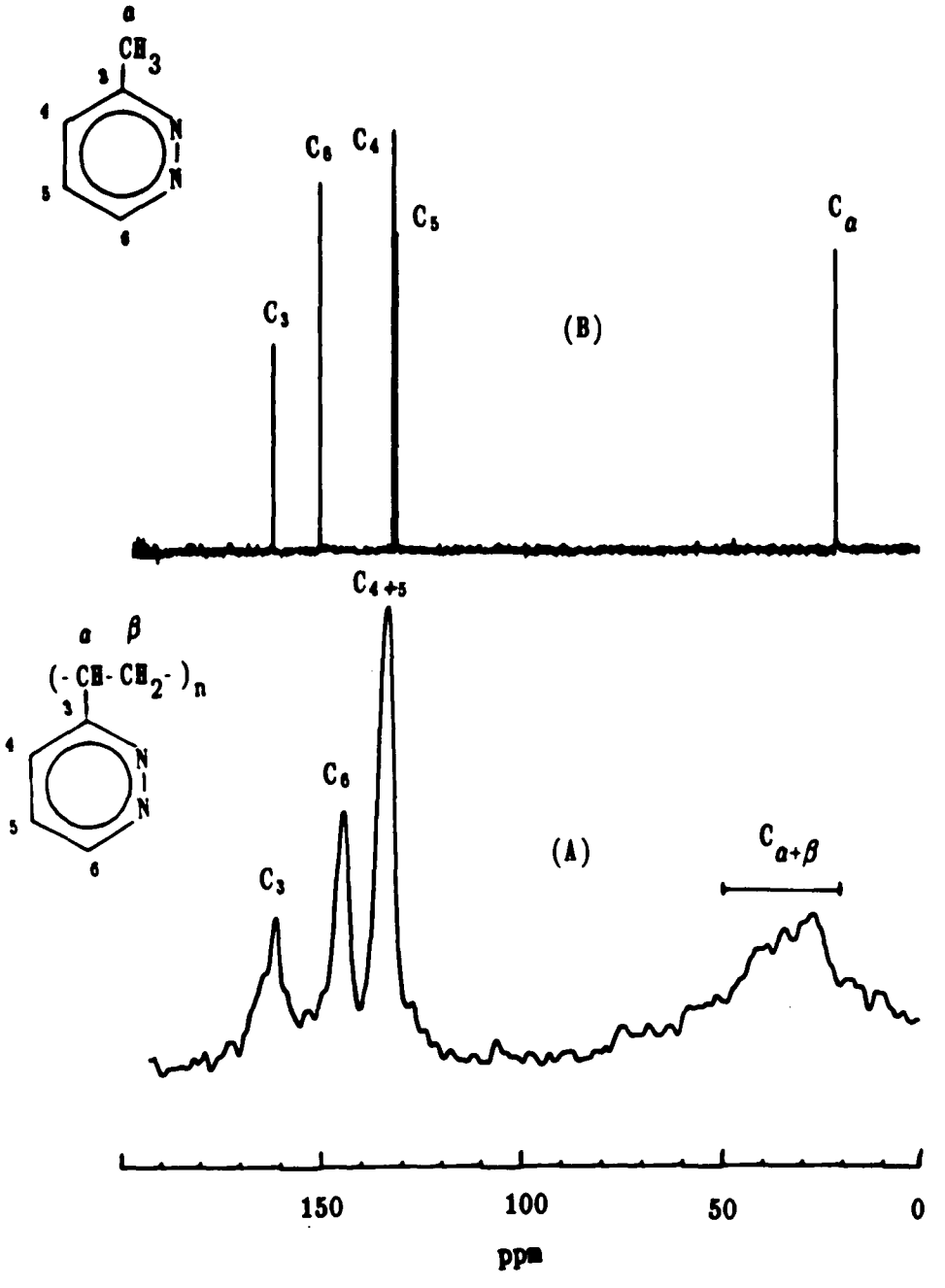

Figure 27. ^{13}C solution NMR spectrum of: A, poly(3-vinylpyridazine) obtained from base dehydration of 3-(β-hydroxyethyl)pyridazine. B, 3-methylpyridazine. Solvent is D_2O plus trace amount of D_2SO_4.

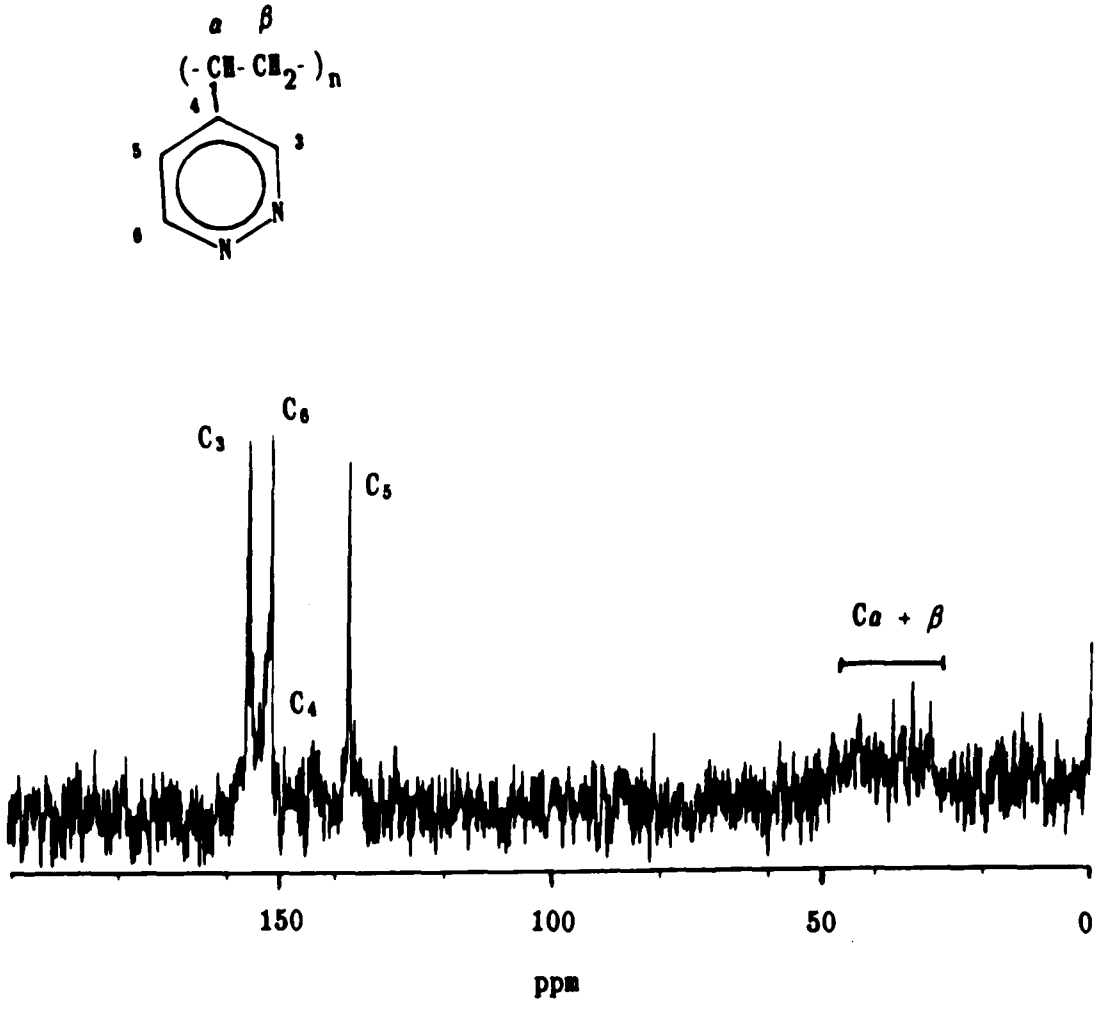

Figure 28. Solution ^{13}C NMR spectrum of poly(4-vinylpyridazine) from self polymerization of 4-vinylpyridazine.
Solvent is D_2O, reference is TSP.
• Absorptions due to starting material, methylpyridazine.

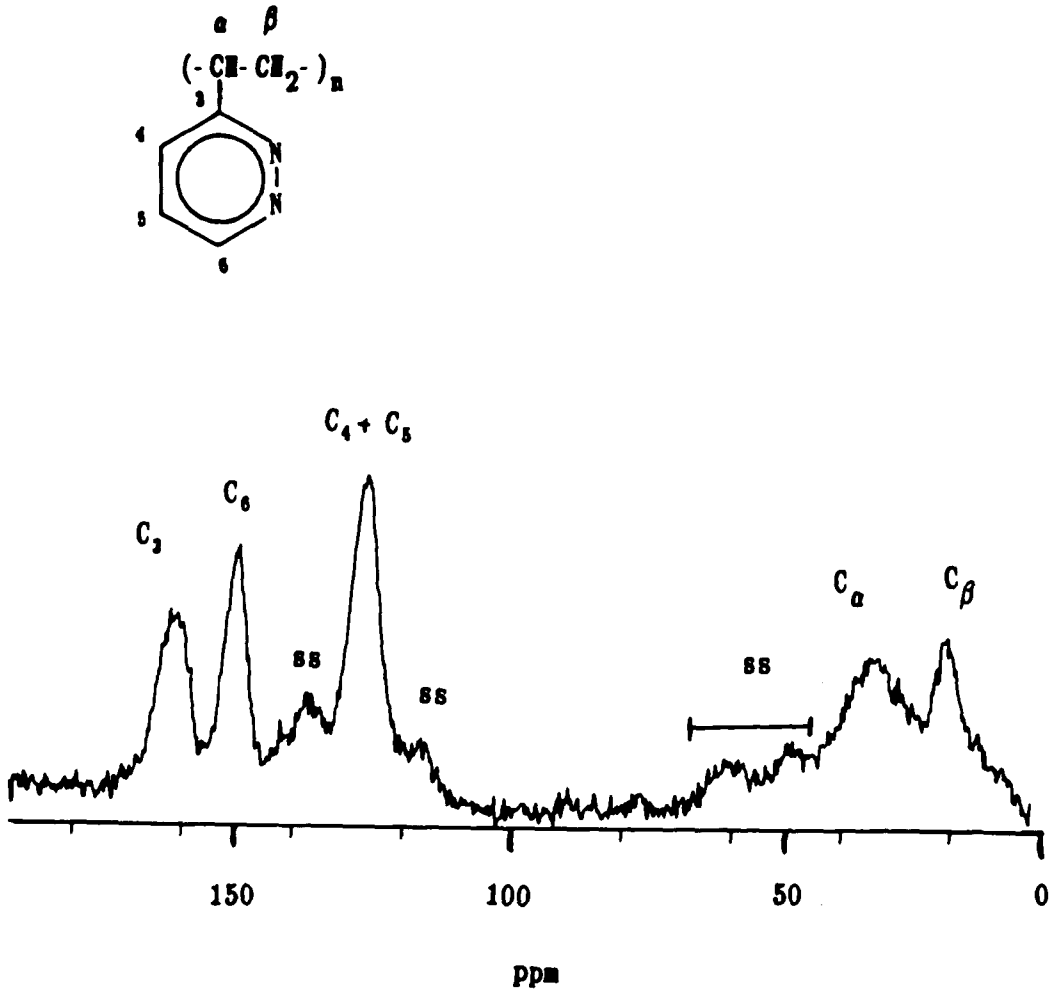

Figure 29. Solid state ^{13}C CP/MAS NMR spectrum of poly(3-vinylpyridazine) obtained from acid dehydration of 3-(β-hydroxyethyl)pyridazine.
ss = spinning side bands

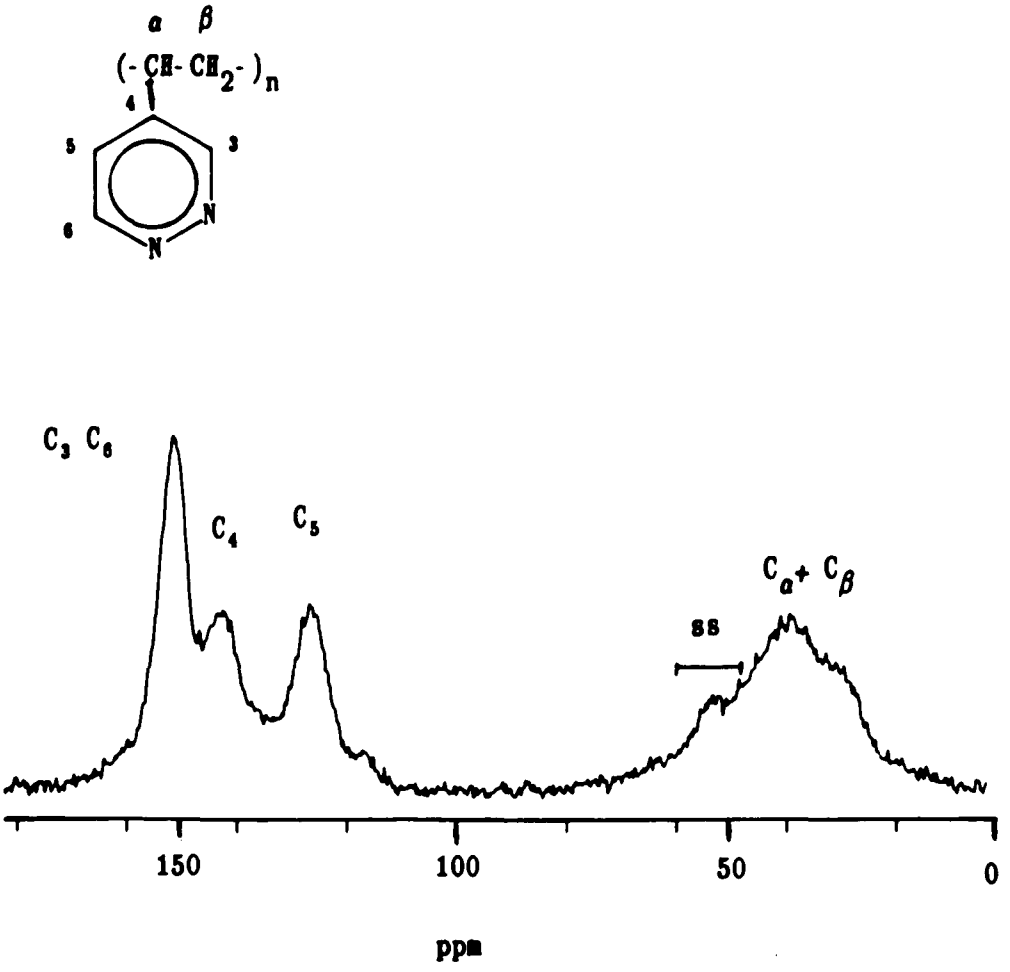

Figure 30. Solid state ^{13}C CP/MAS NMR spectrum of poly(4-vinylpyridazine) obtained from acid dehydration of 4-(β-hydroxyethyl)pyridazine.
ss = spinning side bands

peaks for all carbons as shown in both Figures are broad suggesting the rigidity and lack of stereoregularity. This was the case for all the thermal polymers obtained throughout this work. Solid state ^{13}C NMR was conducted on these apparently high molecular weight thermal polymers in order to avoid the solubility problem and to take advantage of the crosspolarization as well as high concentration in solid.

^{13}C NMR spectra of the thermal and the anionic P3VPd and P4VPd polymers showed in general broad absorptions for the aromatic as well as the aliphatic absorptions. Their quaternary carbons (i.e. C_3 and C_4) showed slow relaxation as the norm, requiring long relaxation delay for their observation in NMR. In contrast, the polymers obtained by radical polymerization showed sharper ^{13}C NMR absorptions for all the carbons including a much narrower and well defined aliphatic region and shorter relaxation delay.

Figure 31 shows a ^{13}C NMR of poly(3-vinylpyridazine) obtained from radical polymerization in bulk of 3-vinylpyridazine at a monomer to initiator ratio of 150. At this ratio the polymer obtained is of relatively low molecular weight and showed good solubility in water. Comparison of this spectrum with that of thermally polymerized P3VPd (Figure 27) reveals a marked difference in the absorption peaks for the aliphatic region (35 to 50 ppm) as well as for the absorption peak for C_3 (158 ppm). The C_3 links the pyridazine ring to the polymer backbone. Its ^{13}C NMR absorption should be tacticity-sensitive.[49] For the thermal polymer the aliphatic absorptions are broad and the C_3

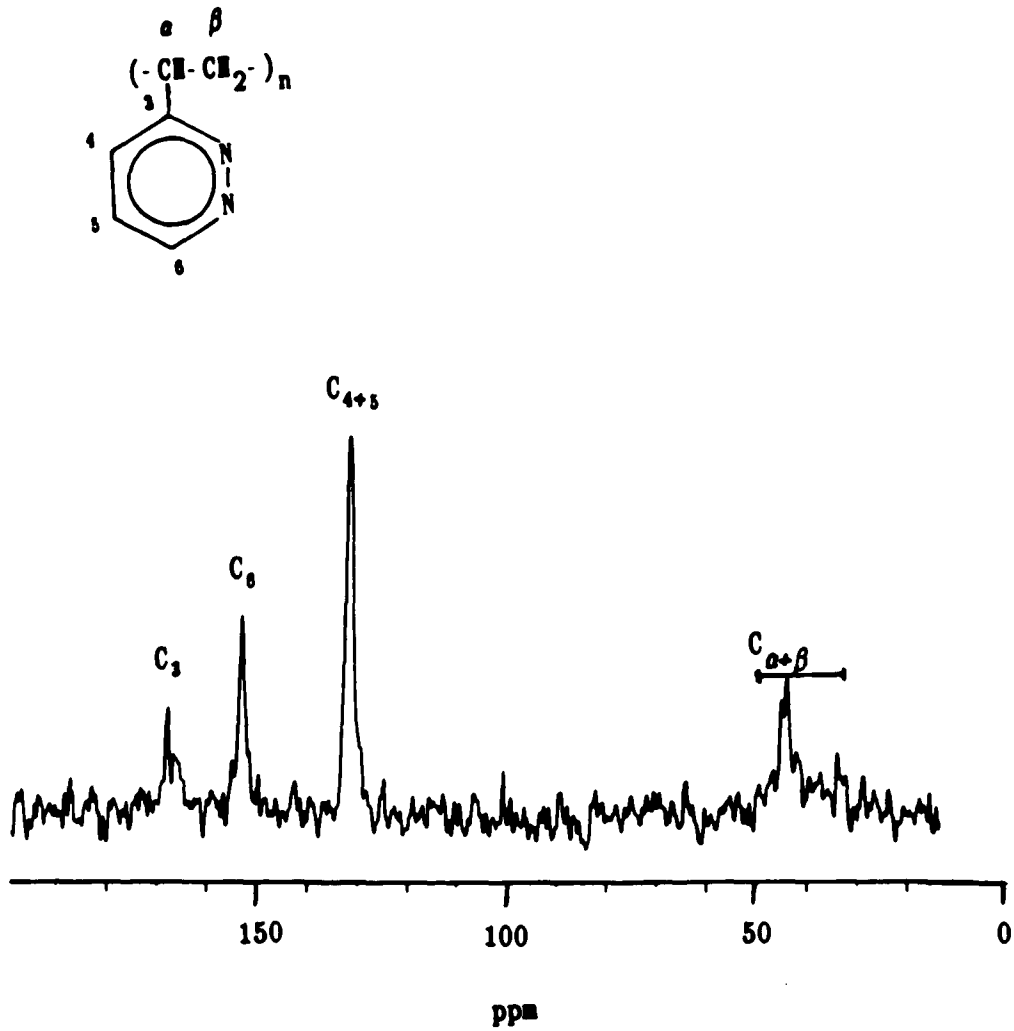

Figure 31. ^{13}C NMR spectrum of P3VPd obtained by radical polymerization in bulk.
Solvent is D_2O, reference TSP.

absorption appears to be composed of several peaks. The spectrum for the radically polymerized P3VPd shows instead narrower aliphatic region absorptions of relatively high intensity and a C_3 absorption composed of 2 peaks. This suggests that radical polymerization occurs in more orderly manner than thermal polymerization. The difference in polymerization temperature, i.e. radical at 105°C vs thermal at 160°C, must play a significant role.

Figure 32 shows a ^{13}C NMR spectrum of poly(4-vinylpyridazine) obtained by radical polymerization in bulk at a monomer to initiator ratio of 120. This spectrum shows narrow and well defined absorptions for all of the carbons in the polymer. The absorption for C_4 of this polymer appears to be a single peak suggesting a high stereoregularity. The absorptions at 41.6, 47.8 and 43.8 ppm are due to $C\alpha$ and $C\beta$.

Figure 33 shows the tacticity-sensitive quaternary carbon absorptions for three different vinyl polymers: A, thermal P3VPd, from Figure 27; B, P3VPd radically polymerized, from Figure 31; and C, P4VPd radically polymerized, from Figure 32. Absorption A is composed of several peaks and spans a width of 16 ppm while absorption B spans only 5 ppm and is clearly composed of two distinct absorptions. Absorption C spans 4 ppm and very clearly shows a single peak. This Figure illustrates clearly the high stereoregularity of the polymers obtained from radical polymerization.

Figure 34 shows a ^{13}C NMR spectrum of P4VPd polymerized in bulk by radical initiation at a monomer to initiation ratio of 270. At

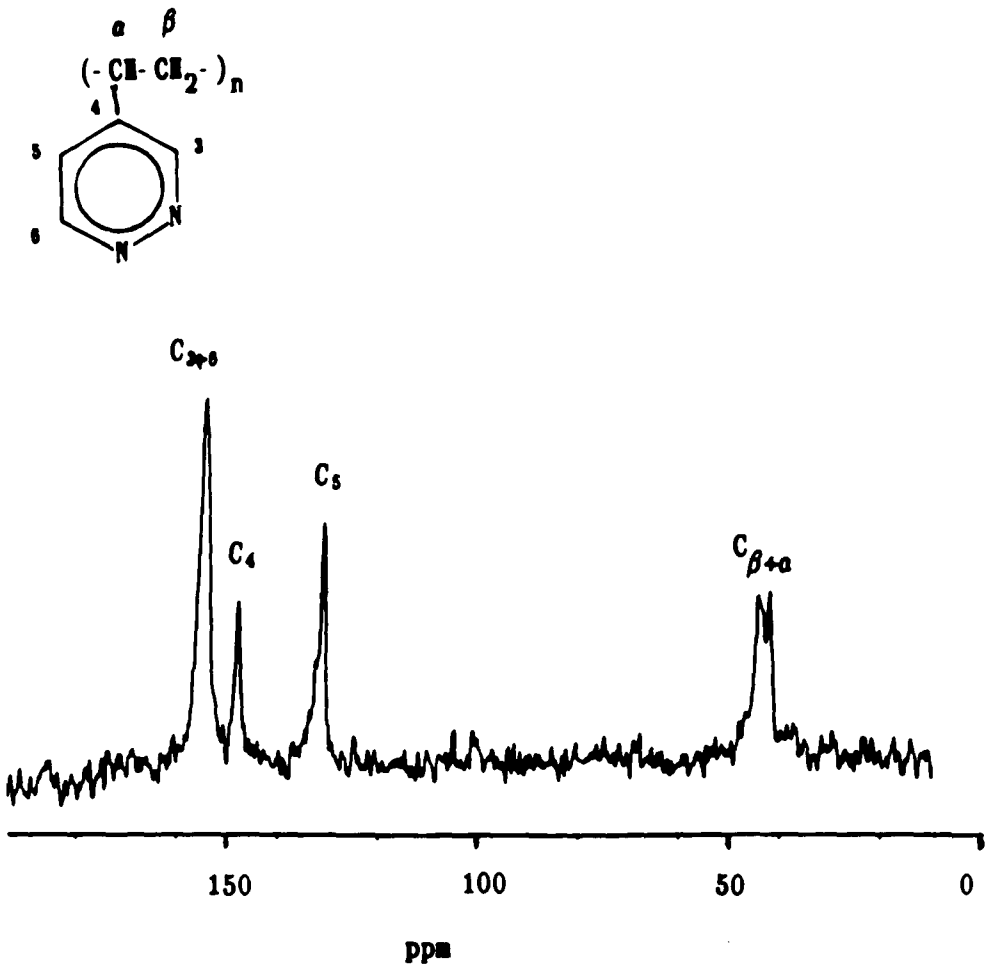

Figure 32. ^{13}C NMR spectrum of P4VPd obtained by radical polymerization in bulk.
Referenced to TSP in D_2O by spectrometer reference.

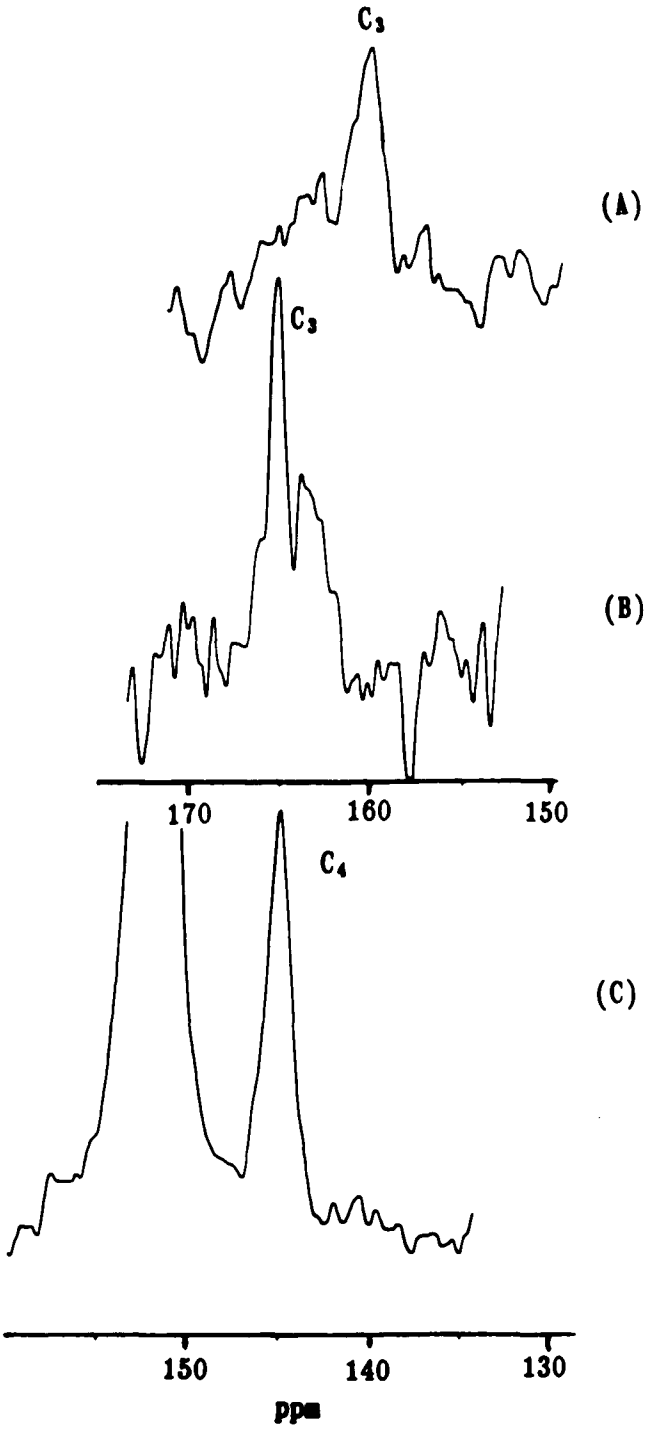

Figure 33. Expanded ^{13}C NMR spectra for quaternary polymer carbons

A. Thermal P3VPd

B. Radical P3VPd

C. Radical P4VPd

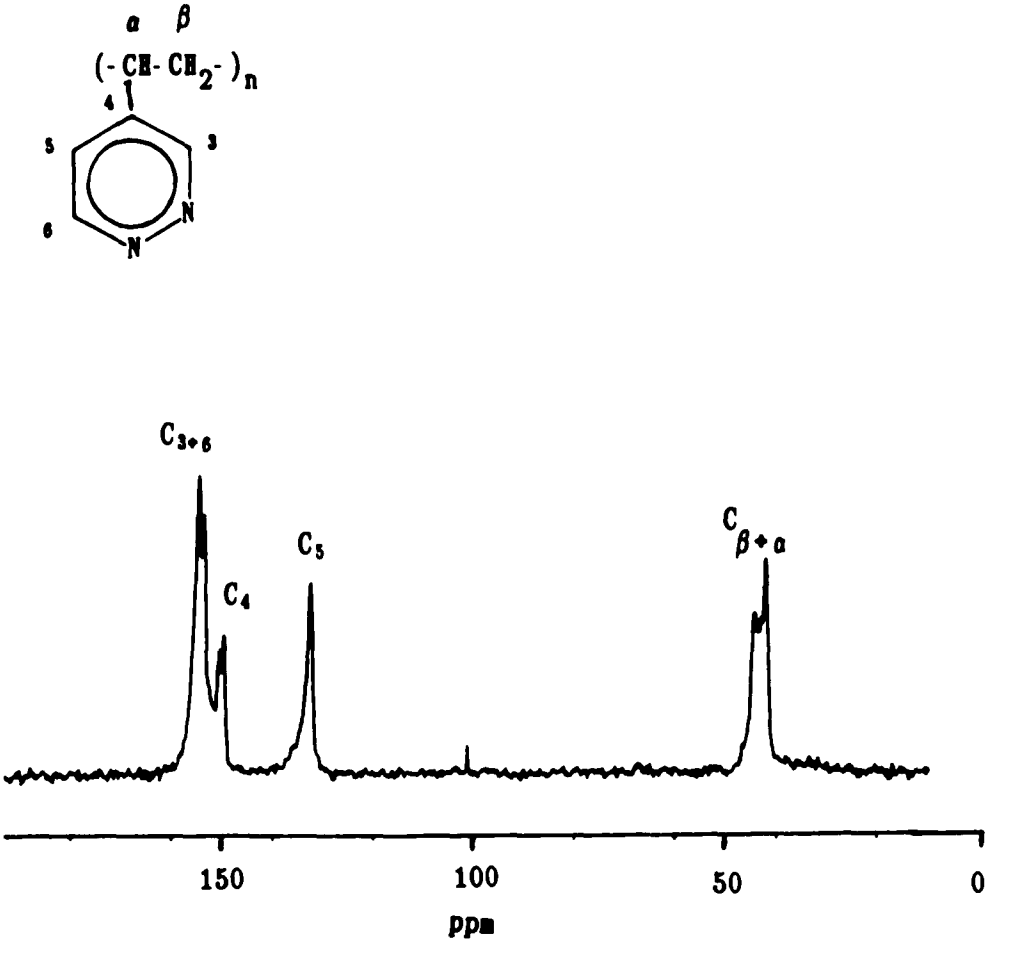

Figure 34. ^{13}C NMR of high molecular weight radically polymerized in bulk P4VPd.
Solvent is D_2O plus trace D_2SO_4, spectrometer reference used.

this ratio the molecular weight of the polymer is high and requires a trace amount of acid, e.g. D_2SO_4 for complete dissolution of the polymer in D_2O. The effect of the acid can be seen by the downfield shift of C_4 by 3 ppm. This Carbon, as seen in Figure 34, is composed of two absorptions, which also suggest a high degree of tacticity for this polymer. Figure 35 shows ^{13}C NMR of P4VPd obtained by radical polymerization in solution using 1.0 N H_2SO_4 as the solvent. The spectrum shows a downfield shift for C_4 and a rather complex aliphatic area. This particular polymer from polymerization at a monomer to initiator ratio of 32 was a hygroscopic material and likely of low molecular weight.

Table 7 shows the results for the elemental analysis of P3VPd and P4VPd obtained by the different polymerization methods. The experimental results for the radical polymers are close to the theoretical values. The presence of oxygen can be explained in part by the water molecules associated with some of the pyridazine rings. After correction for oxygen and hydrogen due to water, a better agreement is achieved. The C/N ratio is within experimental error; the N/H ratio is higher than 0.33%. The radical P4VPd polymer shows far better experimental values compared to the corresponding P3VPd. Table 7 indicates a large disagreement between the theoretical and experimental values for the anionic polymers and a better agreement for the thermal polymers. This disagreement extends to the C/N and C/H ratios as well. It is well known that under conditions similar to the thermal and the anionic polymerizations in this work, the

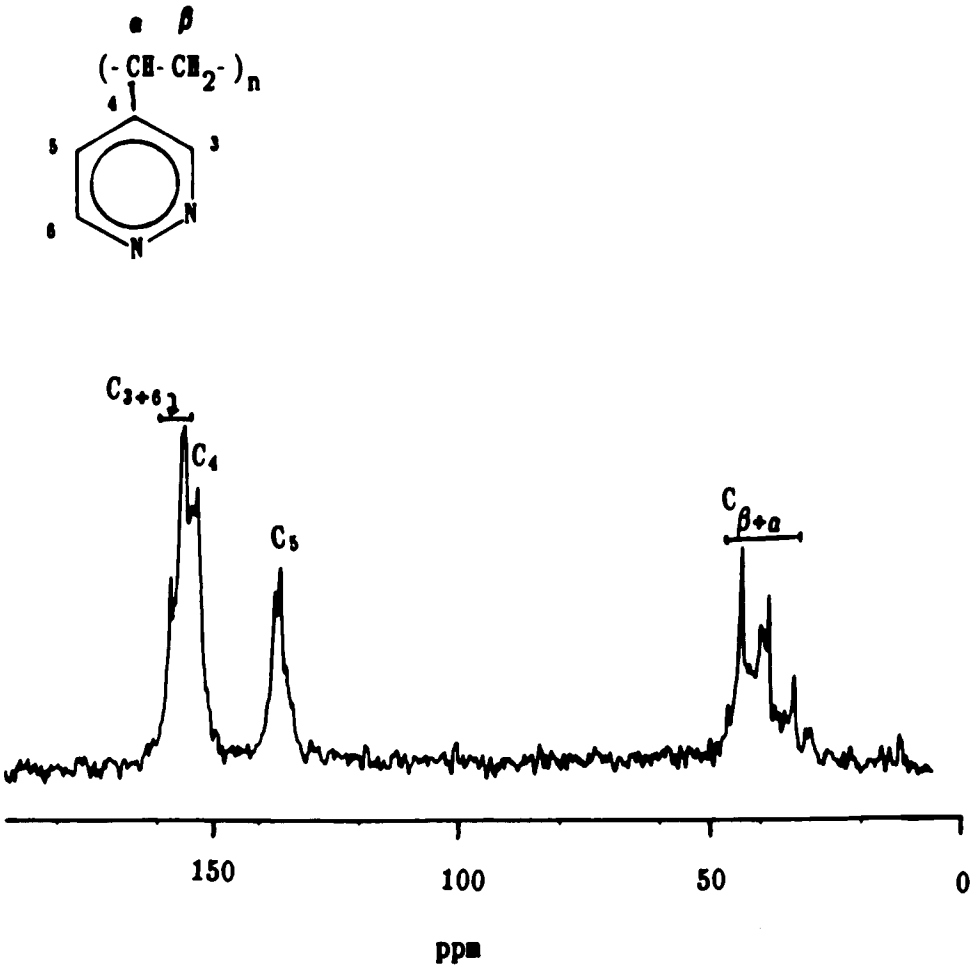

Figure 35. ^{13}C NMR of P4VPd radically polymerized in 0.1 N H_2SO_4 solution.

D_2O solvent, spectrometer reference used.

TABLE 7: Elemental analysis of the new polymers.
Percent by weight.

Sample		C	N	C/N	H	N/H	O
	theor.	67.92	26.41	3.0	5.66	0.33	0.00
1	exp.	63.21	24.30	3.03	4.85	0.44	7.52
	corr.* value	69.15	26.58	3.04	4.27	0.44	
2	exp.	66.00	25.77	2.99	5.30	0.38	3.85
	corr.* value	68.30	26.68	3.09	4.98	0.37	
3	exp.	61.86	21.15	3.41	5.21	0.29	
4	exp.	62.36	21.53	3.37	5.26	0.29	
5	exp.	33.18	11.22	3.45	4.71	0.17	
6	exp.	47.73	17.18	3.23	5.02	0.24	

1. P3VPd (radical)
2. P4VPd (radical)
3. P3VPd (thermal)
4. P4VPd (thermal)
5. P3VPd (anionic)
6. P4VPd (anionic)

* corrected value for the presence of water.

pyridazine ring can open and extrude nitrogen[50]. This ring opening side reaction has the potential for generating defect structures of ethylenic or acetylenic groups pendant to the polymeric backbone.[50] The extrusion of nitrogen leads to the high experimental value for the carbon to nitrogen ratio.

The anionic polymers showed ^{13}C NMR spectra resembling in quality the spectrum shown in Figure 28 with no clear indication of the ring opening products. Although this kind of NMR spectrum is a good indication for the presence of the desired polymer. However the elemental analysis data suggest that besides the desired polymer, other intractable products from ring opening, side reaction and oxygen impurities from $Mg(OH)_2$ are present. NMR observations from the results of anionic polymerization were extremely useful in the beginning of this project in ascertaining the polymerizability of the two new monomers.

The ^{13}C NMR spectra shown along with the elemental analysis in Table 7 strongly support the identity of the polymers obtained by radical and thermal polymerization. Between these two methods, the more desirable is the radical polymerization. This method is simple, effective and allows for the control of the macromolecule size by manipulation of initiator concentration. Radical polymerization was the method used to obtain the polymers on which most of the physical measurements were conducted as described below.

IV.B.3. Polymer Properties

IV.B.3.a. Viscosity Measurements

Molecular weight is an important measurement in the characterization of new polymers molecular weight. In the present study the dilute solution viscosity of the new polymers was measured to estimate molecular size. The viscosity of dilute solutions of P3VPd and P4VPd in methanol was compared with the viscosity of a poly(2-vinylpyridine) standard, a polymer related in structure to the two new polymers (Figure 36).

Curve A shows the reduced viscosity (η_{red}) and inherent viscosity (η_{inh}) extrapolated to zero concentration for poly(2-vinylpyridine), M_w 2 X 10^4. Curves B and C show the η_{red} of P3VPd and P4VPd. Extrapolation to infinite dilution yields an intrinsic viscosity, approximately 0.06 dl/g for P3VPd and 0.049 dl/g for P4VPd.

Assuming that a direct comparison can be made between the two new polymers in solution and P2VP solutions, these values indicate that the polymers P3VPd and P4VPd have approximately one-third the hydrodynamic volume of the 2 X 10^4 molecular weight P2VP standard. This gives a qualitative estimation of the size of these macromolecules. Both the molecular size from viscosity data and the conversion of the vinyl group of the monomer into aliphatic backbone, based on NMR indicate the success of the synthesis of the two new polymers.

The data shown in Figure 36 for the P3VPd and P4VPd solutions were obtained under experimental conditions giving very short flow

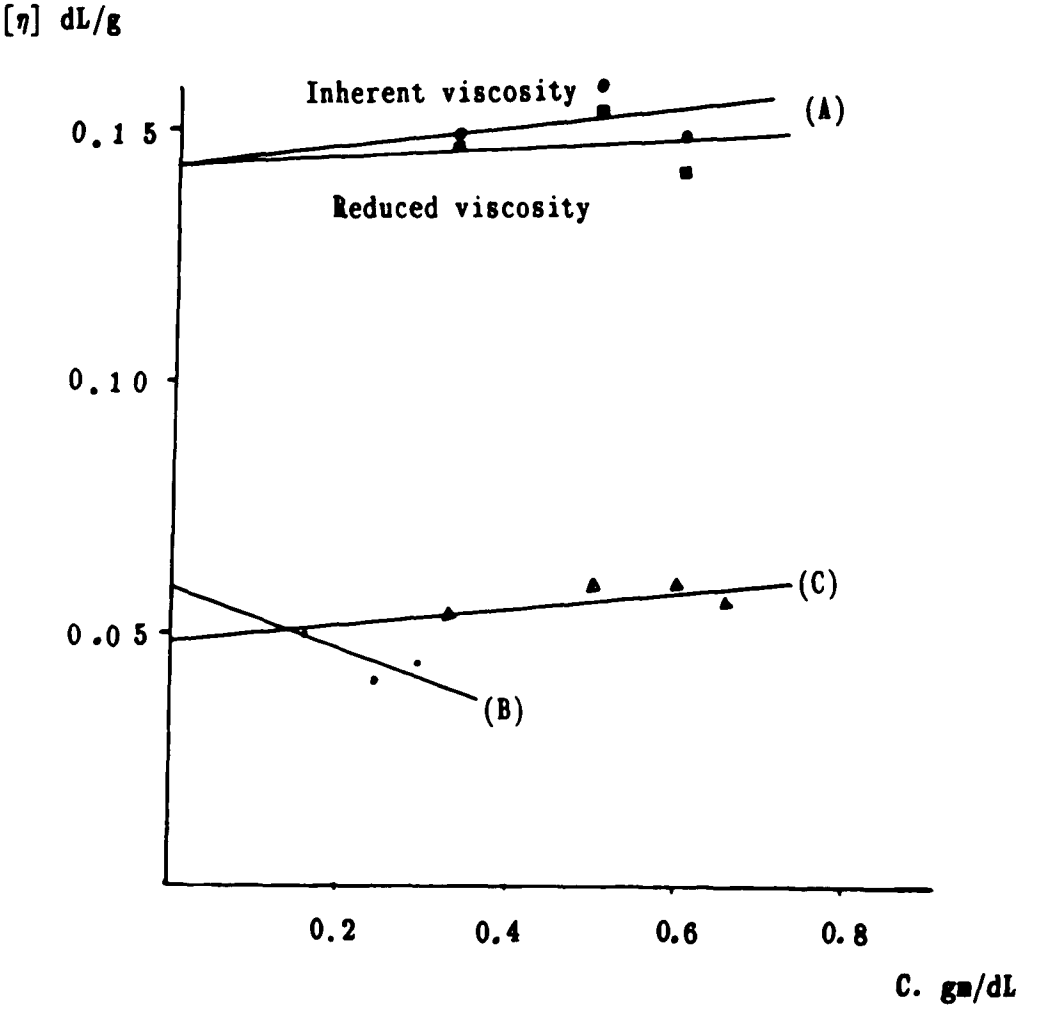

Figure 36. Intrinsic viscosity of: A, standard P2VP M_w 2x10^4 B, P3VPd thermally polymerized and C, P4VPd thermally polymerized.
Solvent used was methanol, thermostated bath at 21°C.

time difference between pure solvent and samples of different concentrations. These data can be utilized, at best, to estimate molecular size. In order to observe in better detail the dilute solution behavior of the two new polymers, further viscosity measurements were conducted in a microcapillary viscometer with much longer flow times, i.e. lower shear.

The dilute solution behavior of two P4VPd samples and one P3VPd sample prepared at different monomer-to-radical initiator ratios were studied. Figure 37 shows the plots of reduced viscosity against concentration for a P3VPd and P4VPd sample. A distinct maximum is observed from both P4VPd systems. The greater value of the maximum for η_{red} is associated with lower monomer to initator ratio. For the P3VPd system no conspicuous maximum is displayed. Two types of systems exhibiting such maxima were documented: polyelectrolytes and rigid rod solutions. For polyelectrolyte solutions, the charges in the polyion can be suppressed by the addition of a salt in high concentration.[56] For this case, the viscosity behaviour of the polyelectrolyte resembles that of uncharged polymers, i.e. a linear increase of η_{red} with concentration. However, for radically polymerized P4VPd in different solvents with different salts at different concentrations, the results always showed the same type of curve with a maximum as shown in Figure 37. The salts used were NaCl and KBr up to a concentration of 1.0 M. Thus the polyelectrolyte effects can be ruled out.

The viscosity behavior of the P4VPd solutions is consistent with

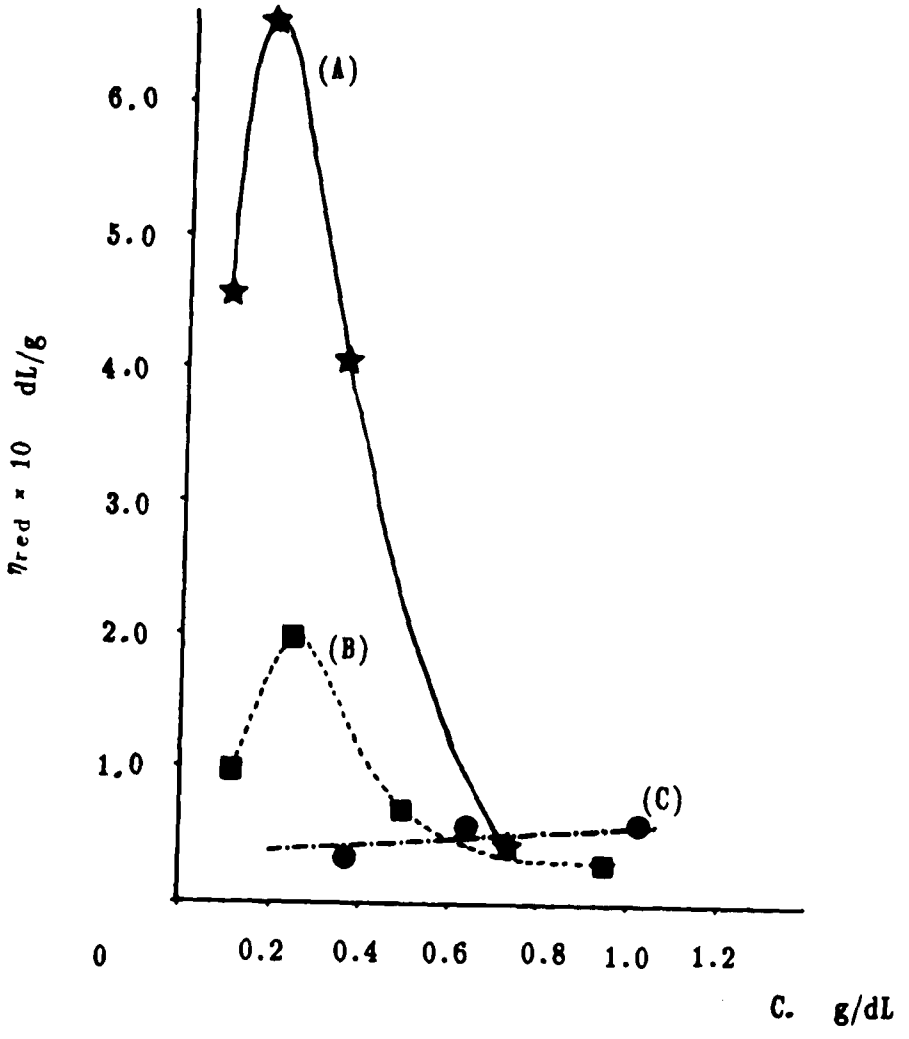

Figure 37. Viscosity measurements in semi-micro viscometer. η_{red} vs. concentration for:

A. P4VPd polymerized in bulk by radical initiation at a monomer/initiator ratio of 270.

B. P4VPd polymerized in bulk by radical initiation at a monomer/initiator ratio of 128.

C. P3VPd polymerized in bulk by radical initiation at a monomer to initiator ratio of 241.

that of rigid rod polymers. At low shear rate, below a critical concentration, the polymer solution is isotropic with the macromolecules unoriented. In this low concentration range, the viscosity of the solution increases with concentration as expected. When the polymer concentration exceeds a critical concentration the polymer solution becomes anisotropic with significant orientation of the macromolecules along the direction of the flow in the capillary viscometer resulting in a precipitous decrease in viscosity.[51] Figure 38 shows plots of polymer solution viscosity vs. concentration. Based on data from Figure 37 and a given viscosity constant for the viscometer (0.003765 centistokes/second). The viscosity plots show much more pronounced maxima compared to the η_{red} plot. A critical concentration of 0.0023 g/mL is obtained from P4VPd prepared by monomer/initiator ratio of 270. A higher critical concentration of 0.003 g/mL for the polymer from a lower monomer-to-initiator ratio of 128 is arrived at as expected, i.e. lower monomer ratio leading to smaller molecular size, requiring a higher critical concentration for orientation.

The dipole interaction between the pyridazine rings of the monomer units can be a strong driving force for the formation of syndiotactic P4VPd polymer. For isotactic propagation there would be a strong dipole repulsive force between the two pyridazine rings of the terminal and the incoming monomers (100 to 200 kcal/mole).[54] The two dipoles with a moment of ca. 4.3 D would be only 2.5 Å apart. It is obvious that the syndiotactic propagation is energetically far more

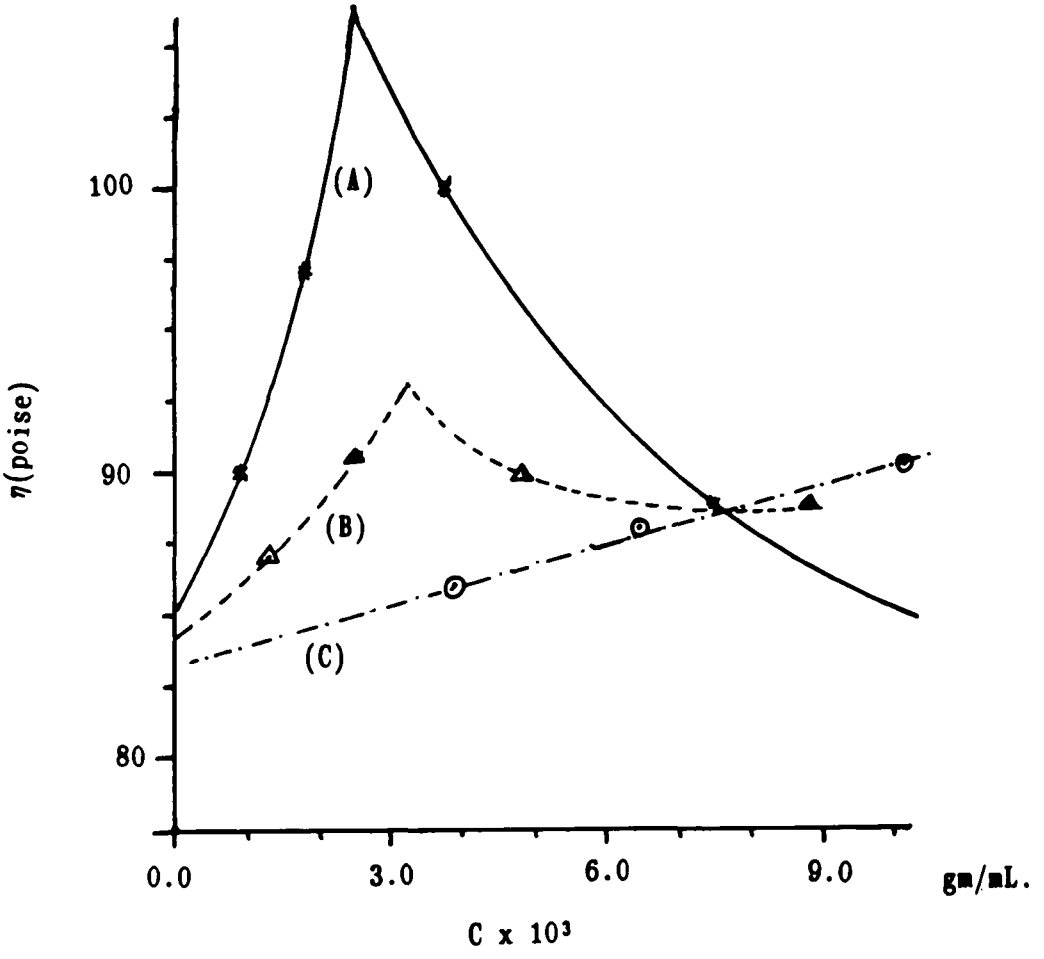

Figure 38. η vs. concentration for:

A. P4VPd polymerized in bulk by radical initiation at a monomer/initiator ratio of 270.

B. P4VPd polymerized in bulk by radical initiation at a monomer/initiator ratio of 128.

C. P3VPd polymerized in bulk by radical initiation at a monomer to initiator ratio of 241.

favorable based on both dipole and steric considerations . Once the syndiotactic polymer is formed, the molecule will tend to assume a planar zigzag conformation with the pyridazine dipoles favorably aligned, i.e. a rigid rod.

For the P3VPd system, the pyridazine dipole is parallel to the double bond functional group in contrast to the perpendicular arrangement for the P4VPd system. The dipole driving force for syndiotactic placement no longer prevails. The resulting P3VPd polymer molecule will not be significantly stereoregular. The rigid rod conformation in solution does not persist, hence absence of a maximum in the viscosity plot (Figures 37 and 38).

The dipole interaction also manifests itself in the high yield of polymer for P4VPd in radical polymerization compared to P3VPd. At a monomer to initiator ratio of 270 for the P4VPd system, a yield of 25% was obtained for a 24 hour polymerization. For the P3VPd system, under the same conditions but with a monomer to initiator ratio of 240, a yield of only 7% was obtained. This difference can be ascribed in part to the dipolar effect. For P4VPd, both steric and dipole effects favor syndiotactic polymerization, while for P3VPd, the steric effect counteracts the dipole effect.

IV.B.3.b. Paramagnetism and direct current conductivity.

The polymers P3VPd and P4VPd in their solid pure form exhibit ESR absorptions between the third and fourth lines of the Mn^{+2} marker, where ESR signals for most organic free radicals in a doublet ground

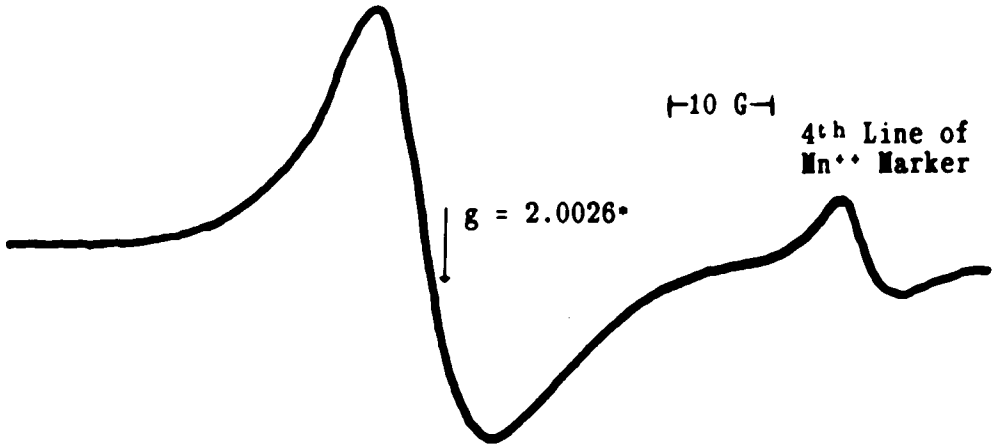

Figure 39. ESR absorption of neat P3VPd radically polymerized

* g ± 0.0005

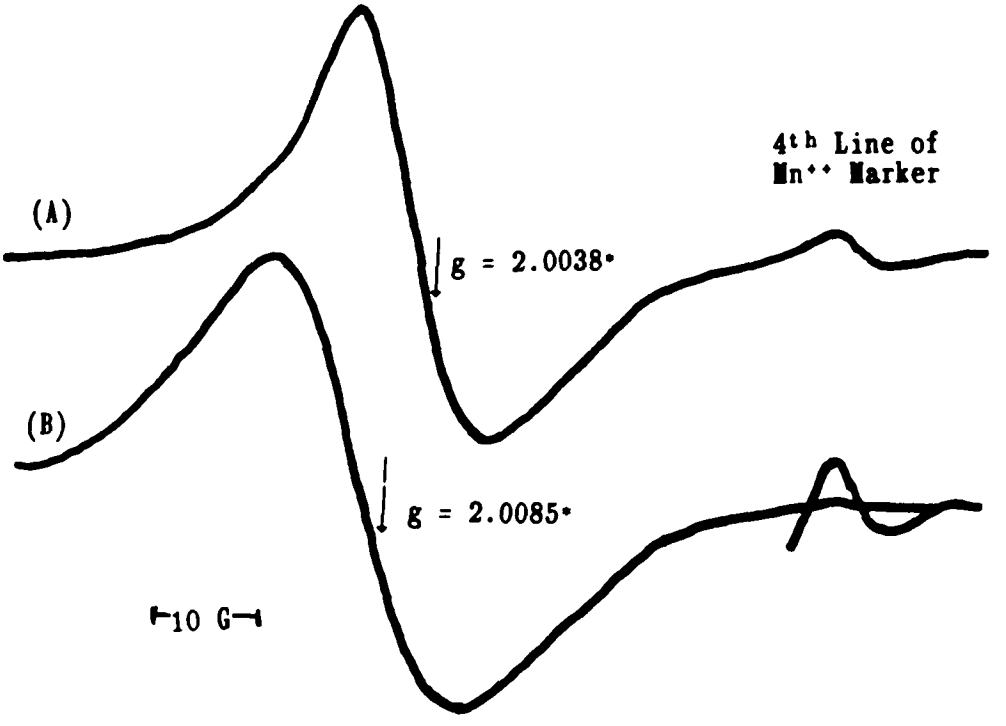

Figure 40. ESR absorption of: A. neat P4VPd polymer obtained by radical polymerization) B. P4VPd/I_2 at 1/1.2 ratio

• g ± 0.0005

state appear. This is in contrast to P2VP which does not show any absorption in its native form. Figure 39 shows a typical absorption for undoped P3VPd. In general, all the ESR signals for doped and undoped P3VPd and P4VPd are structureless singlets, indicating that the unpaired electrons are delocalized. The neat polymer shows ESR signals with ΔH_{ms} of 10 Gauss while the doped polymers, between 15 and 20 Gauss. Figure 40 shows ESR absorptions of P4VPd doped with I_2 at a ratio of 1:1.2, for polymer repeat unit-I_2 curve B, and neat radical P4VPd curve A. A significant shift for the g value of the doped polymer is clearly observed.

Tables 8 and 9 show spin densities, electronic conductivities and g values for a series of thermal P3VPd and P4VPd doped with I_2 at different ratios, as well as radical P3VPd and P4VPd, doped and undoped. All the samples show comparable spin densities, native and doped. The g values for most of the samples appear to be within the same range. Only for the P4VPd/I_2 sample was a significant deviation observed (Figure 40, curve B). The g value shift observed in this case, from 2.0038 to 2.0085, can be attributed to the delocalization of paramagnetic centers into the iodine system which has a spin-orbit coupling parameter[52] of 4060 cm^{-1}. The large g value shift is in agreement with this very high parameter. For example, the 2,3,5,6-tetraiodo-1,4-benzosemiquinone anion has a g value of 2.01217.[53] The neat polymers show a high delocalized spin density. In some cases, even higher compared with the doped polymers. However, the roles of these delocalized spins in electronic conduction are not

TABLE 8: Spin density and conductivity of P3VPd doped with I_2

Sample P3VPD/I_2	Spin Density (spin/g)	Conductivity $\Omega^{-1}\cdot cm^{-1}$	g±0.0005
neat P3VPd	1.14 X 10^{18}	1 X 10^{-10}	2.0026
1:1.5	2.77 X 10^{17}	2.4 X 10^{-4}	2.0048
1:3	8.79 X 10^{17}	1.8 X 10^{-4}	2.0044
1:7	8.25 X 10^{17}	1.0 X 10^{-4}	2.0047
1:10	1.7 X 10^{17}	1.7 X 10^{-5}	2.0041
neat P3VPd*	8.6 x 10^{17}	-	2.0078

TABLE 9: Spin density and conductivity of P4VPd doped with I_2

sample P4VPD/I_2	Spin Density (spin/g)	Conductivity $\Omega^{-1}\cdot cm^{-1}$	g±0.0005
neat P4VPd	4.40 X 10^{17}	1 X 10^{-10}	2.0068
1:1.5	5.40 X 10^{17}	1.7 X 10^{-4}	-
1:3	5.60 X 10^{17}	6.6 X 10^{-5}	2.0046
1:7	2.40 X 10^{17}	1.8 X 10^{-5}	2.0042
1:10	6.75 X 10^{17}	1.9 X 10^{-5}	-
neat P4VPd*	3.96 x 10^{17}	-	2.0038
P4VPd/I_2 1:1.2	1.19 x 10^{18}	-	2.0085

* Polymers obtained by bulk radical polymerization.

yet established. For the native polymers, the conductivities are much lower than 10^{-10} $\Omega^{-1}\cdot cm^{-1}$. Only polymers complexed with I_2 result in a semiconducting system.

This finding clearly indicates that the charge-transfer complex between the polymer and I_2 is responsible for conduction and not the delocalized spins in the native system. Data from Tables 8 and 9 suggest that the conductive behavior of the two new polymers is relatively unaffected by the amount of I_2 present.

IV.B.3.d. Iodine uptake by P3VPd and P4VPd.

In order to ascertain the ratio by which molecular iodine combines with the rings to form the charge-transfer complex in each of the polymers, we conducted sets of" approach to equilibrium" experiments. Figure 41 shows the time required to reach equilibrium for samples of P3VPd-I_2 and P4VPd-I_2 systems. The time Curve A indicates that P3VPd complexes with I_2 in a ratio of 1 pyridazine ring to 1.5 molecules of I_2. The P4VPd polymer combines with I_2 in a ratio of 1 pyridazine ring per 1.2 molecules of I_2, Curve B. These ratios are consistent with those found by Hoare et. al.[9] for monomeric charge-transfer complexes between pyridazine and I_2, i.e. 1.0 to 1.4 moles of I_2 per mole of pyridazine rings.

IV.B.3.d. Thermal analysis

DSC for the thermal P3VPd and P4VPd showed on first heating a

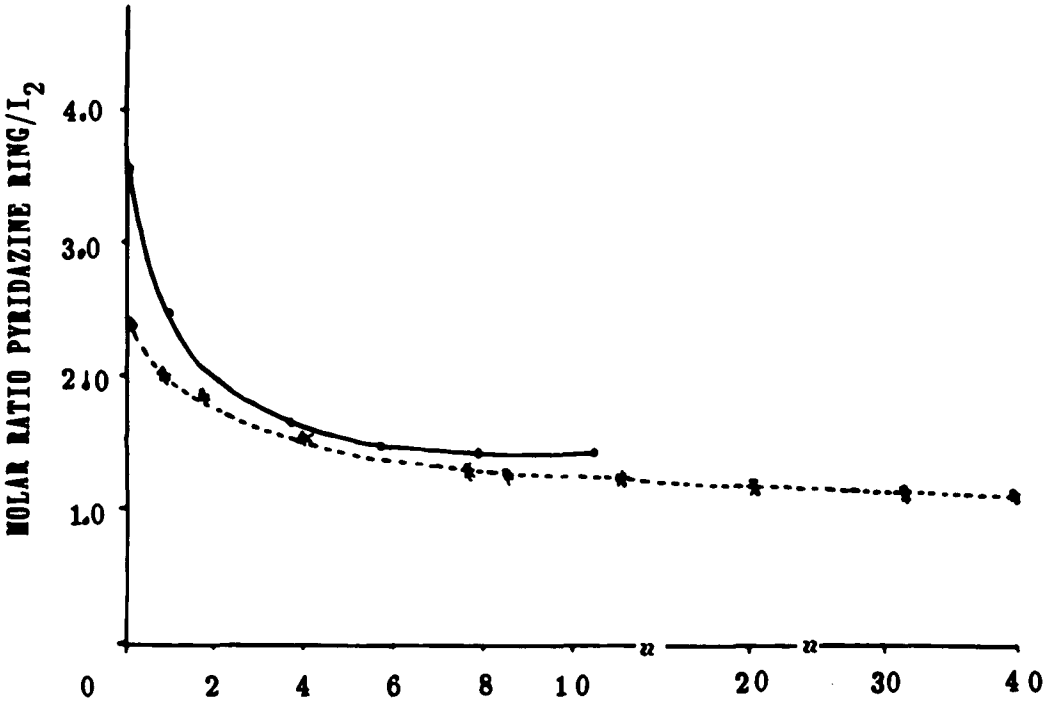

Figure 41. Iodine uptake by:

P3VPd ——

P4VPd .....

broad shallow endotherm between 80-120°C, no additional endotherm was observed up to 260°C. The shallow transition was not observed upon slow cooling back to room temperature and reheating of the same sample. Thermogravimetric studies of these polymers show that this transition corresponds to weight loss, perhaps due to solvent or water molecules associated with the pyridazine rings in the polymers. The absence of observable endotherms for the second heating of this polymer combined with its rigidity and lack of stereoregularity suggests that this polymer is devoid of crystalline organization. A similar situation is observed for the anionic P3VPd and P4VPd. DSC for these polymers shows on first heating a series of sharp endotherms over a wide range of temperature, i.e. 140-220°C. These sharp endotherms are not observed after the sample was cooled slowly to room temperature and reheated. Instead, a rather featureless thermogram is obtained. TGA for these polymers indicates weight loss starting at the temperature of onset of the first DSC endotherm and continuing throughout. It is possible that the endotherms observed correspond not only to the loss of associated solvent and water, but also to chemical reactions ocurring during heating.

Figure 42 summarizes the DSC thermograms for radical and thermal P4VPd, as well radical p3VPd, including first and second heating. For the radical P4VPd, endotherms (curves A and B) were observed at 109°C and 160°C for both the high and the low molecular weight polymers upon heating. The area under the curve for these endotherms corresponds to an energy of 1.86 cal/g and 5.07 cal/g respectively. These energy

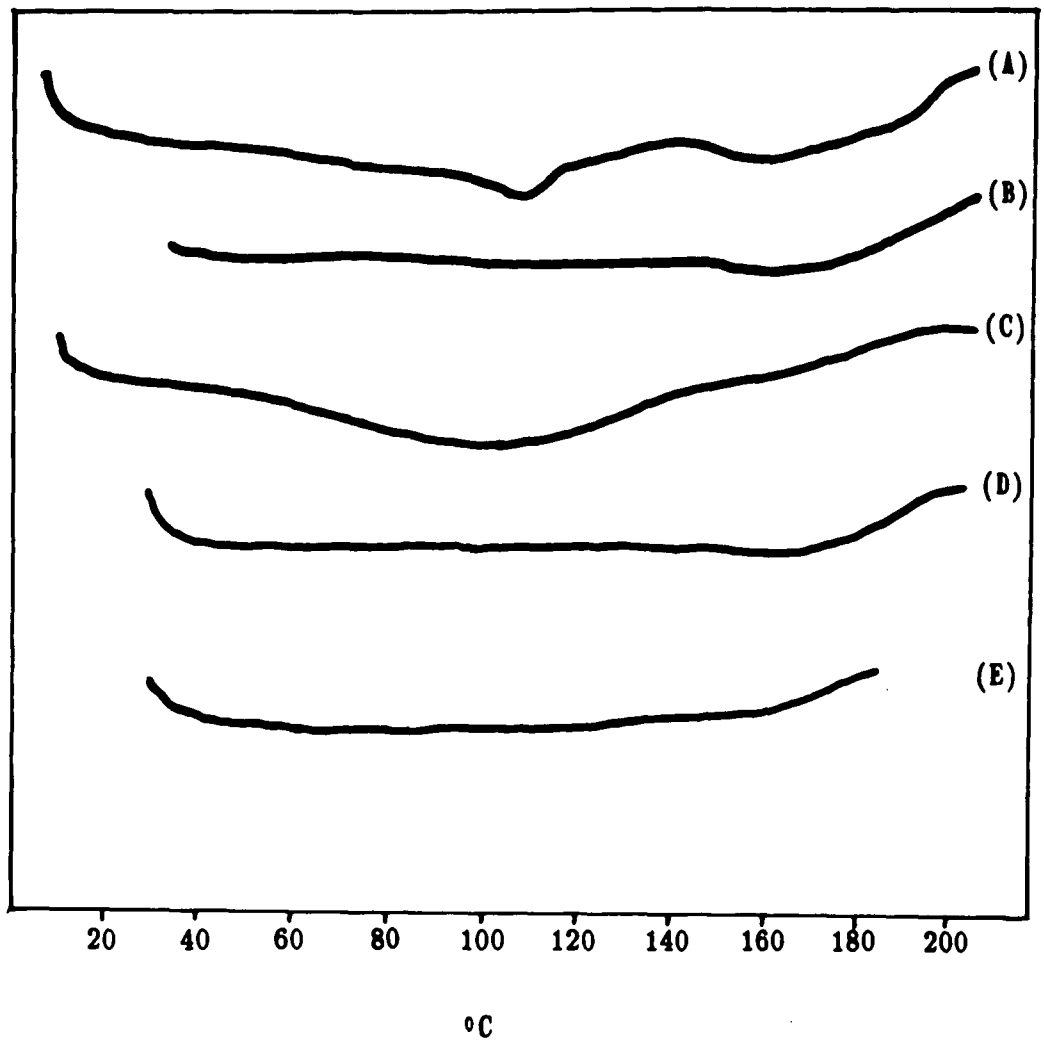

Figure 42. DSC thermograms of:

A. Radical P4VPd, first heating

B. Radical P4VPd, reheat

C. Thermal P4VPd for comparison

D. Radical P3VPd, first heating

E. Radical P3VPd, reheat

values are too low to be attributed to melting of the polymers. TGA showed no weight loss for these samples up to a temperature of 240°C. Slow cooling to room temperature followed by reheating of the samples showed the complete loss of the first endotherm and a diminution of the second. Therefore the second endotherms observed must correspond to changes of order in polymer organization upon heating.

Both NMR and viscosity data support a rigid rod conformation for the stereoregular, most likely syndiotactic, polymer. For such macromolecules, liquid crystal behaviour is expected. The prevailing low energy transition at 160°C can be attributed to melting of the nematic phase of the polymer into an isotropic phase. Curve C shows DSC thermograms of thermal P4VPd for comparison.

Radical P3VPd, curves D and E, shows only an endotherm in the DSC thermogram at 180°C which diminishes upon second heating. ^{13}C NMR data indicate a significant level of isotactic placement (Figure 31). The 180°C endotherm can be attributed to the distortion of the helical fragments of the polymer required by the isotactic stereoregularity.

TGA thermograms for the new radical polymers showed better heat stability for P3VPd and P4VPd compared with P2VP at temperatures below 240°C (Figure 43). The high dipole moment of the pendant pyridazine rings of the new polymers must play an important role. At temperatures above 240°C, the pyridazine ring could be destroyed through nitrogen extrusion.

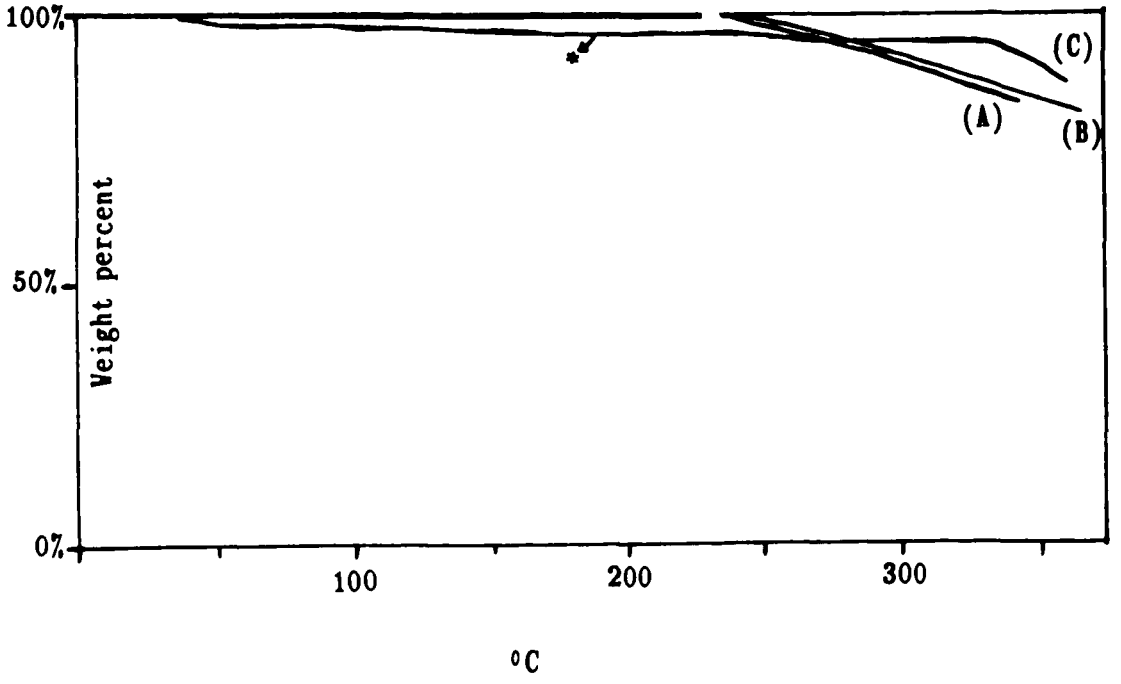

Figure 43 TGA thermograms of:

A. Radical P3VPd

B. Radical P4VPd

C. P2VP

* P2VP melts at this point and turns to a brown charred material.

V. CONCLUSION

The first syntheses and characterization of P3VPd and P4VPd have been accomplished. Solution behavior and charge-transfer complexes of the new polymers with iodine were studied in detail. The preparation of the polymers involved the first synthesis of the monomers 3- and 4-vinylpyridazine. The search for a suitable route to the new monomers resulted in two different methods. Both required the first synthesis of the intermediate alcohols, 3- and 4-(β-hydroxyethyl)pyridazine.

The first method required high pressure and temperature in an aqueous medium to produce acceptable yields of 3-(β-hydroxyethyl)-pyridazine and no recoverable 4-(β-hydroxyethyl)pyridazine. ^{13}C NMR spectra indicated that 3-(β-hydroxyethyl)pyridazine formed six-member cyclic structures through hydrogen bonding of the alcohol hydrogen with the N-2 atom of the pyridazine ring, while for the 4-(β-hydroxyethyl)pyridazine such hydrogen bonding was not favored. The 3-alcohol cyclic structure formed in aqueous medium, could be stabilized by surrounding water dipoles, resulting in good yields for the 3-(β-hydroxyethyl)pyridazine. The conditions of high pressure and temperature applied to the 4-alcohol favored dehydration followed by polymerization of the resulting vinyl monomer, yielding the polymer P4VPd.

The second method, involving an anhydrous molecular formaldehyde reagent solution at low temperature and pressure in a mildly basic

solvent gave a high yield of 4-(β-hydroxyethyl)pyridazine and improved yields of 3-(β-hydroxyethyl)pyridazine over the first method. The two vinyl monomers, 3-vinylpyridazine and 4-vinylpyridazine, were then obtained in good yields by acid dehydration of the intermediate alcohols. The four new molecules resulting from this synthesis were all high boiling liquids caused by their strong permanent dipole moments. The alcohols were stable at room temperature while the 3- and 4-vinyl monomers polymerized on standing for several days.

The methods established in this work for the syntheses of the new substituted pyridazines in acceptable yields are important not only from the point of view of polymer chemistry, but also for pyridazine chemistry in general.

The two new pyridazine monomers were successfully polymerized radically and thermally. Anionic polymerization gave the desired polymers in low yields. However, a better understanding is needed concerning the processes occurring during this type of polymerization. For thermally polymerized polymers, ^{13}C NMR studies combined with thermal analysis suggest rigidity of the chain backbone and lack of stereo- regularity. At high thermal polymerization temperature the orientational effect of dipole interactions on the placement of incoming monomers was overcome by thermal energy.

Radical thermal polymerization of the two monomers was initiated by hydrogen peroxide. The effect of initiator concentration on molecular size of the resulting polymers was observed through viscosity studies. The yield of P3VPd polymers was always lower as

compared to P4VPd. This, we believe, is the result of the difference in resonance stabilization of the propagating radicals by the pyridazine ring in the two monomers. Pyridazine, unlike pyridine, shows two different resonance structures. One of them, with a double bond between the two ring nitrogens, is not favored.[8] This results in only one favorable resonance-stabilized structure for the propagating radical with the pendant ring in the P3VPd system and two favorable resonance stabilized structures for the radicals in the P4VPd system (see below). Thus better overall polymer yields were obtained for the latter system.

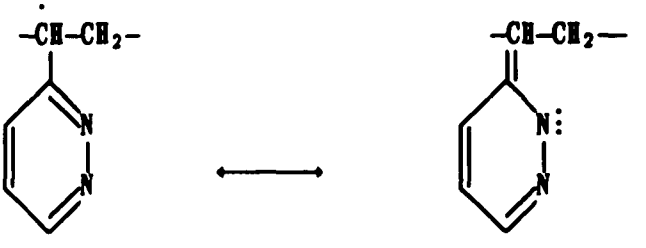

P3VPd

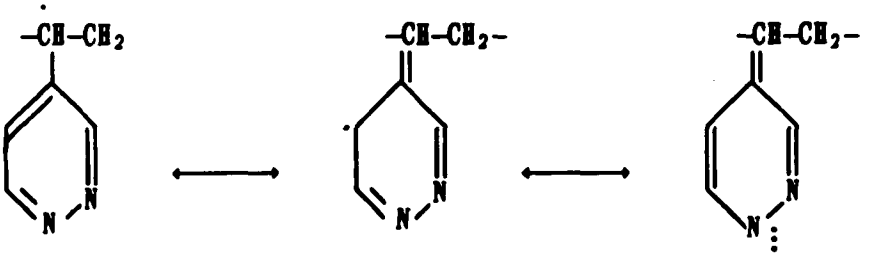

P4VPd

The difference in direction and magnitude of the dipole moment for the two monomers plays an important role in the radical polymerization process as well as in the properties of the resulting

polymers. ^{13}C NMR, thermal analysis and viscosity studies of the radical polymers revealed rigid rod behaviour for P4VPd not observable for P3VPd. Rigid rod behavior is the result of syndiotactic placement of incoming monomers caused by unfavorable dipole-dipole repulsive forces for isotactic placement between pyridazine rings. The isotactic placement is estimated based on a dipole-dipole interaction equation to be at least 200 kcal/mole less energetically favored compared to the syndiotactic placement. The syndiotactic placement imposes stringent structural conformations for the polymer chains, resulting in rigid rod formation and liquid crystal behaviour. For radical P3VPd, a very favorable dipole-dipole interaction, 300 kcal/mole, between neighboring rings in isotactic placement can be achieved through ring rotation to assume a level of head to tail dipole-dipole arrangement. However, steric repulsion plus thermal energy at 400 K does not preclude extensive isotactic placement.

Stoichiometry for charge-transfer complexation of the pyridazine rings in P3VPd and P4VPd with iodine were determined to be of the ratio 1:1.4 and 1:1.2, rings to iodine, respectively. These complexes showed semiconductivity at least at a level similar to the P2VP-I_2 systems, i.e. 10^{-5} to 10^{-4} $\Omega \cdot cm^{-1}$. However, the effect that charge transfer complex formation with iodine had on polymers was found to be different for poly(vinylpyridazine) systems as compared with P2VP. Our study showed that P2VP crosslinks in the presence of iodine at relatively low temperatures while no such process was observed for P3VPd and P4VPd under similar conditions. This difference can be

ascribed to the higher resonance stabilization of pyridine (134 kJ/mol)[55] as compared to pyridazine (52 kJ/mole)[55]. The formation of benzilic radicals followed by crosslinking of the polymer would therefore be more favored in P2VP than in P3VPd and P4VPd. ESR spectra suggesting this type of radical were observed for the P2VP/I_2 system and not observed for the P3VPd/I_2 and P4VPd/I_2 systems. For the three polymer/I_2 charge-transfer complexes, g values were comparable except for the complexes of radically polymerized P4VPd with iodine. These complexes showed a high g value, suggesting a high delocalization of the unpaired electrons into the iodine system. This effect may be caused by the structural regularity of the polymer, allowing special interactions between the pyridazine rings and iodine. The new polymers showed significant differences in solubility compared with P2VP. ESR studies showed high spin density for the native form of P3VPd and P4VPd . no spin density for P2VP.

The effect of the strength and direction of the dipole moment of the pendant rings was observed in the solution properties and structure of the new P3VPd and P4VPd polymers. However, the effect of differences in dipole moments on the properties of the charge-transfer complexes of P3VPd and P4VPd with iodine were not readily observed.

VI. REFERENCES

1. Duke, C.B.; Gibson, H.W. *Encyclopedia of Chemical Technology*, 3rd ed., 1982, *18*, 755.

2. Baugham, R.H.; Bredas, J.L.; Chance, R.R.; Elsenbaumer, R.L.; Shacklette, L.W. "Structural Basis for Semiconducting and Metallic Polymer/Dopant Systems," in *Chem. Rev.* 1982, *82*, 210.

3. Frommer, J.A.; Chance, R.R. in *Encyclopedia of Polymer Science and Engineering*, 2nd ed, Mark, Bikales, Overberger, Menges Eds., Wiley: New York, 1985.

4. Shacklette, L.W.; Chance, R.R.; Ivory, D.M.; Miller, G.G.; Baughman, R.H. *Synthetic Met.*, 1979, *1*, 307.

5. Shacklette, L.W.; Elsenbaumer, R.L.; Chance, R.R.; Eckhardt, H.; Frommer, J.E.; Baughman, R.H. *J. Chem. Phys.*, 1981, *75*, 1919.

6. Druy, M.A.; Rubner, M.F.; Walsh, S.P. *Electrochem. Soc. Ext. Abstracts*, 1984, *84*, 617.

7. Tisler, M.; Stanovik, B. in *Comprehensive Heterocyclic Chemistry*, A.R. Katritzky and C.W. Rees, Eds.; Pergamon Press: Oxford, Vol. 2., 1984.

8. Tisler, M.; Stanovik, B. "Pyridazines and Their Benzo Derivatives" in *Comprehensive Heterocyclic Chemistry*, A.R. Katritzky and C.W. Rees, Eds.; Pergamon Press: Oxford, Vol. 3., 1984.

9. Hoare, R.S.; Pratt, J.M. *J. Chem. Soc., Chem. Comm.*, 1969, 1320.

10. Dratter, R.; Lazlo, P. *J. Chem. Soc., Chem. Comm.*, 1970, 180.

11. Mead, R.T., U.S. Pat. 3 957 533, 1976, CA: *85*, 163333c.

12. Moser, J.R. U.S. pat. 3 660 163, 1972, CA: *76*, 67438m.

13. Schneider, A.A.; Harney, D.; Harney, M.J. *J. Power Sources*, 1980, *5*, 15.

14. Yang, N.L.; Wang, S.S.; Hou, C.T.; Rodriguez, L.; Jolson, J.; Waggoner, J. *J. Chem. Soc., Chem. Comm.*, 1985, 1632.

15. Ohsawa, A.; Uezu, T.; Igeta, H. *Chem. Pharm. Bull.*, 1979, *27*(4), 916-922.

16. Walker, J.J. *ACS Monograph Series*, no. 159, American Chemical Society: Washington, DC, 1964.

17. Mulliken, R.S. *J. Am. Chem. Soc.* 1952, *74*, 811.

18. Kosower, E.M. *J. Am. Chem. Soc.* 1959, *80*, 3253.

19. Larkindale, L.P.; Simkin, D.J. *J.Chem. Phys.* 1971, *55(10)*, 5048.

20. Brandrup, J.; Immergut, E.H. Eds. *Polymer Handbook*, Wiley, New York, 1975.

21. Haas, H.C.; Moreau, P.D. *J. Polym. Sci., Polym. Chem. ed.*, 1972, *15*, 1225.

22. Remy, F.; Muteau, L.; Caze, C.; Loucheux, C. *Polymeric Amines and Ammonium Salts*, E.J. Goethals, Ed.; Pergamon Press: Oxford, 1980, p 295.

23. Andon, R.J.L.; Cox, J.D.; Herington, E.F.G. *Trans Faraday Soc.*, 1954, *50*, 918.

24. Lupinsky, J.H.; Kupple, K.D.; Hertz, J.T. *J. Polym. Sci.*, Part C, 1967, *16*, 1561.

25. Tisler, M.; Stanovnik, B. *Adv. Heterocycl. Chem.*, 1968, *4*, 211.

26. Tisler, M.; Stanovnik, B. *Adv. Heterocycl. Chem.*, 1979, *24*, 363.

27. Neunhoeffer, N.; Wiley, P.F. *Chem. Heterocycl. Cmpd.*, 1978, *33*, 1073.

28. Thulstrup, E.W.; Spangel-Larsen, J.; Gleith, G. *Mol. Phys.*, 1979, *37*, 1381.

29a. Tsujimoto, T.; Kobayashi, C.; Nomura, T.; Lifuro, M. Sasaki, Y. *Chem. Pharm. Bull.*, 1979, *27*, 2105.

29b. Partington, J.R., *An Advanced Treatise on Physical Chemistry*, Vol. 5, Longmans: London, 1966.

30. Japelj, M.; Pollack, A.; Valcavi, V.; Likar, M.; Schauer, P. *Farmaco, ed. Sci.*, 1973, *28*, 46. CA: 78 132243b

31. Itai, T.; Sueyoshi, S.; Nato, K.; Mizuno, D. *Yakugaku Kasshi*, 1969, *89*, 132. CA: *70*, 96480a.

32. R. Qian, *Acad. Sinica*, verbal communication and Chinese patent, GK 85-108688, 1987.

33. Wyard, S.J. *J. Sci. Instrum.*, 1965, *42*, 769.

34. Carr, H.Y.; Purcell, E.M. *Phys. Rev.*, 1954, *94*, 630.

35. Fyfe, C.A. *Solid State NMR for Chemists*, C.F.C. Press: Guelph, Ontario, Canada, 1983, 326.

36. Vold, R.L.; Vaugh, J.S.; Kleln, M.P.; Phelps, D.E. *J. Chem. Phys.* 1968, *48*, 3831.

37. Allerhand, A.; Dodrell, D.; Komoroski, R.J. *J. Chem. Phys.*,1971, *55*, 189.

38. Kuhlman, K.F.; Grant, D.M.; Harris, R.K. *J. Chem. Phys.*,1970, *52*, 3439.

39. David, C.; Verltasselt, A.; Geuskens, G. *J. Polym. Sci.* Part C, 1967, *16*, 2181.

40. David, C.; in *Degradation of Polymers*, C.H. Bamford and C.F.H. Tipper eds.; Elsevier, New York, 1965.

41. Mizzoni, R.H.; Spoerri, P.E. *J. Am. Chem. Soc.*, 1954, *76*, 2201.

42. Brooks, L.A. *J. Am Chem. Soc.*,1944, *66*, 1295.

43a. Matsushita, Y.; Shimizu, K.; Nakuo, Y.; Choshi, H.; Noda, I.; Nagasawa, M. *Polym. J.* 1986, *18*(*4*), 361.

43b. Kommanduer, J. in *Physics and Chemistry of the Organic Solid State*, Fox, D.; Labes, M.; Weissburger, A. Eds.; Interscience Publishers: New York , 1965; p 14.

44. Furve, M.; Sumi, K.; Nozakura, S.I. *J. Polym. Sci., Polym. Lett. ed.*, 1982, *20*, 291.

45. Jones, R.G.; Konfeld, E.C.; McLaughlin, K.C. *J. Am. Chem. Soc.*, 1950, *72*, 3539.

46. Debun, J.D.; Levine, R. *J. Am. Chem. Soc.*, 1959, *81*, 5666.

47. Bremser, W.; Ernst, L.; Franke, B.; Gerhards, R.; Hardt, A. *Carbon-13 NMR Spectral Data*, Verlag Chemie: Deerfield Beach, FL, 1981.

48. Pouchert, J. *The Aldrich Library of NMR Spectra*, vol. *2*, 2nd ed. Aldrich Chem. Co. 1983

49. Matsuzaky, K.; Kanai, T.; Matsubara, T.; Matsumoto, S. *J. Polym. Sci.: Polym. Chem. ed.*, 1979, *14*, 1475.

50. Igeta, H.; Kaneko, C.; Tsuchiga, T. *Chem. Pharm. Bull.*, 1975, *23*(11), 2798.

51. Hermans, J. *J. Colloid Sci.*, 1962, *17*, 638.

52. McClure, D.S. *J. Chem. Phys.* **1949**, *17*, 905.

53. Feher, G.; Kip, A.F. *Phys. Rev.* **1955**, *98*, 337.

54. *Physical Chemistry*, 2nd ed., Moelwyn-Hughes, E.A., Ed. Pergamon Press: London, 1951.

55. Pihlaja, K.; Taskinen, E. in *Physical Methods in Heterocyclic Chemistry*, Vol. VI(23a), Katritzky, A.R. Ed., Academic Press: New York, 1974.

56. Morawetz, H. *Macromolecules in Solution*, *High Polymers*, Vol.XXI, Viley-Interscience: New York, 1975.